MINISTERE DE L'ENSEIGNEMENT SUPERIEUR ET DE LA RECHERCHE SCIENTIFIQUE
Universite Felix-Houphouet Boigny

UNITE DE FORMATION ET DE RECHERCHE SCIENCES DES STRUCTURES DE LA MATIERE ET DE TECHNOLOGIE

RÉPUBLIQUE DE CÔTE D'IVOIRE
UNION – DISCIPLINE– TRAVAIL

RWTH Aachen University

SPONSORED BY THE Federal Ministry of Education and Research

No : 833

INTERNATIONAL MASTER PROGRAM

IN RENEWABLE ENERGY AND GREEN HYDROGEN

SPECIALITY: GEORESSOURCE (WATER,WIN) AND TECHNOLOGY

MASTER THESIS

Topic:

VARIABILITY ACROSS CLIMATE MODEL SIMULATIONS OF FUTURE WIND REGIMES IN WEST AFRICA

Presented on the 25th of September 2025 by:

Kouassi Hervé KOUADIO

Jury members:

Obrou Kouadio Olivier	**President**	Prof.	UFHB
Bamba Adama	**Examiner**	Dr.	UFHB
Kouadio Kouakou	**Major supervisor**	Dr.	UFHB
Hegglin Michaela	**Co-supervisor**	Prof.	FZJ
Mohamadou A. Diallo	**Co-sipervisor**	Dr.	FZJ

Academic year 2024-2025

DEDICATION

I dedicate this humble work to my entire family for their prayer and unwavering support since the beginning of this journey

ACKNOWLEDGEMENTS

First and foremost, I am immensely grateful to God Almighty for granting me the strength, knowledge, abilities, and opportunities to embark on this research journey and to successfully complete it.This success would not have been possible without His grace. The research was funded by the German Federal Ministry of Education and Research (BMBF) under the West African Science Service Centre for Climate Change and Adapted Land Use (WASCAL) project. I would like to thank the WASCAL team and the International Master's Programme in Energy and Green Hydrogen Production (IMP-EGH) for the exceptional training. I equally wish to thank them and guidance they provided during my research trip from Africa and Germany.

My gratitude goes to the Rectors of the University of Université Felix Houphouet Boigny (UFHB), Cote d'Ivoire, Prof. Ballo Zié, University of Lome, Prof. Komla dodzi KOKOROKO and University Abdou Moumouni of Niger, Prof. BARAGE Moussa, to the Director of GSP of Niger Prof. Rabbani Adamou at Abdou Moumouni University, to the Director Prof. Kouassi Edouard of GSP Côte d'Ivoire and the Coordinator of the H2 Program at the GSP Dr.FASSINOU Wanignon Ferdinand, to the Scientific Coordinator Prof. Soro for their tireless efforts in ensuring a conducive learning environment.

I am truly fortunate to have been part of an exceptional research team at the Institute of Climate and Energy Systems - Stratosphere (ICE-4), Forschungszentrum Jülich GmbH, Juelich, Germany. I am especially thankful to my main supervisor , Prof. Dr. Michaela I. Hegglin and my daily supervisor Dr. Mohamadou A. Diallo for their expert guidance, continuous support, and valuable insights. Their mentorship have been invaluable, from shaping innovative scientific research to engaging in fruitful discussions and providing constructive suggestions to enhance the work. Their willingness to share knowledge and experience have been instrumental in shaping the direction of this research. Morevover, I extend my special thanks to the other colleagues at the institute, Dr. Fuzhen, Dr. Veenus and Mr. Gabriel, who also brought me their assistance whenever I was confronted to a challenge.

I would also like to express my gratitude to my local supervisor, Dr. KOUADIO Kouadio, at the Université Felix Houphouet Boigny (UFHB) in Cote d'Ivoire for his significant collaborative support providing both administrative and scientific advice, continuous guidance since Germany and in Cote d'Ivoire.

I extend my sincere gratitude to Prof.OBROU Kouadio Olivier, serving as the President of the Jury, and Dr.BAMBA Adama, as the Examiner from Felix Houphouet-Boigny University as well as my supervisors. Your invaluable contributions as jury members during my dissertation defense have greatly influenced the quality and direction of this work. Your expertise and insightful evaluations have

been instrumental in this academic endeavor. I also extend my gratitude to all my IMP-EGM Promotion mates and classmates, their fellowship and support throughout this academic endeavor.
Lastly I would like to convey my hearfelt gratitude to my dear family for their constant psychological encouragement and prayers since I began this academic adventure.

ABSTRACTS

Reliable wind assessments are essential for energy planning in West Africa, where demand is increasing and decarbonisation targets are becoming more stringent. The purpose of this study is to evaluate both the credibility and the variability of global climate models simulations for wind regimes in West Africa dividided into five sub-regions (Atlantic coastal, southern coastal, sub-Saharan, Sahel, and Sahara), using ERA5 reanalysis as a benchmark for evaluating model performance as well as projecting future regimes under climate scenarios for better energy planning and relevance policy informed decision making. First, the past-to present climatological analysis with the ERA5 wind speed data for the period 1950-2024 show that the Atlantic coastal region and the Saharan have strongest and moderate mean wind speed respectively above 3 m/s or around. While most of the Sahelian, sub-Saharan and southern coastal regions show low mean wind speeds between 1-3 m/s. Secondly the long-term wind speed anomalies shows positive and negative values, with |anomaly| ≥ 0.2 m/s across all subregions, except the sub-Saharan region where anomalies fall below 0.2 m/s in absolute value. Futhermore, findings present a relatively low or almost no trend over the study period. The resuluts of seasonal variability and extremes events across the sub-regions show that high wind speeds occur in DJF, MAM for the Atlantic coastal region, in JJA for Southern Coastal and sub-Subsahara, in DJF for Sahelian and Sahara. Four CMIP6 models (MIROC6, HadGEM3-GC3, CESM2-WACCM, MPI-ESM1-2HR) were used for historical wind speed projections.The historical projections show a robust coastal-inland gradient across models with observed individual biaises: the highest mean winds are found on the Atlantic coast and the Saharan fringe, the lowest in the sub-Saharan belt and variability increases inland. The models were compared to ERA5 and the statistically best performing model MPI-ESM1-2LR (mean bias = +0.07m/s, MAE = 0.41m/s; RMSE = 0.52m/s, r = 0.90; R^2 = 0.78) was used for the 2025-2075 projections under SSP2-4.5 and SSP5-8.5 considering DJF and JJA seasons. The future projections conserve the historical gradient but present a generalised weakening inland, weaker and more irregular in the SSP2-4.5 scenario and more widespread in the SSP5-8.5 scenario, particularly during the JJA period in the southern coastal, sub-Saharan and Sahelian areas; the Atlantic coastal corridor remains relatively robust, while the Sahara shows mixed seasonal changes. These results imply that for better regional energy planning we should prioritise grid-connected coastal and offshore projects, combine wind energy from the south coast with photovoltaic energy and storage to address seasonal variability, adopt hybrid strategies and targeted micro-deployment inland, and take into account transport and maintenance constraints for Saharan options

Keywords: West Africa; wind resource assessment; CMIP6 projections; energy planning

RESUME

Des évaluations fiables des vents sont essentielles pour la planification énergétique en Afrique de l'Ouest, où la demande augmente et où les objectifs de décarbonisation deviennent plus stricts. L'objectif de cette étude est d'évaluer la crédibilité et la variabilité des simulations des modèles climatiques globaux pour les régimes de vent en Afrique de l'Ouest. L'Afrique de Ouest est sub-divisée divisée en cinq sous-régions a savoir la Côte Atlantique Ouest, la Côte Atlantic Sud, la region sub-Sahararienne, le Sahel et le Sahara. La réanalyse ERA5 est utilisée ici comme référence pour évaluer la performance des modèles et projeter les régimes futurs. Les projections sont établies sur la base de scénarios climatiques afin d'améliorer la planification énergétique et les décisions politiques correspondantes.

Tout d'abord, l'analyse climatologique et present historique basée sur les données ERA5 relatives à la vitesse du vent couvre la période 1950-2024. Cette analyse montre que la côte Atlantique et la région Saharienne ont respectivement les vitesses moyennes de vent les plus élevées et les plus moderée, dépassant ou autour de 3 m/s. A l'inverse la vitesse moyenne de vent dans la plupart des regions de la Cote Sud, du Sahel, et du Sub-Sahara est comprise entre 1 et 3m/s. Deuxièmement, les anomalies à long terme de la vitesse du vent présentent des valeurs positives et négatives, avec une anomalie $\geq$ 0,2 m/s dans toutes les sous-régions, à l'exception de la région subsaharienne où les anomalies sont inférieures à 0,2 m/s en en terme de valeur absolue. En outre, les résultats présentent une tendance relativement faible ou presque nulle au cours de la période étudiée. Les résultats de la variabilité saisonnière et des événements extrêmes à travers les sous-régions montrent que les vitesses de vent élevées se produisent particulierement dans les saisons DJF, MAM pour la région côtière atlantique, JJA pour la région côtière méridionale et sub-saharienne, et enfin DJF pour les régions sahélienne et saharienne. Quatre modèles CMIP6 (MIROC6, HadGEM3-GC3, CESM2-WACCM, MPI-ESM1-2HR) ont été utilisés pour les projections historiques de la vitesse du vent. Les projections historiques montrent un gradient robuste entre la côte et l'intérieur des terres à travers les modèles avec des biais individuels observes, indicant que les vitesses de vent en moyenne les plus élevés se trouvent sur la côte atlantique et la frange saharienne, les plus faibles dans la ceinture subsaharienne et la variabilité augmente à l'intérieur des terres.

Les modèles ont été comparés à ERA5 et le modèle statistiquement le plus performant MPI-ESM1-2LR (biais moyen = +0,07m/s, MAE = 0,41m/s; RMSE = 0,52m/s, r = 0,90 ; R^2 = 0,78) a été utilisé

pour les projections 2025-2075 en considerant les scénarios SSP2-4.5 et SSP5-8.5 et en tenant compte des saisons DJF et JJA. Les projections futures conservent le gradient historique mais présentent un affaiblissement généralisé à l'intérieur des terres, plus faible et plus irrégulier dans le scénario SSP2-4.5 et plus répandu dans le scénario SSP5-8.5, en particulier pendant la saison JJA dans les zones côtières méridionales, subsahariennes et sahéliennes. La sous-region côtiere atlantique reste relativement robuste, tandis que des fluctuations saisonnières soient observées dans la zone saharienne. Cette étude démontre qu'une stratégie énergétique régionale efficace doit mettre au devant les infrastructures au niveau des regions côtières et marines qui sont intégrées au réseau électrique. La production éolienne dans les zones côtières du sud doit être intégrée à la production photovoltaïque. Il faut egalemnent envisager les technologies de stockage de l'énergie pour tenir compte des changements saisonniers. Les régions intérieures devraient opter pour des tactiques hybrides et des solutions de micro-déploiement ciblées. Elles doivent tenir compte également des difficultés liées au transport et a la maintenance de le Sahara.

Mots-clés : Afrique de l'Ouest ; évaluation des ressources éoliennes ; projections CMIP6 ; planification énergétique

ACRONYMS AND ABBREVIATIONS

AEJ	:	African Easterly Jet
AMO	:	Atlantic Multidecadal Oscillation
CMIP5	:	Coupled Model Intercomparison Project Phase 5
CMIP6	:	Coupled Model Intercomparison Project Phase 6
CO2	:	Carbon dioxide
CORDEX	:	Coordinated Regional Climate Downscaling Experiment
EASJ	:	EAST Asian Subtropical Jet
ECMWF	:	European Centre for Medium-Range Weather Forcasts
ENSO	:	El Niño–Southern Oscillation
ERA5	:	ECMWF Re-Analysis Fith generation
ESRL	:	Earth System Laboratory
GW	:	Gigawatt
GWA	:	Global Wind Atlas
GWEC	:	Global Wind Energy Council
IFC	:	International Finance Coorporation
IPCC	:	Intergouvernemental Panel on Climate Change
IRENA	:	International Renewable Energy Agency
NAO	:	North Atlantic Oscillation
NOAA	:	National Oceanic and Atmospheric Administration
SDG	:	Sustainable Development Goal
SHL	:	Saharan Heat Low
SSP	:	Share socio-economic pathways
SST	:	Sea Surface Temperature
TWh	:	Terawatthour
UN	:	United Nation
WAM	:	West African Monsoon
WPD	:	Wind Probability Distribution

LIST OF TABLES

LIST OF FIGURES

TABLE OF CONTENTS

Contents

GENERAL INTRODUCTION

GENERAL INTRODUCTION

Climate change has been a pivotal subject at the centre of many rigorous scientific reflections over decades. Several studies revealed an increase in global temperature, changes in rainfall patterns, and wind regimes...etc across the world (IPCC, 2021). Climate change is then universally recognized as a major global crisis that requires immediate and concerted responses from every sector of society, including energy(IPCC, 2021; Zhang, 2025). Therefore, Parties to the Paris Agreement set the urgent goal of limiting global average temperature increase to well below 2°C above pre-industrial levels, and to pursue efforts to limit the temperature increase to 1.5°C with the aim of significantly reducing the risks and impacts of climate change (IPCC, 2021). This means it is crucial to find new alternatives to fossil fuels, which are the major contributors to greenhouse gas emissions, leading to global warming and climate change (Attanayake et al., 2024). As a result, the integration of renewable energy in any transition towards a climate-friendly future is imperative. According to IRENA's flagship reports, World Energy Transitions Outlook 2023 and 2024, the largest shares in the carbon dioxide (CO2) emissions cuts needed to achieve net-zero emissions by 2050 under the 1.5°C pathway will come from the use of renewables in power generation and, directly, in heat and transport, combined with energy conservation and energy efficiency. Many other recent studies also emphasize the need to transition towards Renewable Energy Sources to mitigate carbon emissions and ensure a sustainable future (Feng, 2022; Rehman et al., 2023). As such, renewable energy resources are gaining significant value in the total primary energy supply (Gernaat et al., 2021; IRENA, 2025). According to the recent IRENA Report, Renewable Capacity Statistics 2025, by the end of 2024, renewables accounted for 46% of global installed power capacity. In 2024, the global renewable sector experienced the largest increase to date with the addition of 585 gigawatts (GW) of renewables showing a remarkable increase from the previous year. Renewables accounted for a record 92.5% of global power additions, mostly because of the spectacular growth in solar and wind power. Solar power alone contributed over 450 GW, accounting for three-quarters of renewable additions while wind added 113GW.

Furthermore, Boadu & Otoo (2024) reported that that over 620 million people, representing more than half of the continent's population currently lack direct access to electricity. This number is projected to increase by 45 million over the next ten years as the demand for electricity across the continent is anticipated to surge by 600% spanning 2010 and 2040 (Boadu & Otoo, 2024).

Recently, IFC commissioned research to evaluate the potential for wind power in Africa and discovered that Africa has an impressive technical wind potential of approximately 180,000 TWh per year, which is sufficient to meet the continent's electricity needs 250 times over (Alemzero et al., 2021; IFC, 2020). The study also discovered that 27 countries in Africa have enough wind potential on their

own to satisfy the electricity demand of the whole continent, estimated at 700 TWh annually (IFC, 2020).

The estimated regional technical potential of wind energy available on the African continent is as follows: North Africa with an energy reserve of approximately 11,963 TWh, Southern Africa with a wind energy potential of approximately 6,971 TWh, East Africa with an energy reserve of approximately 6,694 TWh, and West Africa with an energy reserve of approximately 5,152 TWh. The region with the lowest wind energy potential is Central Africa (Mentis et al., 2015). In West Africa in particular wind energy development is still at early stages with Senegal being the leader of the region with an installed capacity of around 158 MW (Niang et al., 2024a).

As such, the development of wind energy in West Africa demands a strong and clear understanding of current and future wind regimes. However, confidence in climate projections still poses a big problem due to uncertainties in how these models represent or simulate climatic conditions due to differing assumptions, physics, parameterizations, and spatial resolutions (IPCC, 2021). Several studies out there on regional climate projection have focused their investigations on mainly precipitation and temperature (Akinsanola & Zhou, 2019; *Climate Change Impacts on Biodiversity and Protected Areas in West Africa*, 2016; Diallo et al., 2012; Dosio et al., 2020; Heinzeller et al., 2018; Klutse et al., 2018; Nkrumah et al., 2025; Taguela et al., 2025; Todzo et al., 2020) but few of them have focused on understanding the wind patterns under a changing climate and their relevance to energy planning. For developing countries in West Africa holding the aim to invest in climate-resilient renewable energy, it is crucial to evaluate the variability across climate models and figure out whether climate models can accurately replicate past to present-day and future wind regimes and to simulate their future changes. Without this critical evaluation, long-term planning decisions risk being based on misleading or unreliable presssumptions. Therefore, this study, aims to evaluate both the credibility and the variability of climate models simulations for wind regimes in West Africa, using ERA5 reanalysis as a benchmark for evaluating model performance as well as projecting future regimes under climate scenarios for better energy planning and relevance policy informed decision making.

To achive this main objective of this study, the following specific objectives will be addressed:

1. Evaluate wind climatology in West Africa from 1950 to 2024 using ERA5 reanalysis
2. Statistically evaluate four climate models for replicating historical wind speed from 1950 to 2014 using ERA5 as a benchmarch.
3. Project wind regimes under SSP2-4.5 and SSP5-8.5 scenarios with CIMP6 models from 2025-2075 and discuss possible implications on wind energy infrastructure planning in West Africa.

Following from the previous specificc research objectives, here are some potential research questions:

1. What are the variability and trends in wind speed over West Africa over the past and recent years from reanalysis?
2. How accurately do CIMP6 climate models reproduce historical observations in wind speed distribution over West Africa?
3. What are the future wind speed changes under moderate (SSP2-4.5) and extreme (SSP5-8.5) climate scenarios and possible implications on wind energy planning?

The thesis is structured as follow: in chapter 2, some scientific background is presented, regarding the current state of wind energy in Africa, the key drivers of variability as well as the past and future projections studies conducted in litterature. Chapter 3, the method used for the conduction of the research is presented. In chapter 4, results regarding the wind climatology, model's performance evaluation, and projected wind speed under SSP scenarios are presented. Finally, conclusions and directions for further work are discussed in last chapter.

CHAPTER I: LITERATURE REVIEW

CHAPTER I: LITERATURE REVIEW

This chapter situates the work within the global scientific refelexion giving an overview of wind and its systems. Three sections are covered including first, an overview of the state of wind in Africa, secondly an understanding wind regimes and key drivers in Africa and finally, past and future projections in wind patterns in West Africa.

1.1 Current state of Wind in Africa

The literature consistently emphasizes the paradox between Africa's vast technical wind potential and its modest level of deployment. The technical wind capacity of the continent is estimated at 100 GW, yet less than 1% has been harnessed, with deployment concentrated in North and Southern Africa (Boadu & Otoo, 2024). For instance, Merven et al. (2021) and Laura El-Katiri (2021) have written about how South Africa and Morocco, respectively, have become leaders in the continent through coherent and serious policy frameworks, investment incentives, and integration of wind farms into national power plans. Similarly, Siyi (2024) showed that Morocco's liberalized energy sector attracted foreign investors, contrasting with Nigeria, where weak institutional frameworks and inconsistent wind maps impede progress (Olujobi et al., 2023). However, Kruger & Eberhard (2018) cautioned that even in relatively advanced countries, the high cost of capital and inadequate transmission infrastructure remain binding constraints.

The regional comparisons shows significant differences. While Egypt and Moroco increaseded their capacity to reach above 1 GW each, most of West African countries are still at exploratory stages. Pillot et al. (2019) and Ajah (2019) discovered that Sub-Saharan Africa suffers from fragmented energy governance and poor grid connectivity, posing then difficulties to the integration of large-scale wind. In contrast, Van der Zwaan et al. (2018) emphasised that Northern Africa benefits from stable regulatory sytems regimes, reducing their investment risks.

Yet, even in well-performing contexts, social acceptance and environmental concerns, such as land competition and biodiversity impacts, are emerging challenges (Alemzero et al., 2021; Boadu & Otoo, 2024; Haidi & Cheddadi, 2022). At the technical scale, several authors have stressed the importance of high-resolution wind mapping. Gruber et al. (2019) and Gruber et al. (2022) argued that earlier reliance on sparse station data significantly underestimated site-specific variability, while Adekunle et al. (2025) used ERA5 reanalysis to identify viable wind-wave opportunities along Nigeria's coast. Similarly, Ayugi et al. (2020) demonstrated promising wind resources in East Africa but highlighted strong intra-annual variability that raises concerns for energy planning. These findings resonate are consistent with

other studies (Bloomfield et al., 2022; Thomas et al., 2021) ,who noted that reanalysis products tend to underestimate near-surface wind speeds, necessitating bias corrections with local observations or datasets such as the Global Wind Atlas. However, precautions must be taken that in regions with weak observational networks, even bias corrections may still embed uncertainties (Ramon et al., 2019).

Other studies have shwn that the countries with strong independ power producer (IIP) systems including South Africa, succeeded in reducing their costs by the means of competitive auctions (Kruger & Eberhard, 2018) . On the other side, in Nigeria, feasibility studies sometimes do not succeed to concretize in real projects (Akhator et al., 2019). This is caused by regulatory frameworks that are sometimes uncertain. This difference then support common point in the literature that technology cannot be the only alternative. We need an effective governance, a good financing system, as well as stable policy.

1.2 Wind regimes and key drivers in Africa

The wind regimes of West Africa are strongly modulated by the complex interplay of atmospheric circulation systems, land–atmosphere interactions, and large-scale teleconnections. Several studies converge on the central role of the West African Monsoon (WAM) as the dominant driver of seasonal wind variability (Nicholson, 2013; Yaro & Hesselberg, 2016).

During boreal summer, southwesterly moist winds from the Atlantic penetrate inland, while in winter, the Harmattan a dry northeasterly flow dominates much of the Sahel (Sultan & Janicot, 2003).These contrasting regimes establish a marked seasonality, which, as Sultan et al. (2003) observed, directly translates into strong intra-annual variability of near-surface winds and thus energy potential. However, while this monsoon–Harmattan duality is well-documented, its implications for sub-regional heterogeneity remain less thoroughly explored.

Several authors emphasize the latitudinal gradients within West Africa. For example, Abiodun et al. (2012) classified the region into Guinean, Savannah, and Sahelian climatic zones, showing systematic northward decreases in wind speed due to the weakening influence of maritime air masses. More recent work by Ogunjobi et al. (2018) Kouogang Tchuenkam et al. (2022) and AYUGI et al. (2021) reinforced this gradient but also highlighted that coastal areas, particularly the Gulf of Guinea, experience significant diurnal variability linked to land–sea breeze circulations. This coastal influence contrasts with the inland Sahel and Saharan regions, where desert heating amplifies pressure gradients, often generating localized wind maxima (Parker et al., 2005).

In addition to local and regional processes, large-scale teleconnections have a substantial impact. The Atlantic Multidecadal Oscillation (AMO), for example, has been presented to modulate wind

strength and persistence over decades (Knight et al., 2006a; Li et al., 2024a; Lübbecke et al., 2011; Martin & Thorncroft, 2014; C. Zhao et al., 2022). In the same perspective, Joly & Voldoire (2009) found that ENSO phases influence Harmattan strength, with El Niño years typically resulting in stronger northeasterlies. Meanwhile, Gaetani et al. (2017) and Danso et al. (2019) demonstrated that the Saharan Heat Low (SHL) modulates both wind direction and intensity by altering the meridional pressure gradient that controls monsoon flow penetration. Despite these insights, there is still no agreement on the relative magnitude of these drivers across sub-regions, with some authors prioritizing AMO while others highlight SHL dynamics.

The understanding of wind patterns have known a significant improvement these years , even though we cannot deny the existence of some biases. A concrete exemple is a test conducted by Sterl et al. (2018) on the reanalysis using station data from West Africa. He discovered that there is a reasonable agreement with near surface winds. Having said that, ERA5 continues to underestimate extremes. For exemple a previous study identified significant biases in ERA5 (Ramon et al., 2019).The same studies showed that costal areas better perform than inland areas. These divergences in the results clearly stresses the necessity to combine several datasets to evaluate wind patterns.

An emerging body of literature connects wind regimes to dust transport and aerosols, particularly over the Sahel and Saharan zones. Prospero & Mayol-Bracero (2013), Kaufman et al. (2005), and Schepanski et al. (2017) suggested that dust-laden Harmattan winds influence radiative balance and feed back into circulation strength. More recent analyses by Yeo et al. (2025) and Alamirew et al. (2018) aargueed that dust–radiation interactions can strengthen the SHL, indirectly altering wind speeds at low levels.

This line of inquiry underscores the multi-layered and coupled nature of the drivers but remains insufficiently integrated into wind energy feasibility studies. From an energy perspective, several authors argue that the spatial and temporal variability of wind regimes complicates resource assessments. Attabo et al. (2023) and Ayodele et al. (2021) found that although mean wind speeds in coastal Nigeria were moderate, their seasonal variability made them less reliable without hybridization wth solar. Similarly, Nefabas et al. (2021) demonstrated that interannual variability in Ethiopia, partly modulated by ENSO, influenced wind power generation potential by as much as 20%. Translating these insightss to West Africa reveals an underexplored question: how resilieent would wind energy systems bee to suchs teleconnection-driven variability?

1.3 Past and future projections in Wind patterns in West Africa

The this analysis of past and future wind patterns in West Africa has increasingly attracted scholarly attention, particularly in light of renewable energy planning and climate adaptation needs. Historical assessments of wind variability often rely on reanalysis products such as ERA-Interim and ERA5, which provide consistent long-term datasets. For instance, Sterl et al. (2018) demonstrated that ERA5 more accuraletly represents near-surface winds over West Africa than its predecessor, particualray in coastal zones, while Gleixner et al. (2020) showed ERA5 outperforms ERA-Interim in capturing interannual variability. However, Ramon et al. (2019) and Bloomfield et al. (2022) cautioned that ERA5 has biases in low wind speed regimes, which can constrain wind energy resource assessments. This suggests that while ERA5 provides an improved reference baseline for historical climatology, reliance on a single reanalysis may obscure uncertainties in different wind regime patterns.

Trends in historical winds have produced mixed findings. Maidment et al. (2015) identified no significant long-term trend in reanalysis-based wind speeds over much of West Africa, consistent with the global "stilling" debate reported in other regions Zeng et al. (2019). By contrast, Meulenbroeks et al. (1989) found localized increases in wind speeds in the Sahel during recent decades, attributed to intensified meridional pressure gradients. Similarly, Fall et al. (2025) noted that the declining rainfall trend in the Sahel since the 1970s may have participated to subtle adjustments in wind circulation patterns. These discrepancies showcase methodological differences, particularly in the dataset choice, trend detection methods, and spatial aggregation, raising questions about the reliability of historical conclusions.

Looking ahead, future wind regimes projections under climate change scenarios reveal even greater divergence. Several CMIP5 and CMIP6 studies project modest decreases in mean near-surface wind speeds globally (Deng et al., 2020; Miao et al., 2023; Zha et al., 2021). However, regional research on West Africa produce conflicting narratives. For example, Ogunjobi et al. (2022) predicted heterogeneous changes in wind patterns, with wind power projected to decrease in the Guinea and Savannah zones during the winter months due to pressure gradient changes and decreased land-sea temperature differences. In contrast, by the end of the century, the Sahel is expected to experience considerable increases in wind energy potential, particularly during the monsoon season, due to increased land surface heating and atmospheric instability.

In addition, a recent study demonstrated that the wind power density will increase in West Africa considering the scenario RCP5.8.5 in the near future by 20% (Ndiaye et al., 2022). And this can still increase up to 40% by the end of the 21st century (Ndiaye et al., 2022).

Sawadogo et al. (2019a) similarly reported an overall rise in wind speed and WPD over West and Northern Africa under both low and high emission scenarios, with Southern Africa showing the most regional variability. In contrast, the findings of Akinsanola et al. (2021) reported conflicting results: He found an increased summer wind energy density along the Guinean coast and in savanna regions, coupled with decreased winter wind energy density in the Sahel, indicating seasonal and regional variations.

Esnaola et al. (2024) validated this diverse trend by observing a sharp increase in summer wind density along the Guinean coast and a decrease in the Sahel region. This highlights the importance of regional-scale studies in future wind energy planning. These studies reveal considerable regional and seasonal variations in projected wind regime transitions in West Africa. This highlights the complex prospects for wind energy expansion in the region. Another avenue of study focuses on variability and extremes rather than mean changes. Batibeniz et al. (2023) reported that future projections under the SSP5-8.5 scenario will increase in extreme wind events, particularly in tropical countries. These changes leading to concomitant rainfall and more frequent wind extremes.

Similarly, it was found that while mean wind speeds may remain stable, the frequency of winds exceeding the 95th percentile is projected to rise, posing implications for both wind energy production and infrastructure resilience as to (IPCC, 2021) and (Wang & Liu, 2021). These findings challenge the assumption that climate change impacts can be adequately captured by analysing mean wind speed alone.

In oder to better understand projections and their reliability, it is really important to evaluate climate models. The West African Monsoon circulation was proven to be difficult to captured by climate model. For example, CMIP5 models most of the time show low performance to capture West African Monsoon circulation (McSweeney et al., 2015). This contrains the confidence in their capabilities to to estimate wind patterns. Howver, the CIMP6 models, namely MIROC6 and MPI-ESM1-2-HR, are presented to have higher resolution and and improved parameterization (Eyring et al., 2016; Gebrechorkos et al., 2023; Kunchala et al., 2024).

However, several additional studies have found that even CMIP6 demonstrates significant inter-model dispersion over West Africa. This is particularly when simulating regional circulation features like the Saharan Heat Low (Toolan et al., 2024; Zhang & Li, 2022). This suggests that ensemble methods with careful bias adjustment against reanalysis data, are required for reliable projections.

From a renewable energy perspective, these projections can lead to significant implications. Pryor & Barthelmie (2010) highlighted that due to the cubic relationship between wind speed and electricity

generation, even minor fluctuations in average wind speeds can lead to disproportionately large variations in energy output. Recent work conducted by Ramon et al. (2019) also confirmed that uncertainties in wind projections do not facilitate investment decisions in African energy systems.
The combination of climate projections and statistical downscaling have improved the reliability of wind energy assessments in Ethiopia (Nefabas et al., 2021). This finding demonstrates the need for more specific evaluations in West Africa.

In conclusion the analysis of previous studies highlights Africa's significant but untapped potential, which is limited by infrastructural, political and data-related issues. While climatic factors such as the monsoon, the East African jet stream and teleconnections such as AMO and ENSO play a crucial role, their relative influence remains debatable. Advances in reanalysis datasets and CMIP6 models have improved understanding.However, persistent biases still limit their direct application. It is essential to address the gaps through refined regional analyses and better integration of models and data in order to move from general climatological understanding to concrete wind energy planning.

CHAPTER II: DATA AND METHODS

CHAPTER 2 : DATA AND METHODS

This chapter outlines a methodological framework for assessing the wind climatology and variability in West Africa, with particular emphasis on its implications for renewable energy planning. It began by explaining the research region and then explained the datasets used. This included ERA5 reanalysis data, CMIP6 simulation data, and the Atlantic Multidecadal Oscillation (AMO) index.The research technique is divided into two phases: first, characterizing wind field patterns through wind speed, wind direction, and statistical distribution aspects. Second, using statistical analysis to find trends, anomalies, and severe events while evaluating climate model performance.
These steps collectively establish a rigorous multi-scale assessment system capable of analyzing historical and projected wind field patterns across West Africa's five sub-regions in a better way.

2.1 Study area description

The study area covers the West African domain situated between 4°N–20°N latitude and 18°W–15°E longitude and includes all West African countries (Figure 1). The region offers a huge renewable energy potential including solar, water and an untaped wind resources (Alemzero et al., 2021; Aliyu et al., 2018; Boadu & Otoo, 2024; Gunnell, Mietton, Touré, & Fujiki, 2023). The region is endowed with pronounced climatic and ecological gradients, strongly influenced by the West African moonson (WAM) system and the Saharan Heat low Low (Biasutti, 2019; Nicholson, 2013). During boreal summer between June-September, moist southerwesterly monsoon winds from the Atlantic Ocean bring substantial rainfall to southern latitudes, while in boreal winter November-February), dry northeasterly Harmattan winds doninates, transporting Saharan dust across much of the region (Nicholson, 2013). Both temperature and rainfall and their annual cycle depend on the way in which dry and moist air masses interact over the year (Climate Impacts in the Sahel and West Africa, 2016).

In this study, for analytical purposes , we dividded the study area into five distinct sub-regions (Figure 1), namely the Atlantic Coastal Zone (6–20°N, 18–15°W) , the Southern Coastal Zone (4–6°N, 18°W–15°E), the Sub-Saharan Zone (6–10°N, 15°W–15°E), the Sahelian Zone (10–16°N, 15°W–15°E), the Saharan Zone (16–20°N, 15°W–15°E). This regional subdivision ensures that the spatial heterogeneity of wind regimes is adequately captured, allowing for meaningful comparisons across ecological facilitating insights for renewable energy planning.

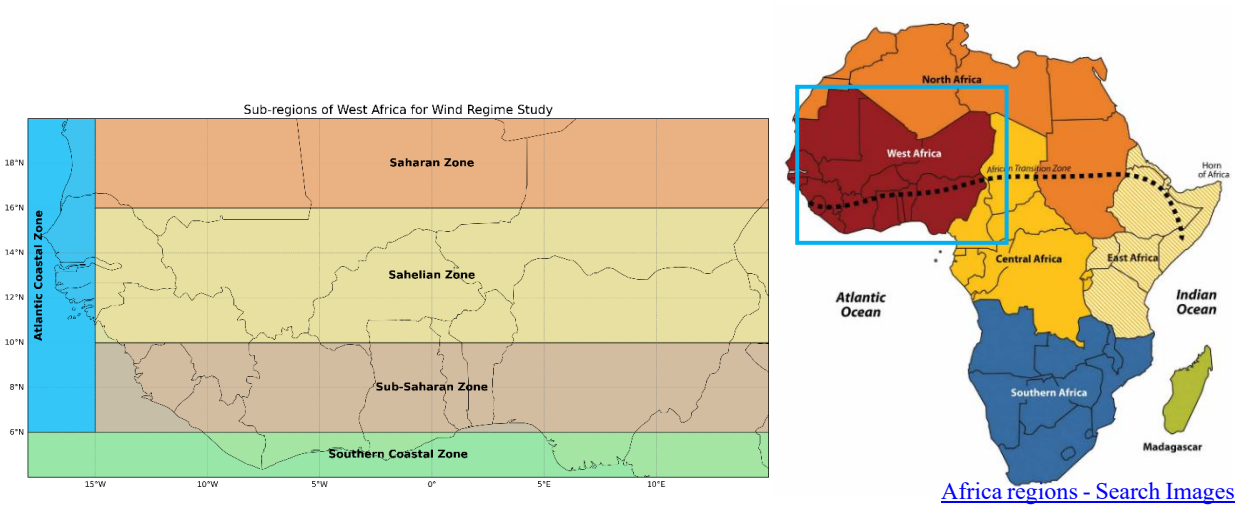

Africa regions - Search Images

Figure 1: Study area with the five climatic zones (Atlantic coastal, Southern coastal, sub-Sahara, Sahel, Sahara) and the topography in West Africa (left) and regional map of Africa (right).

2.2 Data

This study employs a combination of reanalysis datasets, climate model simulations outputs, and large-scale climate indices to evaluate past-to-resent, and future wind regimes over West Africa. The reanalysis dataset is used to characterise past and current wind climatology, climate model outputs are used for historical and to project future wind patterns, and the AMO index is analysed to investigate possible teleconnections with wind variability in the region.

2.2.1 ERA5

The European Centre for Medium-Range Weather Forecasts (ECMWF) produces ERA5, the fifth generation of atmospheric reanalysis, as part of the Copernicus Climate Change Service (Hersbach et al., 2020a; Poli et al., 2016). It succeeds its predecessor, ERA-Interim (Dee et al., 2011), with significant improvements in geographical resolution, temporal frequency, data assimilation methodologies. It also adds new observational datasets.

This dataset provides a physically consistent global climate record from 1940 to the present, featuring hourly temporal resolution and a horizontal grid spacing of approximately 31 kilometres (0.25° × 0.25°). The data span 137 mixed sigma-pressure vertical layers extending from the surface to 1 hPa (approximately 80 kilometres altitude). This dataset is generated from the Integrated Forecasting System (IFS) run 41r2, using a four-dimensional variational (4D-Var) data assimilation scheme. Data assimilation is achieved through optimised fusion of short-term forecasts with an extensive assimilated observational data.

These observations include in situ measurements from ships, buoys, radiosondes, and aircraft, as well as satellite-based instruments such as QuikSCAT, ERS-1, ERS-2, and SSM/I. All these improvements is crucial for building confidence in their application on various cliamate variables as confirmed in the study of (Gbode et al., 2023). However, although this dataset dates back to 1940, it should be noted that prior to the satellite observation era (approximately before 1970), the constraints on reanalyzed data were not yet fully established. Therefore, caution is warranted when interpreting trends from earlier periods.

Reanalyses are in fact hybrid products that combine a so-called frozen state-of-the-art numerical model with the assimilation of past observations from several sources (Fujiwara et al., 2017) to generate uniform in time and space datasets of multidecadal (e.g., ERA5;(Hersbach et al., 2020a) and even centennial (Compo et al., 2011) length. The assimilation of observations drives the model close to the actual variability of the variable of interest (Dee et al., 2011). In the case of wind-related variables, this enables producing wind resource, typically after downscaling the large-scale information to regional or local-scale products through using meso- and micro-scale models (Hahmann et al., 2020; Rohrig et al., 2019), or directly using regional reanalyses. Reanalysis products provide large inter-model consistency and virtually an observational quality in areas of larger observational density and still offer useful information as a means of physical interpolation in areas of data scarcity (Hersbach et al., 2020b; Ramon et al., 2019).

In this study, 10 m and 100 m (zonal (u) and meridional (v)) wind components were retrieved from ERA5, monthly means (by hour of day on single levels) to evaluate past -to-current wind climatology over West Africa for respective periods 1950-2024 (10-m) and 1980-2024 (100-m). This reanalysis data also served as a benchmarch for model performance evaluation.

2.2.2 CMIP6 Data

Future wind projections are derived from the sixth phase of the Coupled Model Intercomparison Project (Eyring et al., 2016), European Centre for Medium-Range Weather Forecasts (ECMWF), which represents the most recent coordinated ensemble of global climate model (GCM) simulations for climate change assessment. CMIP6 improves upon CMIP5 (Taylor et al., 2012) through enhanced model physics, higher spatial resolution, refined aerosol–cloud interaction schemes and updated forcing datasets. The projections used in this study are part of the Scenario MIP experiment (O'Neill et al., 2016), which employs Shared Socioeconomic Pathways (SSPs) to explore different potential greenhouse gas emission trajectories. Two scenarios are considered: SSP2-4.5, representing a medium stabilisation pathway, and SSP5-8.5, representing a high-emissions pathway.

For this study four CMIP6 global models (Table 1) were particularly selected based on data availability, horizontal resolution, and prior evaluation of their ability to simulate African climate variability (Almazroui et al., 2020; Monerie et al., 2020; Spinoni et al., 2020). For each model, near-surface wind speed data were directly extracted at daily resolution for both the historical period (1950–2014), and future projections (2025–2075). Historical simulations are forced with observed atmospheric composition, including greenhouse gases, aerosols, and solar variability, while future simulations are driven by the SSP-specific forcings.

The estimation of the future wind regime were done using historical simulations (1950-2014) and future scenarios derived from the CMIP6 ensemble (2025-2075). The MPI-ESM model was the one selected for future assessment among the four models considered in the study.

This is because of its higher spatial resolution and superior performance during the statistical assessment phase. Projections were performed using two separate shared socioeconomic pathways (SSPs). The moderate scenario (SSP2-4.5) and a worst case scenario (SSP5-8.5). This permiited to determine the possible effects of climate change on regional wind regimes.

To ensure comparability with ERA5, all 4 CMIP6 model outputs (for the historical projections) were harmonized and regridded to a common 0.25° × 0.25° spatial resolution using bilinear interpolation, and the same West African spatial domain was applied. Models are described in the table below (table 1).

Table 1 : Overview of the global climate models used in this study, including information on the name, the available scenarios and times

N	MODEL NAME	INSTITUE OR MEDELLING CENTER	RESOLUTION Long X Lat	PERIOD	REFERENCE
1	**MIROC6**	Japan Agency for Marine Earth Science and Technology (JAMSTEC), The University of Tokyo, Japan	**256 × 128**	Historical (1950-2014)	(Ando et al., 2021; Nooni et al., 2023a)
2	**MPI-ESM1-2-HR High Resolution**	Max Planck Institute for Meteorology, Germany	**384 × 192**	Historical (1950-2014)	(Nooni et al., 2023a)
	MPI-ESM1-2-LR Low Resolution	Max Planck Institute for Meteorology, Germany	**192 × 96**	Projections (2025-2075)	(Nooni et al., 2023a)
3	**HadGEM3-GC3.1-MM**	Met Office Hadley Centre, United Kingdom	**432 × 324**	Historical (1950-2014)	(Nooni et al., 2023b; Zhao et al., 2021)
4	**CESM2-WACCM**	National Center for Atmospheric Research, USA	**288 × 192**	Historical (1950-2014)	(Zhao et al., 2021)

2.2.3 Atlantic Multidecadal Oscillation (AMO) Index

To investigate the possible mechanisms of large-scale climate variability on West African wind regimes, the Atlantic Multidecadal Oscillation (AMO) index was included in the analysis. The AMO is a long-term fluctuation in North Atlantic Sea surface temperatures (SSTs) with a typical cycle of 60–80 years, known to influence atmospheric circulation patterns and climate over West Africa, including the West African Monsoon system (Knight et al., 2006b; R. Zhang & Delworth, 2006). The monthly AMO index used in this study is obtained from the National Oceanic and Atmospheric Administration (NOAA) Earth System Research Laboratory (ESRL), calculated as area-averaged SST anomalies over the North Atlantic basin (0°–70°N, 75°W–7.5°W) following the methodology of Enfield et al. (2001). The index is provided as a time series from 1948 to the present adapted to our study period (1950-2024), which allows for correlation and composite analyses with the ERA5 reanalysis to assess possible teleconnection influences on wind variability across West Africa. Furthermore, in the case of our study monthly AMO index was processed to annual index to evaluate the possible long-term connections with surface wind anomalies.

2.3 Methods

The method used in this study can be conceptualized by the following flowchart

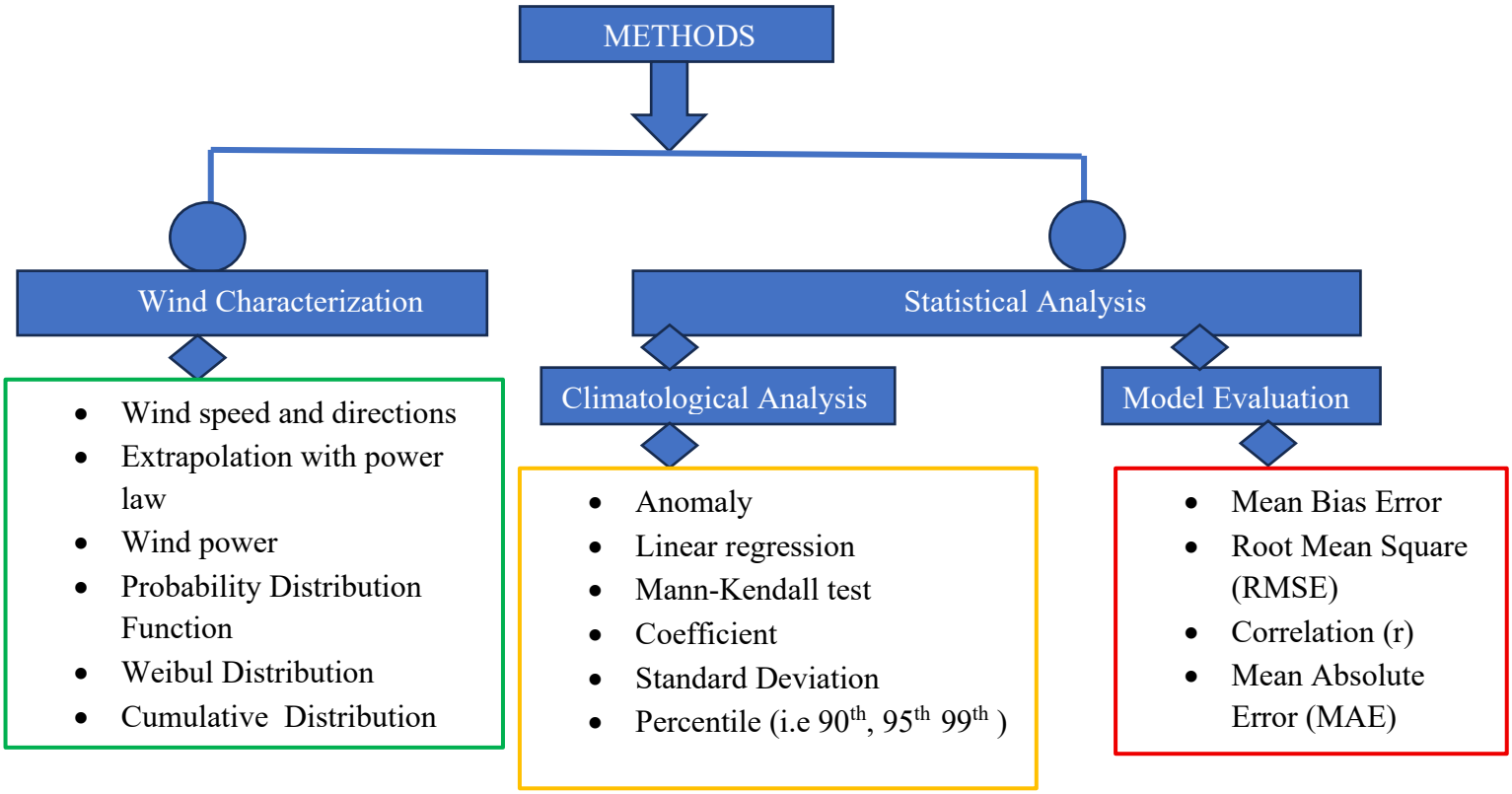

Figure 2: Method flowcharts

2.3.1 Wind characterization

To characterize the wind resources in West Africa, near-surface wind speed was derived from zonal (u) and meridional (v) components of wind from the ERA5 reanalysis. These components allowed us to determine the resultant wind speed (v) as well as its direction (θ) at each point on the spatial grid. The wind speed was then calculated using:

$$U = \sqrt{u^2 + v^2} \qquad \text{Equation (1)}$$

where u and v are the zonal and meridional wind components, respectively (Atsu et al., 1976; Niang et al., 2024b)

Wind direction is also an important aspect affecting the wind energy when evaluating wind characteristics in a certain area. Gugliani et al. (2018) contended that analyzing wind power at a specific location without considering wind direction yields inconclusive results, making such evaluations ineffective. Han & Chu (2021) also emphasized that the available wind resources change with the wind direction, especially in the low-speed and complex terrain areas.

Thereby, wind direction was determined from the same (u10 and v10) and (u100 and v100) components, allowing the orientation of airflow to be visualized. Wind roses were produced to summarize the frequency distribution of wind directions and highlight dominant flow regimes in each climatic zone. This was complemented by vector field plots (see figure A5 in appendices) to illustrate seasonal circulation patterns associated with the West African Monsoon and Harmattan winds. The wind direction was then computed as follow:

$$\theta = 180/\pi \; mod(\pi + \tan^{-1}(u, v) + 2\pi) \qquad \text{Equation (2)}$$

where u and v are horizontal wind components and θ is the resolved wind direction in degrees. The wind direction is expressed in meteorological convention indicating the direction 'from' which the wind blows. These are standard formulations used in wind climatology studies. (Atsu et al., 1976; Niang et al., 2024b).

The near-surface wind speed can be also extrapolated to the turbine hub height (100 m) above ground level using the power-law relationship (Abolude et al., 2020; Hueging et al., 2013) as shown in Eq. (3). While extrapolating wind speeds above 100 m with this approach can result in underestimations in stable atmospheric conditions and overestimations in unstable conditions, it is widely regarded as a reliable method to approximate wind speed at hub heights (Aririguzo & Ekwe, 2019):

$$\frac{U(z)}{U(z_r)} = (\frac{z}{z_r})^{\alpha} \qquad \text{Equation (3)}$$

where U(z) is the wind speed at height z (such as hub height), U(z_r) is the wind speed at the reference height z_r (commonly 10 m), and α is the empirically determined power-law exponent. The value of α varies with elevation, wind speed, vegetation cover, temperature, etc. (Kikumoto et al., 2017)

Usually, the value of α is higher (lower) in a stably stratified (unstable) atmosphere and/or high (low) surface roughness (Jung & Schindler, 2021). In this study, we have taken the power exponent as 0.14 following the one-seventh factor of land representation (Storm et al., 2009). The varying value of alpha is day time or night time wind speed is not considered as mean daily wind speed is used, hence reducing the biasness towards atmospheric stability.

In wind studies, one of the parameters is key to know is the wind power density (WPD; unit: W/m2) since wind power in a wind flow is directly proportional to the cube of the wind speed (Sawadogo et al., 2019a), it is expressed as follow:

$\text{WPD} = \frac{1}{2}\rho V^3$ Equation (4), where ρ is the air density (usually about 1.225 kg/m^3) (Aririguzo & Ekwe, 2019; Jabbar, 2021).

Equation (4) is used to assess wind energy resource over the study area. WPD indicates also how much energy is available at the site for conversion by a wind turbine (Sawadogo et al., 2019a; Tushar K. Ghosh and Mark A. Prelas, 2011).

Although this evaluation is not performed here, we mention it because it provides useful context for interpreting later results.

Weibull distribution function, the most used probability density function (PDF) for wind speed distribution because of its adaptability in expressing a broad spectrum of wind conditions (Abbas et al., 2025; Burton, 2011; Ouammi et al., 2010; Wang & Liu, 2021), was used to characterise wind over the West African region. The Weibull PDF (Eq.5) and cumulative distribution fonction CDF (Eq.6) is expressed mathematically as foollow:

$$f(v_m) = \left(\frac{v_m}{c}\right)^{\kappa-1} exp\left[\left(-\frac{v_m}{t}\right)^{k}\right] \quad v_m > 0,\ c,\ \alpha > 0 \quad \text{Equation (5)}$$

$$F(v_m, c, \alpha) = 1 - e^{(\frac{v_m}{k})^c} \qquad v_m > 0,\ c,\ \alpha > 0 \quad \text{Equation (6)}$$

where f(v_m) is the probability of the measured wind speed v_m, k is the Weibull shape parameter (dimensionless) and c is the Weibull scale parameter (m/s). k and c are defined as:

k = $(\frac{\sigma}{vm})^{-1.086}$

$c = \frac{v_m}{\Gamma\left(1+\frac{1}{k}\right)}$, where v_m is the mean wind speed, σ is the standard deviation and Γ is the gamma function (Aririguzo & Ekwe, 2019). The scale parameter k indicates the average wind speed, the shape parameter c higher controls the wind speed variability. A lower c indicates more wind variability and a higher c signifies more stable wind speeds. Since this distribution may define a large variety of wind regimes depending on c, it is flexible enough to be used with wind speed data. (See figure A1 in appendices)

2.3.2 Statistical analysis

All analyses in this study were performed rigorously in Python, which provided a flexible environment for data processing and visualization. The main libraries included xarray and pandas for data handling, NumPy for numerical computations, matplotlib and seaborn for visualization, and scipy for statistical tests and regressions.

The statistical analysis was systematically designed to assess the variability, reliability, and future evolution of wind regimes across West Africa in a comprehensive manner. First, diagnostic and climatological analyses were conducted at different temporal scales (monthly, seasonal, and annual) and across the five climatic sub-regions. To conduct variability, standard descriptive statistics such as the mean, standard deviation, and percentiles were employed, while anomalies were calculated relative to a climatological baseline in order to highlight deviations from long-term averages.

To further characterize the the variability across space and time, the coefficient of variation (Molina et al., 2021) was computed, enabling comparisons between regions with different wind speed magnitudes. In addition, extreme events were identified based on percentile thresholds (90th, 95th, and 99th), (IPCC, 2021), which allowed us to distinguish between moderate, extreme, and severe wind episodes. For each category, the duration of events was determined by tracking consecutive time steps exceeding the threshold, while the number of occurrences was obtained from event counts, and the longest episodes were identified as the maximum length of consecutive exceedances. Long-term changes in these metrics were assessed through trend analysis using robust non-parametric methods, specifically the Mann–Kendall test for

statistical significance and Sen's slope estimator for trend magnitude (Aksay et al., 2025; Jurasz et al., 2021; Natarajan et al., 2020).

Following this, model evaluation was carried out to assess the skill of four CMIP6 climate models namely, MIROC6, MPI-ESM, HadGEM3, and CESM-WACCM against the ERA5 reanalysis. Several statistical skill metrics were applied, each providing a complemantary perspective. The root mean square error (RMSE) quantified the average magnitude of model errors relative to observations (Wang & Liu, 2021), while the mean absolute error (MAE) (Piotrowski et al., 2022) measured overall deviations without exaggerating outliers, mean Bias (Babaousmail et al., 2021) were calculated. Correlation coefficients (Piotrowski et al., 2022; Wang & Liu, 2021) were calculated to capture temporal agreement between simulated and observed series. In addition, a radar chart (figure A17 in appendice section) and heatmap was designed employed to provide a visual synthesis of multiple model performance metrics simultaneously, enabling easier comparison across models.Based on these diagnostics, a performance ranking was established so as to identify the model best suited for reproducing historical wind climatology.

The methodogy flow described above is the pathway to abtain the results presented in the next chapter. It combined data and the methods employed for the analysis of the climatology related to wind and also the evalution of models for future projections.

CHAPTER III: RESULTS AND DISCUSSIONS

CHAPTER 3 : RESULTS AND DISCUSSIONS

This chapter presents the results of wind climatology and variability analysis for West Africa, aiming to examine both historical trends and future projections. First, it describes the distribution characteristics (see annex figure A1) of wind speed and direction, covering anomalies, seasonal cycles, and long-term spatial patterns. Subsequently, it analyzes interannual variability and extreme wind events across five major subregions, and explore explore the influence potential drivers such as the Atlantic Multidecadal Oscillation (AMO) on wind speed varitions. Finally, the report presents future wind speed projections under the medium emissions scenario (SSP2-4.5) and high emissions scenario (SSP5-8.5), highlighting regional and seasonal variation patterns. Through a comprehensive analysis of these findings, the report underscores their significant implications for West Africa's renewable energy potential and strategic planning.

3.1 Wind climatology over west africa

3.1.1 Wind speed distribution across West Africa

This analysis is based on data from the ERA5 reanalysis covering the period of 1950 to 2024. It reveals the spatial structure of West Africa's wind regimes at both 10 m (Figure 1a and b) and 100 m**,** providing an overview of the region's wind potential. At 10 m, the long-term climatology shows a pronounced gradient between the coast and inland. As a matter of fact, the Atlantic coastal zone (Mauritania, Senegal) consistently has the strongest winds, with averages above 3 m/s, while most of the Sahelian, sub-Saharan and southern inland coastal zones remain in the low wind category (1-4 m/s). Extrapolated to a hub height of 100 m, the spatial distribution of ressource potential remains similar, but absolute wind speeds increase in all regions due to reduced surface friction and the increased influence of free atmospheric flow at altittude.

This verticall amplification is particularly important in moderately windy areas, where mean speeds at 10 m of around 3-4 m/s can translate into speeds at 100 m approaching or exceeding the thresholds for viable wind energy (>5 m/s). The persistence of the coastal and Saharan fringes as the windiest areas aligns with the influence of marine inflow, subtropical anticyclones and seasonal Harmattan flows, while the relative weakness inland reflects seasonal monsoon stagnation, vegetation drag and continental thermal contrasts. This is clearly consistent with previous assessments (Davis et al., 2023; Otunla & Umoren, 2022; Sedzro et al., 2022) indicating that strategic wind energy development should prioritise the Atlantic coastal belt and some Saharan margins, while marginal inland areas require detailed hub height

profiling prior to investment. Ultimately, the combined 10m-100m perspective highlights the need for multi-level wind assesssments to capture the vertical structure of the wind, reduce uncertainty and optimise site selection for renewable energy expansion in West Africa

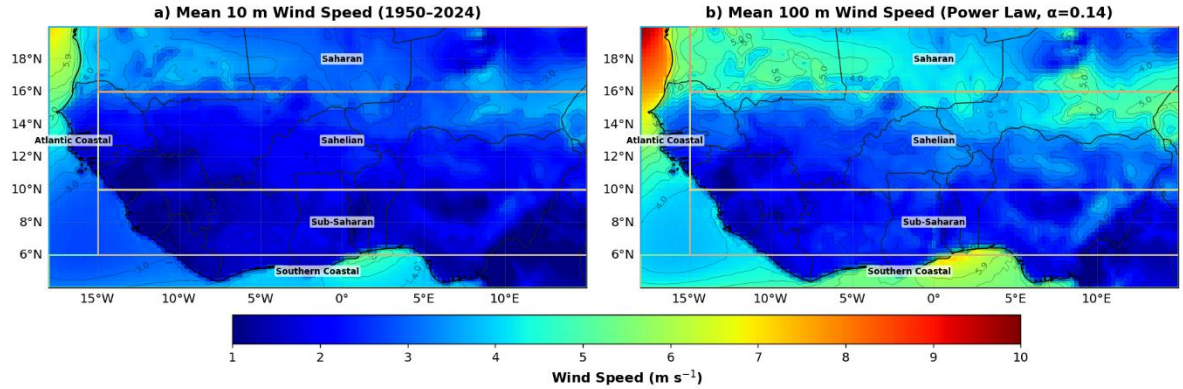

Figure 3: Mean annual wind speeds over West Africa (4-20N, 18W-15E) from 1950–2024 using ERA5 reanalysis at 10 m from ground (top) and extrapolated to 100 meters hub height (bottom).

3.1.2.Wind directions considering per sub-region-Wind rose (100m)

The figure 4 presents presents wind roses at 100 m for the five west-African sub-regions. All the five wind rose panels quantify the directional persistence and wind speed distribution at 100 m in the main sub-regions of West Africa, providing a detailed spatial characterisation of the regional wind climate. As predicted by the West African monsoon-harmattan regime, coastal and humid areas are mainly influenced by south-westerly winds, while the Sahel and Sahara regions are controlled by north-easterly trade winds.

Firstly, the Southern Coastal and the Sub-Saharan areas show strong SW-WSW flows (around 210-250°), with most wind occurrences in the 2-8 m/s range and relatively low calm frequencies (around 2-3%). This pattern corresponds well with marine inflow during the monsoon season and suggests the presence of moderate and relatively regular winds suitable for Class III onshore turbines, particularly in coastal areas where surface roughness is low.

As far as the Sahelian region is concerned we two directions NE and ENE winds (around 30-70°) which are the most dominant and having higher speeds. Also the most occurring wind speeds are in between 6 and 10 m/s. A seasonal alternation between the Harmattan and the monsoon is preceeded by the weaker SW branch that is continuously present.

Moreover, winds in the Saharan region are focused in a narrow north-eastern sector, with considerable contributions in the 8-12 m/s speed class and the lowest percentages of quiet

(about 1-1.5%). This high directional persistence and wind speed implies a significant potential for wind resources.

Finally, the Atlantic coastal zone shows a more diffuse wind pattern, with lower frequencies per sector and wind speeds mainly below 8 m/s, which highlights the heterogeneous exposure of the coastline and the greater diurnal variability of the sea breeze. From the point of view of the energy system, these spatial contrasts offer a number of advantages. In particular, the north-east-dominated Sahel and Sahara regions and the south-west-dominated coastal and sub-Saharan regions are seasonally out of phase, meaning that geographical diversification, combined with north-south grid interconnection, could effectively reduce overall portfolio variability. In addition, the pronounced directional persistence in the Sahel and Sahara regions provides crucial guidance for the micro-selection of wind farms, which means turbine arrays should be oriented with their long axes approximately orthogonal to prevailing wind directions in order to minimise wake losses, while more isotropic arrangements may be more appropriate for coastal sites with less directional coherence. Given that most winds are below 12m/s, turbine selection should favour low to moderate wind speed designs, with robust dust protection inland and corrosion protection in coastal environments.

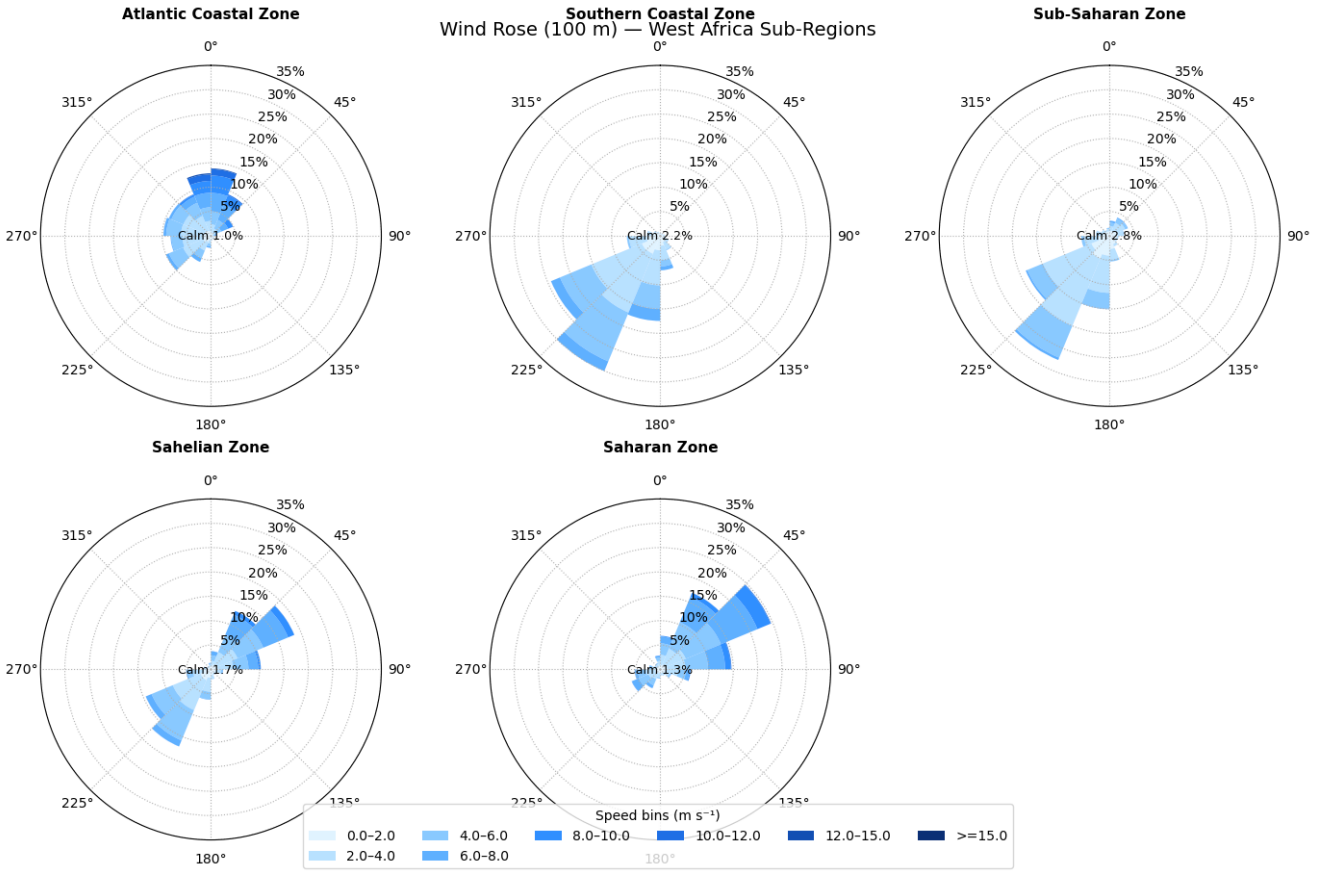

Figure 4:Wind roses at 100-m wind direction and speed for West Africa subregions over the period 1980-2024

3.2. Wind speed anomalies

The figure below informs aboutb the long tern variability of ERA5 10-m wind speed over West Africa for the period 1950-2024. This information is crucial for assessing wether multi-decadal fluctuations could affect climatological baselines and subsequent energy-yield or hazard analyses. Studies as Pryor & Barthelmie (2010) and (Dunn et al., 2016) confirm itt is essential to analyse decadal wind variability for accurate energy resource assessment. The result show negative anomalies over the past years especially form 1950 to around late 1975 and strong positive anomalies over the recent years. This present the spatially averaged interannual anomalies, revealing significant superimposed on weak upward trend. The fited linear trend of about 0.021 m/s per decade indicating a moderate strengthening of wind speeds trend during the study period. This pattern aligns with the global decadal wind speed trend documented by Mcvicar et al. (2012). Troccoli et al. (2012) , and Azorin-Molina et al. (2017) similarly observed wind speed recoveries in various regions following earlier declines, supporting the interpretation of the positive multidecadal signal abserved in this study. These studies reinforce conclsuions that, despite the dominance of short term variability , near-surface wind speeds increasing have shown a subtle yet consistent increasing trend since the 20th century.

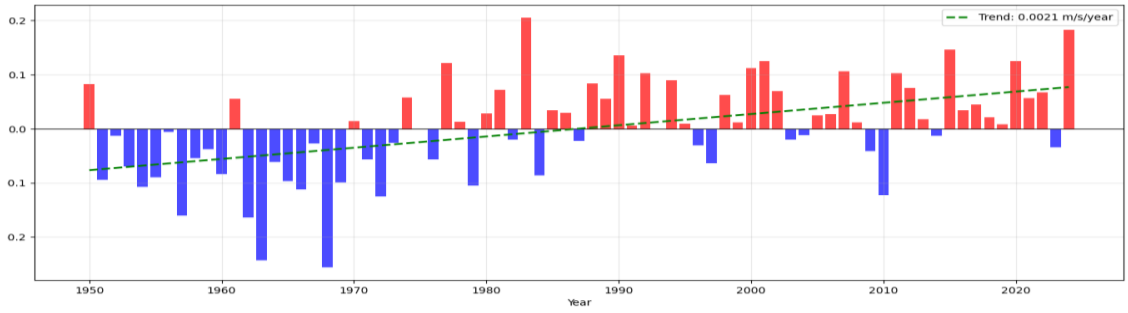

Figure 5: Wind speed anomlies and trend from 1950-2024 over West Africa

3.3. Wind speed variability and trend analysis

The figure below offers a compariative overview of surface wind regimes across the five West African sub-regions, revealing a clear coastal-to-inland gradient in mean wind speeds. The Atlantic coastal region (approximately 3.6 m/s) and the Sahara region (approximately 3.0 m/s) have higher average wind speeds than the southern coastal zone (around 2.6 m/s), the Sahel region (approximately 2.3 m/s), and the sub-Saharan region (around 1.6 m/s). However, the variability which is measured by the coefficient of variation (CV) increases with distance inland rising from approximately 20% along the Atlantic coast to about 32% in the Sahel and

Sahara regions.This indicates that areas with the highest average wind speeds do not necessarily offer the most stable operating conditions. All the regions have a weak but positive linear trend, with the Sahel (approximately $+3.1\times10^{-3}$ m/s/year) and Sahara (approximately $+2.9\times10^{-3}$ m/s/year) showing the greatest increases. Although these trends are limited in magnitude, their cumulative effect could reach approximately 0.3 m/s per century, holding significant implications for long-term resource planning.

These results have several implications for wind energy development and planning. Firstly, coastal and Saharan regions present the most promising sites for wind power projects, though strategies must be devised to address the high coefficient of variation (up to 30%) in inland areas. Detailed statistics and individual sub-regional insights are gathered in the appendice section, see tables A1, A2 , figures A11-A15. Secondly, the southern coastal zone offers advantages for hybrid development with solar energy, as its peak wind conditions coincide with the JJA months when photovoltaic output typically declines due to cloud cover.

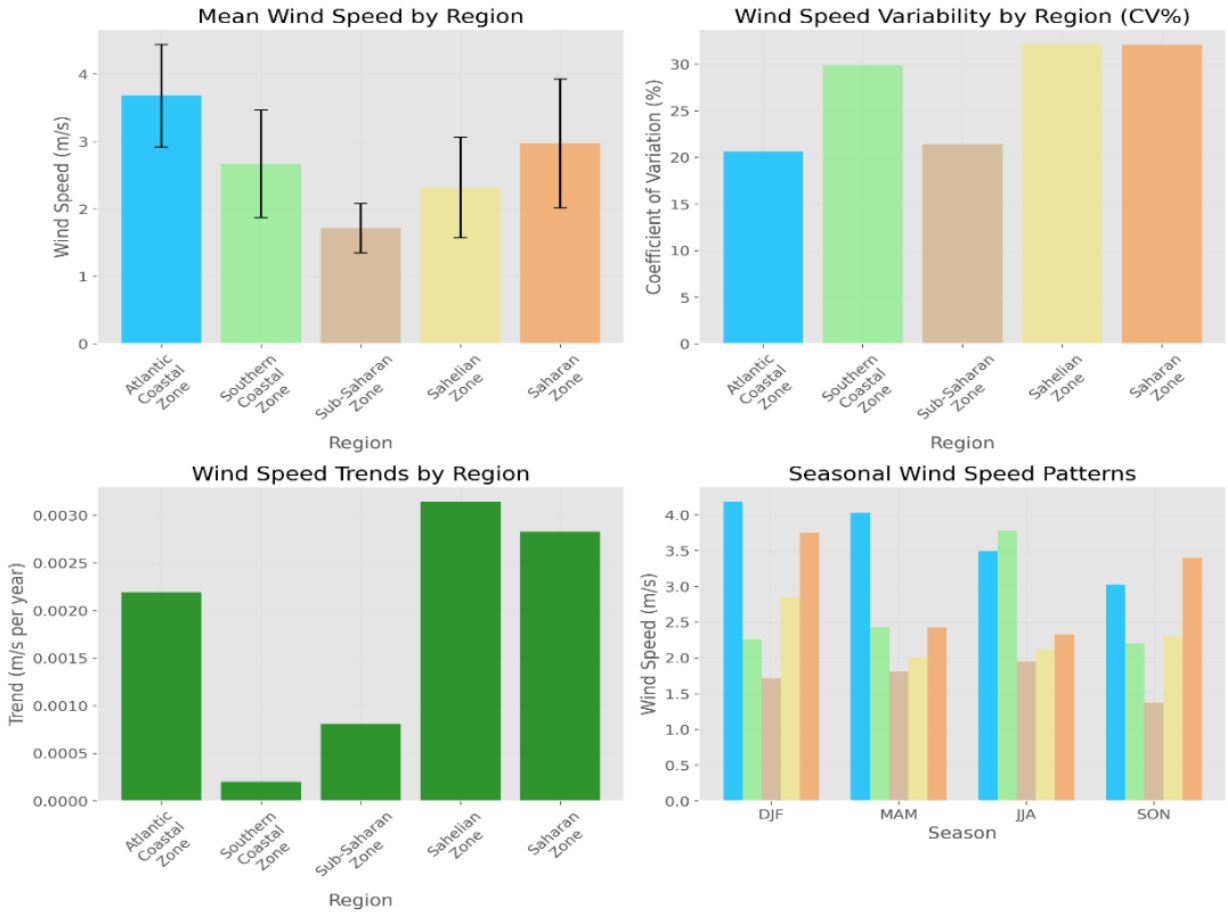

Figure 6: Multipanel barplots summarizing near-surface wind statistics across five West African sub-regions (Atlantic Coastal, Southern Coastal, Sub-Saharan, Sahelian, and Saharan Zones) 1950-2024.

3.4. Extreme wind analysis by region

3.4.1.Atlantic Coastal region

The figure 7 below comprises five panels. Together the panels provide an overview of near-surface extreme winds in the Atlantic coastal zone and their relevance to energy planning. The figure 7 (a) shows significant year-to-year variability in the annual extreme wind counts, using fixed percentile thresholds for the entire record (90^{th}: 4.64 m/s, 95^{th}: 4.85 m/s, 99^{th}: 5.16 m/s). The years with increased activity at the 95^{th} percentile are scattered throughout the time series, punctuated by calmer periods, but there is no clear upward or downward trend, indicating that synoptic-scale variability remains the dominant influence in driving extremes rather than long-term changes.

The figures 8 (b) and 8 (e), which show the monthly climatology and the thermal map of the year during the season, highlight strong and operationally significant seasonality. Detailed information about the occurrence of extremes in this region are gathered in the table A4 in the appendice section.

The figure 8 (c) investigates the persistence of extreme winds. It indicates that most events are brief or transient.

The extreme median lasts 5 hours, the mean is 5.8 hours, and the duration distribution shows a long upper tail which includes some 24-hour breaks, such as the notable episodes of March 1974 and February 2009. The time series with the exceedance values shaded in figure 7 (d), together with the summary statistics (mean 3.68 0.76 m/s, range 1.51-6.08 m/s), clearly show that these extreme winds are episodic peaks defined in generally moderate wind conditions (see tables A1, A2. A4 in appendice section).

The operational implications for the power system are distinct: managing rapid, intra-day changes in wind power will be more important than concerns about the survivability of structures. The greatest challenges come from short periods of rapid generation increase or potential reduction, particularly during the MAM and DJF peak seasons, as 95^{th}-99^{th} percentile winds (around 4.9-5.2 m/s) are well below turbine cut-off speeds. To remedy this, flexibility resources (such as storage or reserves) designed for durations of 4 to 6 hours are well suited to the typical duration of episodes. It is advisable to give priority to the programming and pre-positioning of resources according to the forecasts for late winter and spring, and to concentrate maintenance activities in the SON when the risk of extreme winds is practically non-existent or, incidentally, in the JJA.

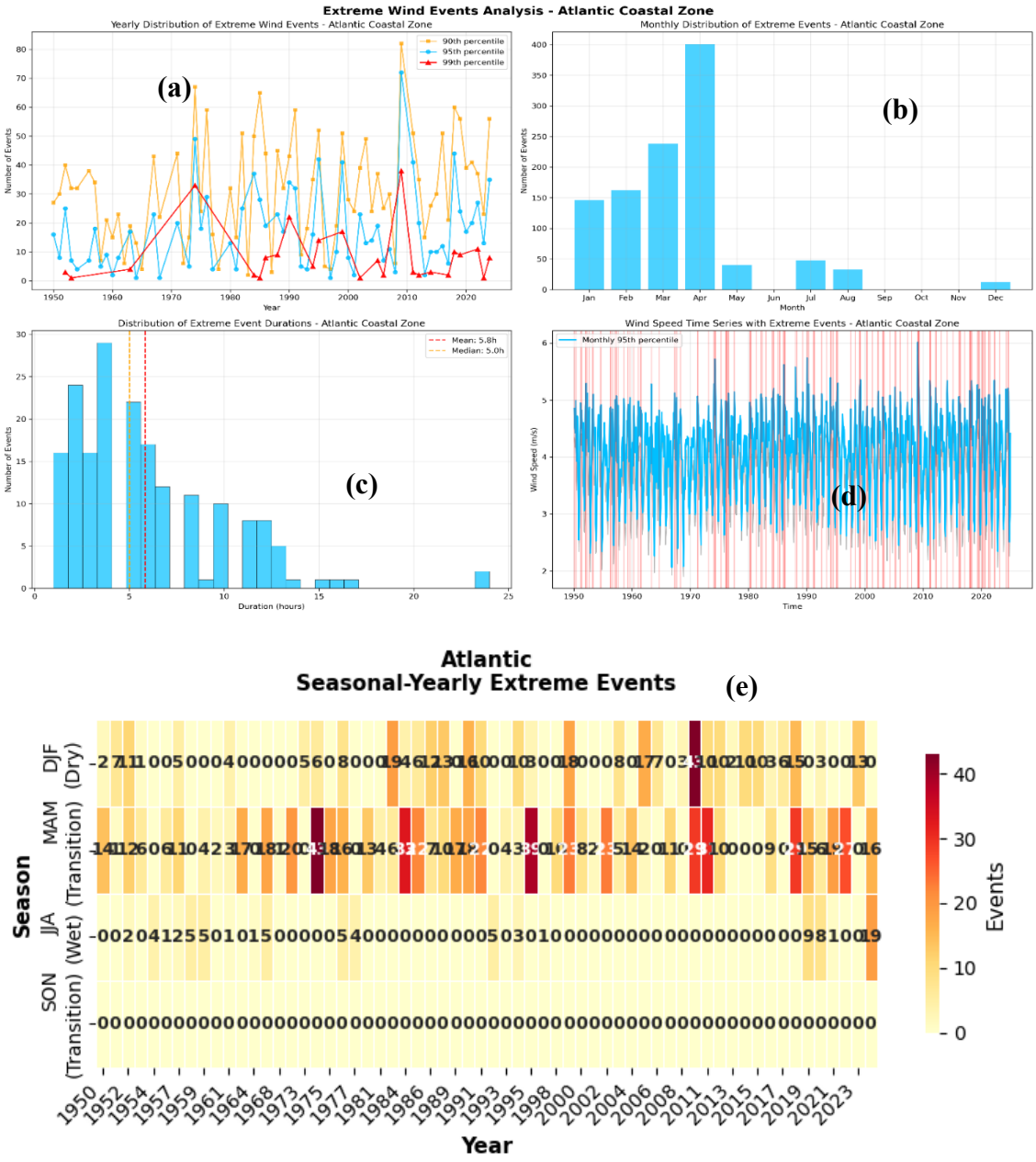

Figure 7: Multi-panel summary of Atlantic Coastal Zone extreme wind events, 1950–2024 (hourly data). (a) Annual counts above the 90th, 95th, and 99th percentiles; (b) monthly counts; (c) histogram of event durations (hours); (d) wind-speed time series with hours above the monthly 95th percentile shaded; (e) season–year heat map (DJF, MAM, JJA, SON).

3.4.2.Sub-Saharan region

The figure 8 below provides a comprehensive assessment of sub-Saharan extreme winds over the period 1950–2024, covering 21,600 hourly observations with an average wind speed of 1.71 0.37 m/s and using 90th, 95th and 99th percentile thresholds at 2.19, 2.34 and 2.67 m/s, respectively. The figure 8 (a) shows the annual wind counts exceeding these percentiles, revealing pronounced multi-decadal variability: early periods and years post 2010 have higher

extreme frequencies, while a relative lull extends from the 1970s to the 1990s. This pattern suggests variability over decades rather than a clear long-term upward or downward trend.

The figure 8 (b) shows that most 95th percentile winds occur in the middle or late of the boreal summer, with August being the most frequent and having only minor activity in spring, especially between April and June. This distribution aligns with the monsoon dynamics in the region. By supporting this, the figure 8 (e) demonstrates that the rainy season (JJA) accounts for about 82% of all extreme wind episodes, with occasional contributions from MAM, rare events in DJF and little or no activity during SON detail statistics are found in the appendice section (see table A 3). It is also important to keep in mind that this strong seasonal trend remains constant over time, even though the number of events fluctuates from year to year.

The figure 8 (c) characterizes the persistence of these extreme winds, showing that they are generally short-lived, with a median duration of 3 hours and an average of 4.2 hours, although some rare events last up to 22 hours. Notably, the longest episodes occur during JJA, indicating that the rainy season sees not only more frequent extremes but also the most persistent. The the figure 8 (d) contextualizes these extremes, confirming that they occur at relatively modest absolute speeds rarely greater than 3.3 m/s, so that the designation "extreme" is relative to local conditions rather than representing a structural danger for modern wind turbines. The main operational challenge lies in rapid changes of several hours in wind speed rather than concerns about the survival of wind turbines.

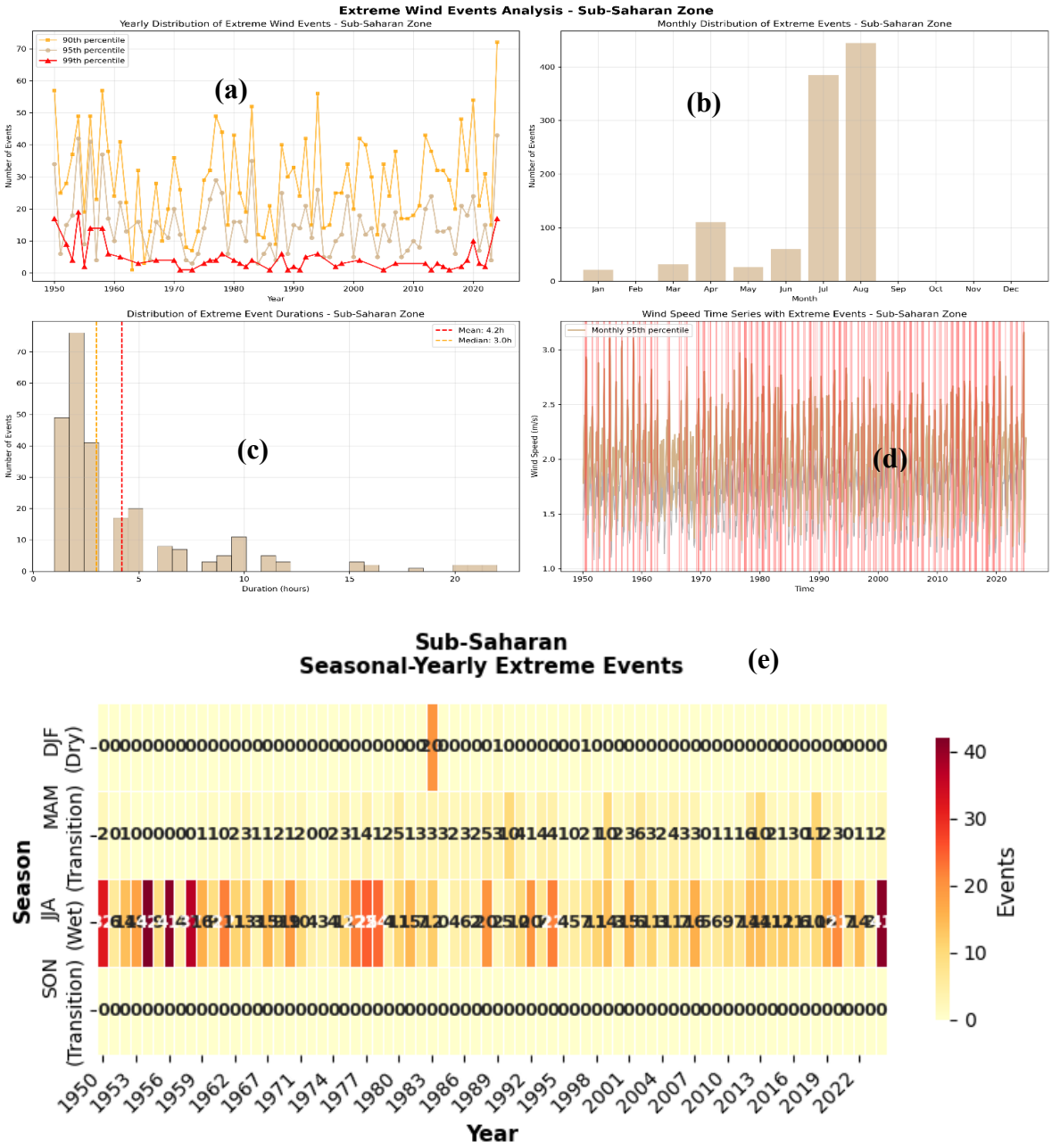

Figure 8: Multi-panel summary of Sub-Saharan extreme wind events, 1950–2024 (hourly data). (a) Annual counts above the 90th, 95th, and 99th percentiles; (b) monthly counts; (c) histogram of event durations (hours); (d) wind-speed time series with hours above the monthly 95th percentile shaded; (e) season–year heat map (DJF, MAM, JJA, SON).

3.4.3.Saharan region

Figure 9 provides a detailed summary of the Saharan extreme winds over 1950–2024, analyzing 21,600 hourly observations with an average wind speed of 2.97± 0.95 m/s and using thresholds of 4.20, 4.54 and 5.25 m/s for the 90th, 95th and 99th percentiles. Figure 9 (a) shows that annual exceedances of these extreme wind thresholds vary considerably from one record to another, with notable gusts in the 1960s-1980s and again after 2010, but without a persistent

long-term trend. Extremely extreme events (99th percentile) remain rare, highlighting the predominance of interannual variability in wind hazard formation.

Figure 9 (b) shows a distinctly seasonal pattern, with extreme winds peaking in January, February and December, and near-absence of events from late spring to summer. This result is reinforced by the heat map of the season–year in figure 9 (e), which reveals a substantial dominance of the dry season (DJF): 83.4% of 95th percentile events occur in winter, while MAM and SON represent only 7,1% and 7.7%, and the JJA is almost absent (1.8%) (see table A5 in appendice for more details).

Besides, active winter extreme weather clusters reappeared in the 1980s-1990s and 2010s, yet their intrinsic seasonal characteristics remained consistent. Figure 9 (c) describes event duration, revealing a right-skewed distribution: most events lasted between 1 and 6 hours (median 4 hours, mean 5.3 hours), though a small number extended up to 24 hours. The three longest-lasting events all occurred during the DJF months. This chart indicates that the dry season not only concentrates the frequency of strong wind events but also their duration.

The figure 9 (d) situates these episodes in the broader annual cycle, indicating that exceedances coincide with periods of high wind speeds up to 6.96 m/s material for power generation but well below turbine cut-off thresholds. Thus, the main operational risk lis not is not structural load, but rather in managing the frequent fluctuations in wind power output over several hours

Based on the above information, energy system planning in the Sahara region should focus on three core strategies: First, allocate resources during the dry season (DJF) when extreme storms occur most frequently and persistently to ensure short-term flexibility and demand response capabilities; Second, schedule maintenance activities during late spring and summer when extreme wind risks are lowest. Third, leverage the seasonal complementarity of hybrid energy portfolios since robust DJF monsoon winds can offset potential declines in solar generation caused by winter dust storms and atmospheric attenuation.

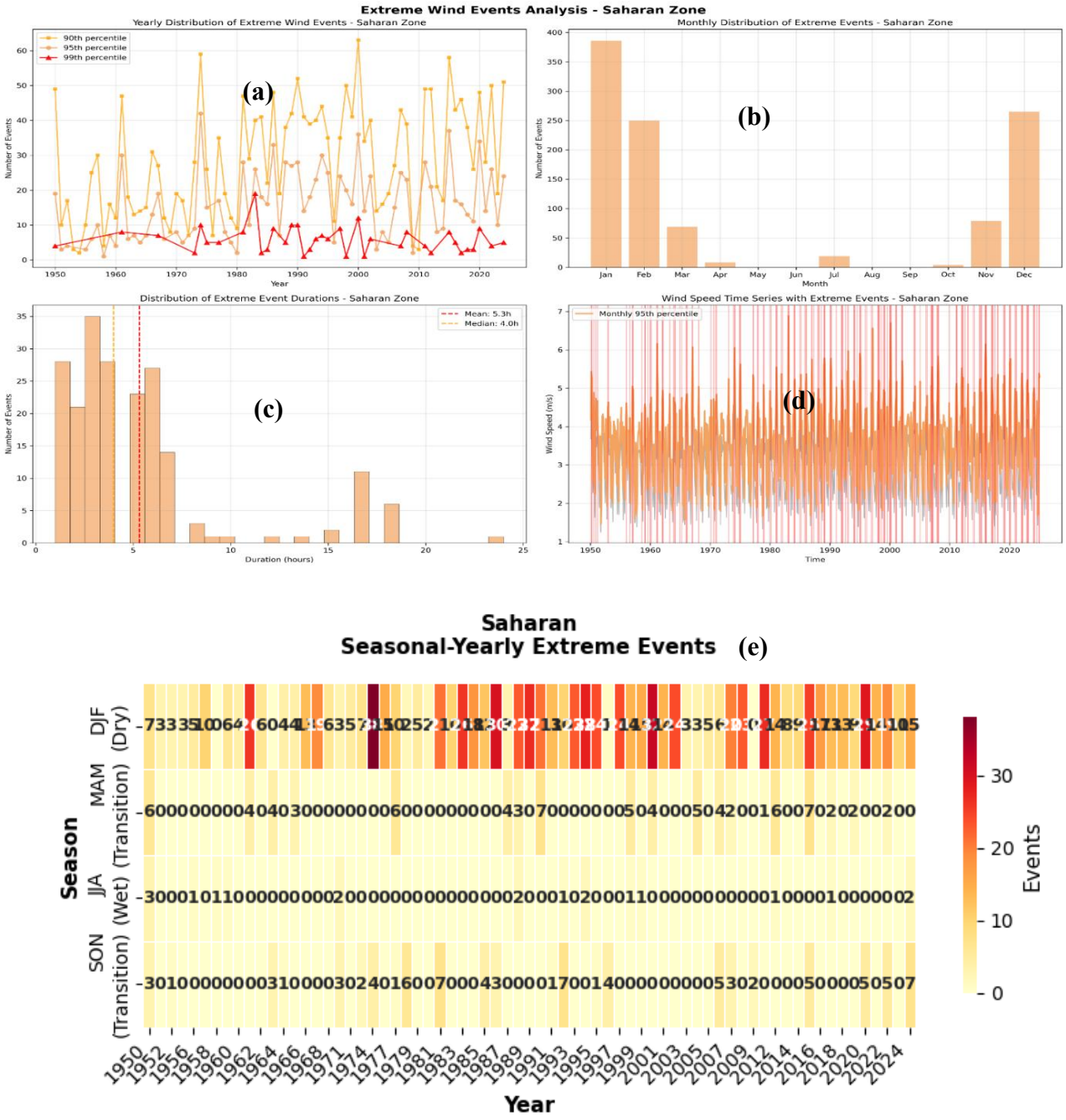

Figure 9:Saharan extreme winds, 1950–2024. (a) Annual counts above the 90th/95th/99th percentiles; (b) monthly counts; (c) event-duration histogram ; (d) wind-speed time series with hours ≥ monthly 95th percentile shaded; (e) season–year heat map (DJF-MAM-JJA-SON).

3.4.4.Sahelian region

The figure 10 presents a multi-faceted assessment of Sahelian extreme winds during 1950–2024, based on 21,600 hourly observations with a mean wind speed of 2.32 ± 0.74 m/s and percentile thresholds at 3.29m/s , 3.60 m/s , and 4.12 m/s for the 90th, 95th, and 99th percentiles, respectively. Figure 10 (a) shows that annual exceedances vary appreciably from year to year,

with moderate extremes (≥90th percentile) becoming more frequent since the 1980s, while severe events (≥99th percentile) remain sporadic.

This pattern indicates that the primary source of risk stems from variability rather than a clear long-term trend.

Figure 10 (b) has a pronounced bimodal seasonal trend. In fact, most extreme events occur during the dry season (December-January-February), with a secondary peak during the early rainy season (June–July). Subsequent months show relatively lower frequencies of extreme events. Figure 10 (e) demonstrates the persistent stability of this seasonal structure: DJF months (January–March) account for 69.4% of events exceeding the ≥95th percentile threshold, JJA months (June–August) for 25.6%, while MAM months (March–May) and SON months (September–November) combined contribute only 5% (see figure A6 in appendice for more details). This clustering of dry-season activity persists over decades with no evidence of shifting climatic patterns.

Figure 10 (c) investigates event duration, revealing that most events are short-lived and densely clustered, with a median duration of 3 hours, an average of 4 hours, and a standard deviation of 2.6 hours. Event durations rarely exceed 18 hours, with the three longest events all occurring between December and February of the following year, indicating that such events are both frequent and persistent during the dry season. Figure 10 (d) places these extremes within a broader time-series context. In fact, exceedance events follow an annual cycle, with wind speeds reaching 5.48 m/s significant for power generation but well below wind turbine cut-out speeds. Thus, the primary operational challenge lies in managing power ramping processes lasting several hours, rather than structural wind loads.

From an energy planning perception, these findings demonstrate that short-term flexibility and demand response are crucial for managing frequent and occasionally prolonged strong wind events during the dry season (DJF). The sub-peak demand in summer (JJA) can be utilized for seasonal diversification, while maintenance tasks should primarily be scheduled between the rainy season (MAM) and winter (SON), especially when the probability of extreme events is lower. Overall, the wind resource pattern depicted in Figure 10 for the Sahel region presents a dry-season-dominated stable system characterized by short-duration, moderate-intensity extreme events. This shows the greater importance of implementing variability management and seasonal portfolio coordination strategies over reinforcing wind-resistant structures.

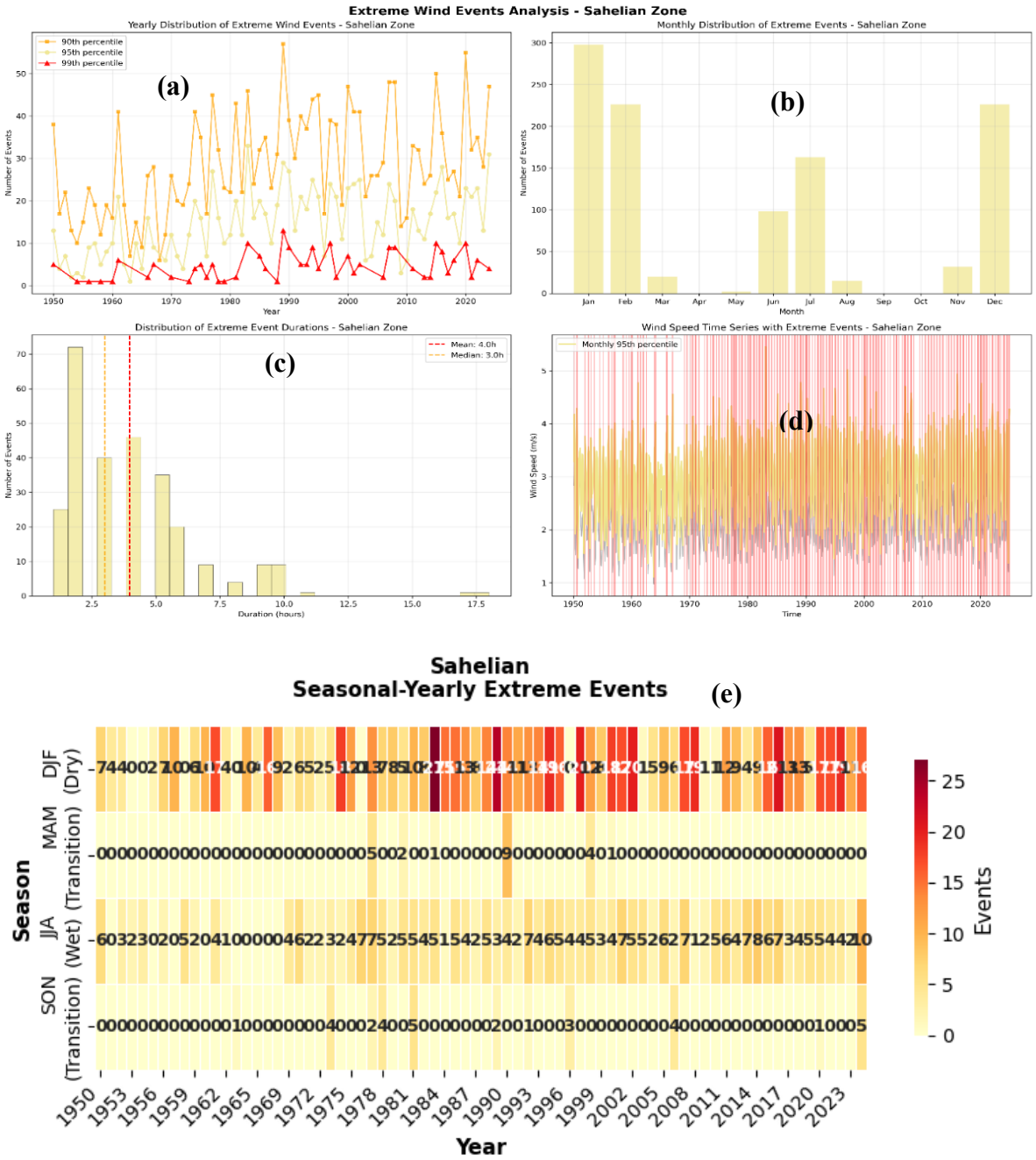

Figure 10:Sahelian extreme winds, 1950–2024. (a) Annual counts above the 90th/95th/99th percentiles; (b) monthly counts; (c) event-duration histogram ; (d) wind-speed time series with hours ≥ monthly 95th percentile shaded; (e) season–year heat map (DJF-MAM-JJA-SON).

3.4.5.Southern coastal region

The figure (Figure 11) integrates five perspectives on Southern Coastal extreme winds over 1950–2024, drawing on 21,600 hourly observations with a mean wind speed of 2.67 ± 0.80 m/s and using 90th, 95th, and 99th percentile thresholds at 3.95 m/s, 4.18 m/s, and 4.52 m/s, respectively. Panel (a) highlights pronounced interannual variability in the annual counts of wind extremes, with higher activity during parts of the 1950s–1970s, a subdued interval around the early 2000s, and a clear rebound in the 2010s–2020s. Still, there is no persistent upward or

downward trend, and severe (≥99th percentile) events remain limited, seldom exceeding a dozen per year.

Figure 11 (b) showss a sharply focused seasonal pattern: nearly all events exceeding the 95th percentile occur in July and August, with peak frequency in August and a secondary maximum in July. June and September contribute only modestly, while the remainder of the year is essentially inactive.

September contributed only a small number of events, while the remaining months were largely inactive. Figure 11 (e) validates this seasonal structure: JJA (June–August) accounted for 95.3% of all extreme events, SON (September–November) for 4.7%, while DJF (December–February) and MAM (March–May) recorded none highlighting a stable monsoon-driven pattern across decades of records

Figure 11 (c) analyzes event duration, revealing a right-skewed distribution: local events persist longer than inland ones with a median of 8 hours, mean of 8.4 hours, standard deviation of approximately 5.7 hours, and maximum duration of 24 hours. Notably, all three longest events occurred during JJA. This indicates that while periods of strong winds occur less frequently, they often have significant persistence when they do occur.

The figure 11 (d) the total sequence of wind speeds. It shows the area of concentration of exceedances, especially around the middle of the year and peak at low wind speeds, below 5 m/s.

From a planning perspective, several implications emerge: First, deploy short-to-medium-term flexible resources (such as 8-24 hour energy storage or demand response) primarily during July-August, when extreme wind conditions are concentrated and persistent. Second, schedule major maintenance between December and May, when strong winds are virtually absent. Third, the complementary nature of wind and solar energy should be actively leveraged since the strongest wind months coincide with monsoon-related cloudy conditions, which helps stabilize power generation output in hybrid systems. More details are grouped in the appendice section (table A7)

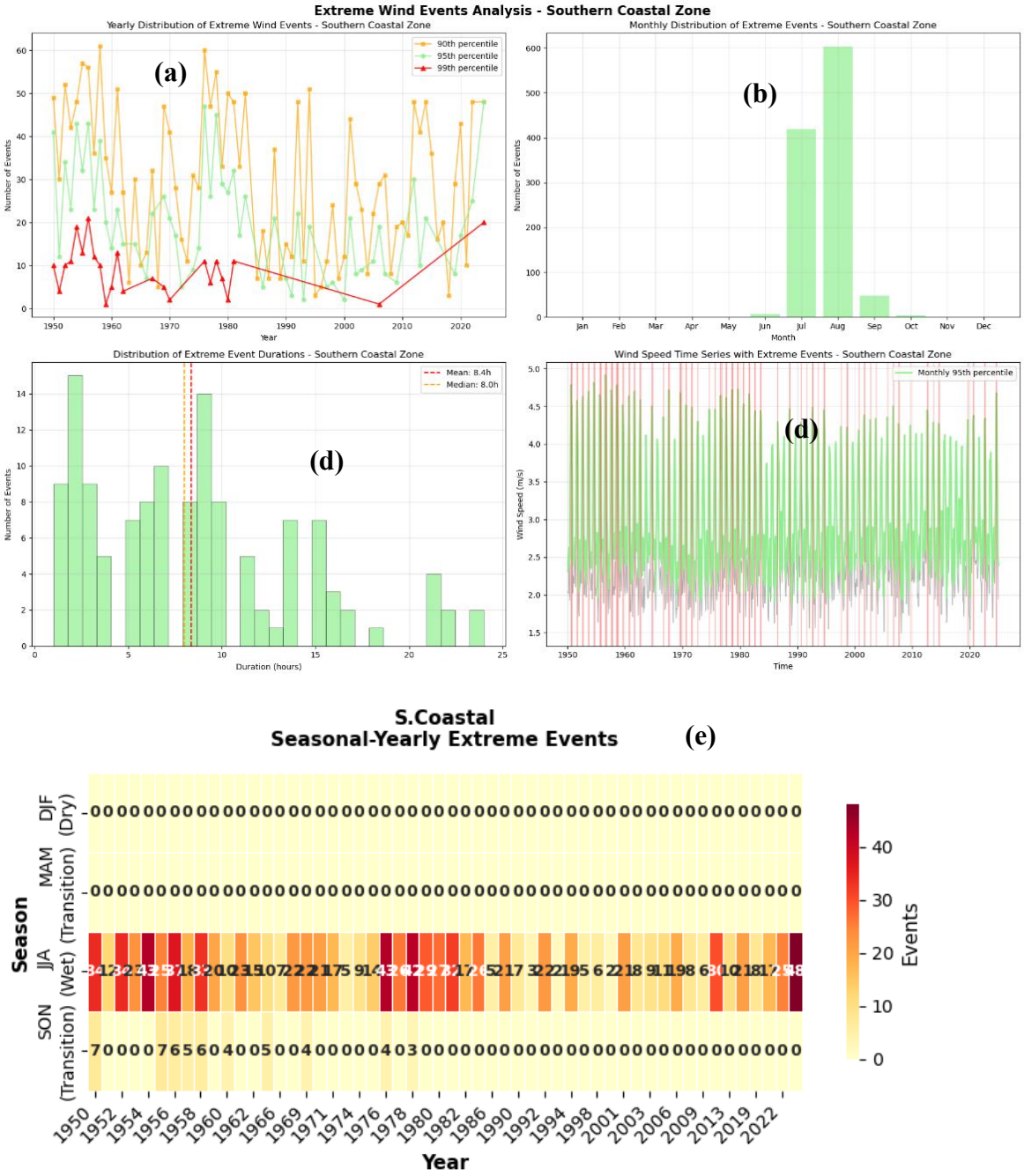

Figure 11: Southern Coastal extreme winds, 1950–2024. (a) Annual counts above the 90th/95th/99th percentiles; (b) monthly counts; (c) event-duration histogram ; (d) wind-speed time series with hours ≥ monthly 95th percentile shaded; (e) season–year heat map (DJF-MAM-JJA-SON).

3.5.Possible mechanism or drivers of the interannual variability

3.5.1.Possible influence of the Atlantic Multidecadal Oscillation (AMO) on the wind speed multidecadal variability

This result as the previous ones is relevant as it aims to understand or assess the possible influence of global climate drivers particularly the Atlantic Multidecadal Oscillation on the decadal or multi-decadal variability on the wind speed in West Africa. The continuous reduction in near-surface wind speed (NSWS) before 2010, commonly referred to as 'stilling', has been widely observed across land areas in the Northern Hemisphere (NH) (Azorin-Molina et al., 2017). The concept of NSWS stilling has been proposed for over a decade, yet a significant scientific gap persists in fully understanding this phenomenon (Zha et al., 2024). The motivation behind conducting this analysis is that in other parts of the world studies were conducted on the possible link of the AMO and wind patterns. For instance, Li et al. (2024b) conducted a study over China and found that the Atlantic Multidecadal Oscillation influences wind patterns primarily by modulating large-scale atmospheric circulation and temperature gradients in the Northern Hemisphere (NH). More specifically, their results showed that the hist-resAMO (refering to a "pacemaker" climate model experiment under the Coupled Model Intercomparison Project phase 6 (CMIP6)) and historical model simulations successfully replicate the significant influence of AMO in driving NSWS stilling, offering strong dynamical evidence supporting the observational findings. Specifically, a positive AMO phase leads to a weakened EASJ (East Asian Subtropical Jet) and diminished vertical momentum transport, which in turn weakens NSWS over China. Using MPI-ESM LEs, they further discovered that the uncertainty in simulated NSWS changes among different ensemble members is primarily induced by AMO. Notably, the standard deviation of NSWS trends could be reduced by 19% if the effect of AMO is accounted for, suggesting that improving our understanding of leading modes of internal climate variability, such as the AMO, could help reduce uncertainty in future projections of NSWS changes over China in particular and globally (Li et al., 2024b).

In this study, considering figure 12 below, from 1950 to 2024, wind speed anomalies are predominantly negative during the 1950s-1970s, with a dip around the mid-1960s, followed by a transition to persistent positive anomalies from the mid-1990s. The 5-year running meann (orange) rises from around -0.08 m/s in the 1960s to about 0.05-0.08 m/s in the years 2010-2020, indicating a multi-decadal variation rather than purely interannual noise. At the same time, the Atlantic Multidecadal Oscillation (AMO: blue dotted line, right axis) is negative for most of the mid-century, becomes neutral or positive in the 1990s, and reaches high positive values in the most recent years. This shows a plausible inter-relationship between the two AMO

SST and changes in wind partterns. The next figure (figure 13) will give more elucidation on this inter-relationship making use of a statical evaluation.

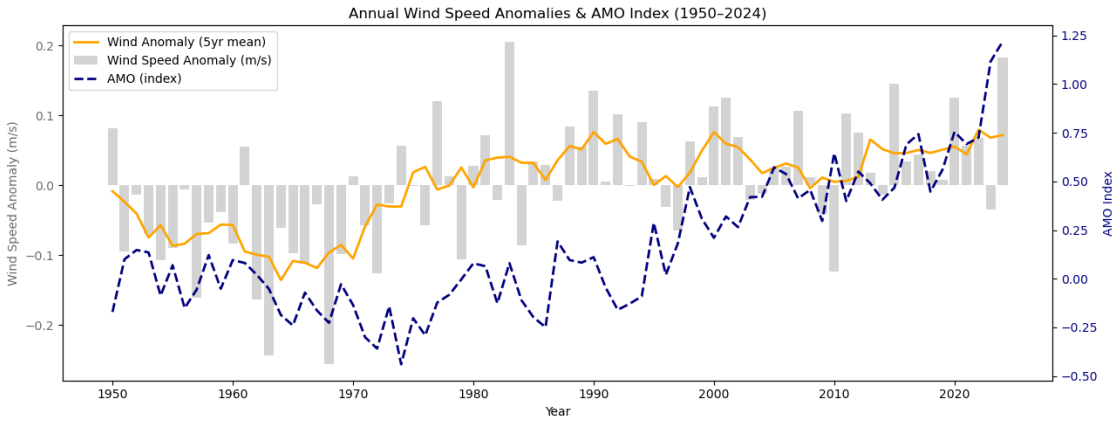

Figure 12:Time series of annual wind-speed anomalies (gray bars, m/s), five-year running mean of wind-speed anomalies (orange line, left axis), and the Atlantic Multidecadal Oscillation (AMO) index (blue dashed line, right axis) from 1950 to 2024.

3.5.2.Statistical evaluation of relationship between AMO and wind pattern

First, the zero-lag relationship between the Atlantic Multidecadal Oscillation AMO index and the annual wind speed anomaly between 1950 and 2024 is positive and statistically significant with ($r = 0.36$, $p= 0.002$). In other words, years in which the AMO is in a warm phase tend to coincide with above-normal winds in West Africa, whereas cool phase AMO tends to align with weaker winds. Nonetheless, the scatter is substantial. The simple linear fit explains on the order of 13 % of interannual variance ($r^2 \approx 0.13$), which implies that other modes of variability such as ENSO, NAO and local processes also contribute materially to the wind climate.

Secondly, the lagged correlation analysis shows stronger associations when the AMO precedes wind anomalies by several years. Correlations increase from around 0.2 for short negative lags to around 0.4–0.45 for positive lags of around +5 to +10 years, with many of these values reaching conventional significance (green markers). This structure is consistent with a physical picture in which Atlantic-scale SST anomalies associated with the AMO modify large-scale pressure gradients and storm track behaviour, with a delayed expression in regional winds via coupled ocean-atmosphere pathways and ocean memory. Conversely, when winds lead (precede) the AMO (negative lags), correlations are weaker, allowing us to cautiously conclude that winds are not the main driver of AMO variability in this case. Finally, the relevance of these pieces of information in the context of energy is that it brings awareness and informs energy planners to consider AMO influence as a contextual background state in long-term wind power planning.

In real application, operators can update these perspectives annually, combining AMO with NAO/ENSO predictors, and using sliding baselines to avoid over-attributing short-term anomalies to the multidecadal cycle.

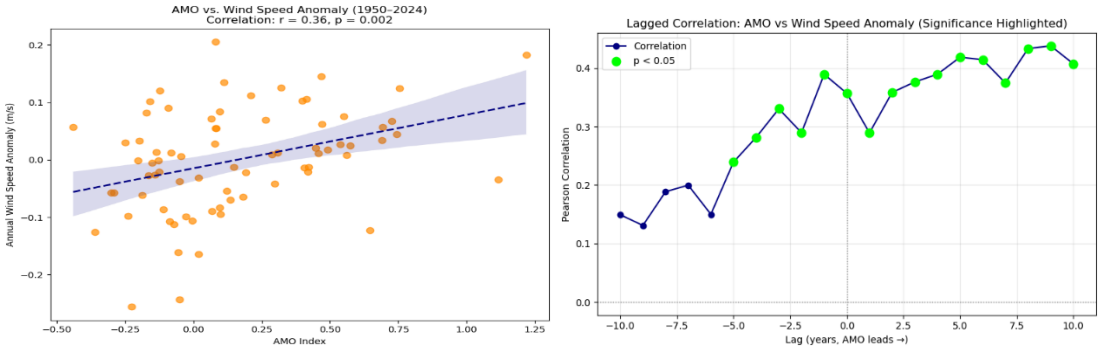

Figure 13:Left panel: Scatterplot of the Atlantic Multidecadal Oscillation (AMO) index the annual wind-speed anomaly in West Africa. Right-panel: L agged Pearson correlations between the AMO index and annual wind-speed anomalies for lags −10…+10 years (x-axis; positive lags mean AMO leads).

3.6. Model performance evaluation: era5 vs cmip6 models

3.6.1.Wind Speed distribution over West Africa (1950-2014).

Thie figure 14 below presentts the average wind speed from 1950 to 2014 near the surface in West Africa, using ERA5 as an observation reference to evaluate four models CMIP6 MIROC6, HadGEM3, MPI-ESM and CESM2-WACCM, the same models used for historical climate projections. ERA5 (left single panel) reveals a distinct southern gradient: the winds are strongest along the Atlantic margin of Mauritania–Senegal and northern Sahara and gradually weaken as they move south through the Sahelian and sub-Saharan belt to the weak-wind Gulf of Guinea.

The panels on the right show the CMIP6 model findings, which essentially duplicate numerous key ERA5 features. These features include a gradient strong in the north or weak in the south, a coastal jet maximum over the Atlantic edge. Additionnally models show relatively weak winds over the Southern Coastal Region.

However, many studies out there using Global or Regional historical or future projections under SSPs scenarios also confirmed particularly this regional variations across the four models (Akinsanola et al., 2021; K.O et al., 2022; Ndiaye et al., 2022; Sawadogo et al., 2019b) and (Gunnell, Mietton, Touré, Fujiki, et al., 2023; Youm et al., 2005). Most of them recognized that the costal region holds the highest potential in wind and low or moderate winds appear in other regions like the Sahel.

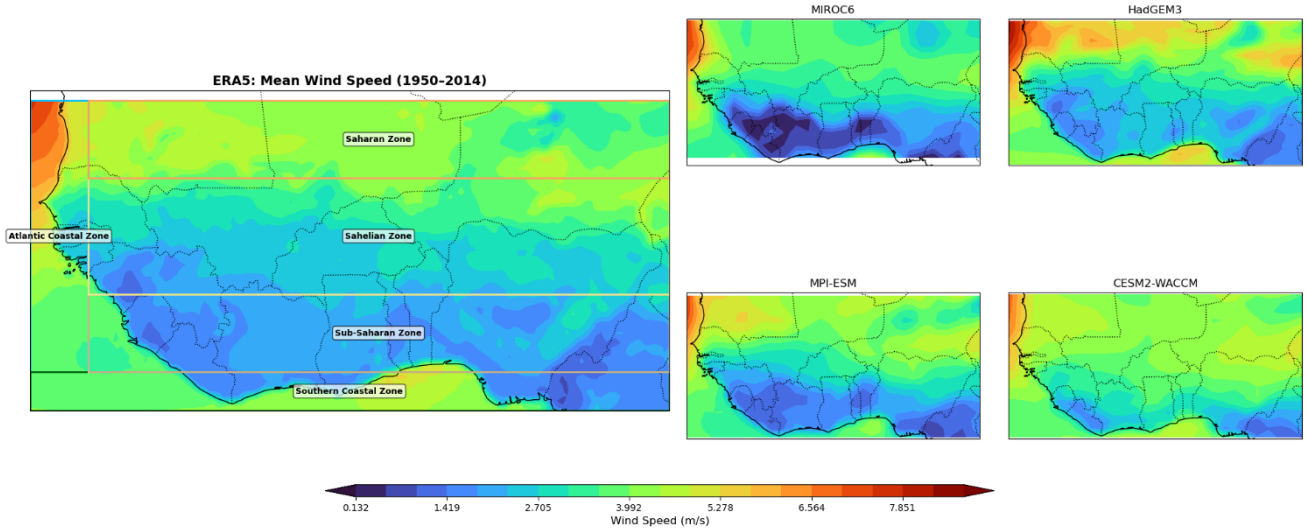

Figure 14: Historical projections with climate models. ERA5 on left panel and CMIP6 models on right panels, same period (1950-2014).

3.6.2. Wind speed anomalies across models

The figure 15 below shows the percentage wind speed anomalies for the 1950-2014 climatology over West Africa, using ERA5 as the observational reference and comparing four CMIP6 models. In panel a (ERA5), the anomalies are slightly positive over most of West Africa particularly pronounced in the Sahel, sub-Saharan and southern coastal belts while the extreme north of the Sahara and some areas along the eastern Gulf of Guinea are almost neutral or slightly negative. This indicates that the period saw a weak regional acceleration of the wind, the strongest to the south of around 15°N.

As far as the models are concerned, panel b (MIROC6) amplifies this pattern, producing a band of positive anomalies of +3-5% from about 5-12°N, but also introducing negative anomalies in the northern Sahara and along parts of the immediate coast. This suggests that MIROC6 simulates a strengthening of the monsoon belt wind regime but a weakening of the Saharan trade winds. In panel c, the (HadGEM3) model largely matches the ERA5 anomaly pattern, with positive anomalies in the Sahelian and sub-Saharan zones, although it displays stronger amplitudes and retains spotty negative anomalies along the margins adjacent to the ocean, thus overestimating the ERA5 signal. Panel d (MPI-ESM) shows positive anomalies in the western regions of the Sahel and Guinea but presents a marked west-east dipole with negative anomalies in the south-east of the Gulf of Guinea (Nigeria-Cameroon), which diverges from ERA5 and indicates a different view of recent decadal wind variability. Panel e (CESM2-WACCM) shows widespread positive anomalies in the sub-Saharan and southern coastal

regions, with slight negative anomalies in the far north, echoing the meridional gradient of ERA5 with larger and smoother spatial contrasts.

Overall, the figure shows broad agreement between the datasets that the period 1950-2014 was generally windier south of around 15°N, but not markedly so in the Sahara. However, the models differ in the strength, spatial resolution and coastal detail of these anomalies. Most tend to exaggerate the anomaly, smooth out the sharp coastal features and (in the case of MPI-ESM) reshape it into an east-west dipole. Neverthless, these observations are not yet rigorously sufficient to prove the performance of each model considering theirr individual internal structure.

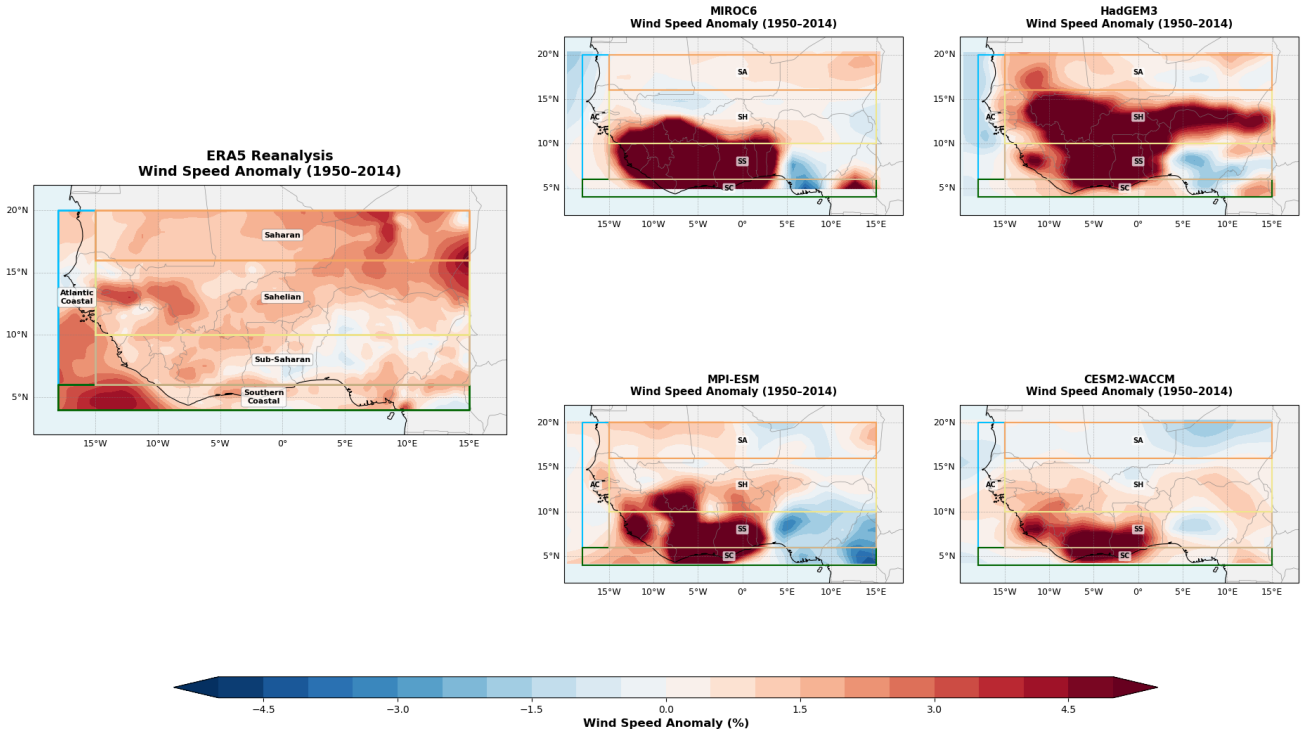

Figure 15:Percentage anomalies in near-surface wind speed for 1950–2014 climatology over West Africa, comparing CMIP6 models with the ERA5 benchmark. (Left-panel) ERA5 anomalies; (right-panels) anomalies from MIROC6, HadGEM3, MPI-ESM, CESM2-WACCM.

3.6.3.Heat map of subregional mean wind-speed bias

Figure 16 illustrates the spatial distribution of systematic wind speed biases in the four CMIP6 models within the key climatic subregions of West Africa. This is to highlight that these errors show pronounced regional heterogeneity in model performance rather than uniform behaviour. The analysis demontrastes that MIROC6, for example, produces some of the largest deviations, significantly overestimating wind speeds in the Sahelian zone by +0.17 m/s while underestimating them in the southern coastal zone by -0.76 m/s. In contrast, the MPI-ESM model performs comparatively better, with biases consistently below |0.30| m/s in three of the

five sub-regions, indicating a more balanced representation of wind climatology. In addition, in all the sub-regions the CESM2-WACCM model overestimates. This range in model performance reflects an analysis that is specific to a region. This is because a model deemed reliance in one region can produce serious distortions in another region. Furthermore, the practical implications of these errors go beyond areas related to climate. For instance, an overestimation of +0.65 m/s in the Atlantic coastal zone by HadGEM3 could inflate wind energy density estimates by more than 20%. Therefore this bias would compromise the accuracy of feasibility assessments and planning for subsequent investments in wind infrastructure.

Therefore, the results highlight the indispensable role of applying model and region-specific bias correction approaches before using CMIP6 results in quantitative assessments of wind resources in West Africa and related development strategies. More details on the biases are provided in the (see table A8 in appendices).

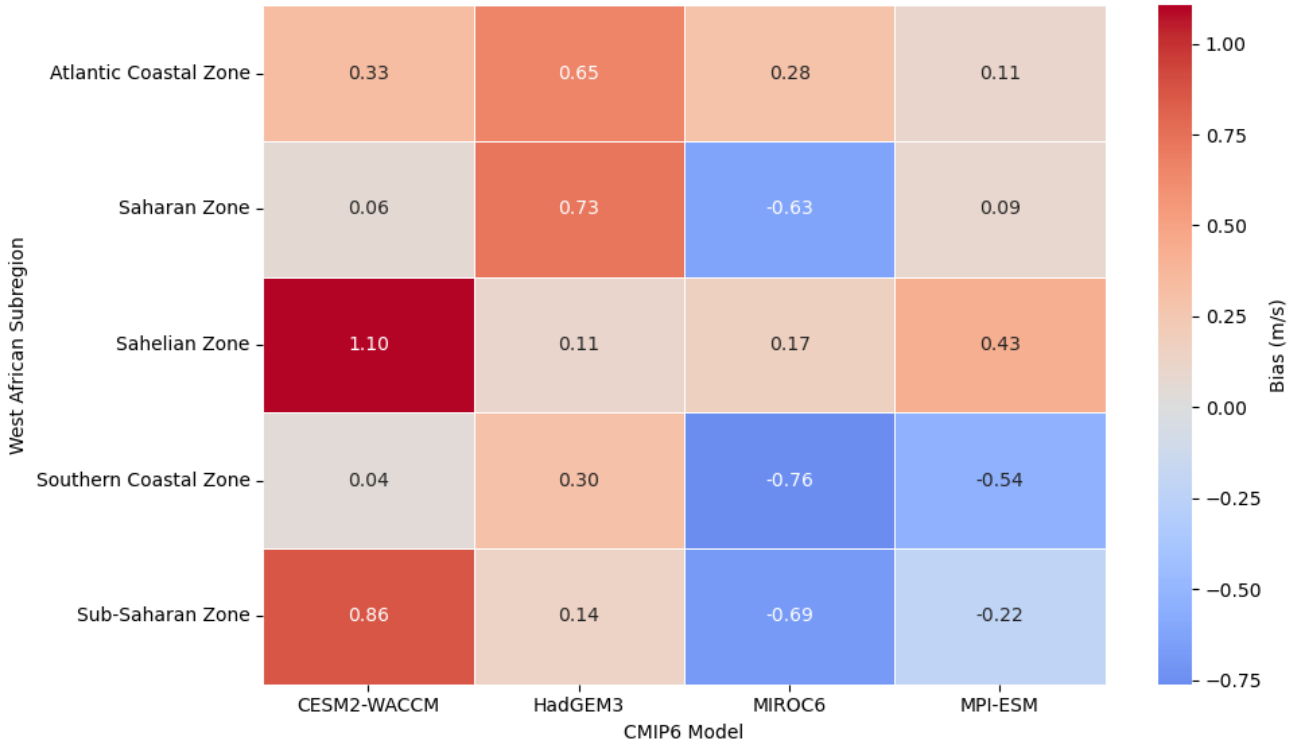

Figure 16: Heat map of the sub-regional bias in mean wind speed (Model - ERA5, m/s) for 1950-2014, summarising the performance of CMIP6 compared to the ERA5 reference in five West African zones.

3.6.4.Statistical Model Performance Evaluation

The figure (figure A17 see appendice (radar chart)) and 17 (heat map) presented together offer a compact but comprehensive assessment of the performance of the four CMIP6 models

used in this study compared with the ERA5 reference over West Africa. In particular, the use of standardised metrics in the radar map facilitates a direct and fair comparison of the different skill parameters, revealing that while all models capture the general climatological structure, their skill varies both by metric and by domain. More specifically, MPI-ESM appears to be the most robust overall, as indicated by its large radar footprint and dominant position in the heatmap exhibiting the lowest mean bias (+0.07m/s), MAE (0.41m/s), and RMSE (0.52 m/s), as well as a high correlation ($r = 0.90$) and an R^2 of 0.78. In addition, its standard deviation (model $\sigma = 1.22$ m/s) closely matches the ERA5 reference ($\sigma = 1.11$ m/s), confirming the realism of the amplitude representation.

The performance off this model has been proven in other studies, for instance Li et al. (2024a) conducted a study where the MPI-ESM shows strong performance in simulating the spatial climatology and range of summer precipitation trends over the Mongolian Plateau, enabling credible analysis of internal variability contributions to observed changes.

Lakku & Behera (2022) also conducted a study on simulating wind speed over South Asian Domain using regional and global climate models. After rigorous examination of all climate models' skill, he recommended the MPI-ESM model for onshore wind energy and air pollution modelling. In addition, Ganea & Rusu (2024) conducted a study to assess the offshore wind energy along the European cost using the MPI-ESM-LR as it offers high-quality, scientifically credible, and comprehensive datasets that are well-suited for assessing offshore wind energy potential in Europe under both current and projected future climate conditions. His Results show that current wind conditions at key sites especially the Gulf of Lion, Odesa, and Constanta are sufficient for offshore wind farms, with future climate scenarios projecting up to 60% increases in wind intensity and energy production.

Conversely, HadGEM3, despite having the highest spatial correlation ($r = 0.95$) and a high R^2 (0.73), tends to over-amplify variability, as evidenced by its positive mean bias (+0.33 m/s) and inflated standard deviation (model $\sigma = 1.39$ m/s), consistent with its overly strong Sahelian or interior winds. This overestimation aligns with the pattern noted by (Fiedler et al., 2016). In contrast, in other context of study the same model underestimates patterns, that is the case of Toste et al. (2018), whose study identifies that HadGEM2-ES underestimates near-surface sea surface temperatures (SST) over the western South Atlantic.

Meanwhile, MIROC6 systematically underestimates mean wind speed, specially in the coastal and southern belts, as evidenced by its negative mean bias (-0.28 m/s), higher MAE (0.57 m/s), higher RMSE (0.71 m/s) and lower correlation ($r = 0.85$), with a model standard deviation of 1.24 m/s.

This underperformance is corroborated by Abatan et al. (2021), who highlighted the difficulties encountered by the MIROC family of models in reproducing monsoon characteristics. Finally, CESM2-WACCM has the lowest agreement between measurements, with the highest mean bias (+0.62m/s), the highest MAE (0.72 m/s), the highest RMSE (0.91m/s), the lowest correlation (r = 0. 81), and lowest R^2 (0.34); notably, its sub-ERA5 variability (model σ = 0.85m/s) suggests a wind field that is too uniformly windy but too smooth. However, this model has been proven to be the best performer when conducting studies or applications that focus on precipitations (Guo et al., 2021). Moreover, Liu et al. (2019) conducted a study to where he compared major sudden stratospheric warming event in CESM1-WACCM and CESM2-WACCM. His study revealed that while both models capture key features of vortex split and displacement SSWs, CESM2-WACCM exhibits some new biases compared to CESM1-WACCM, especially regarding the seasonal timing and surface temperature responses.

Importantly, these diagnostic results which link amplitude, error, variability and spatial model collectively highlight the need to consider both the specific application and the dynamic context when selecting models for regional energy or climate impact analysis. While some models excel in model fidelity, others are better at preserving amplitude or minimising systematic biases, which is why multi-metric evaluations, as demonstrated here, remain indispensable. In addition, the broad consensus emerging from this and previous studies highlights the recurring strengths and weaknesses of structural models, particularly with regard to the representation of coastal jets and the low-level wind regime in the Sahel, highlighting areas where parameter refinement and coordinated model development will be required.

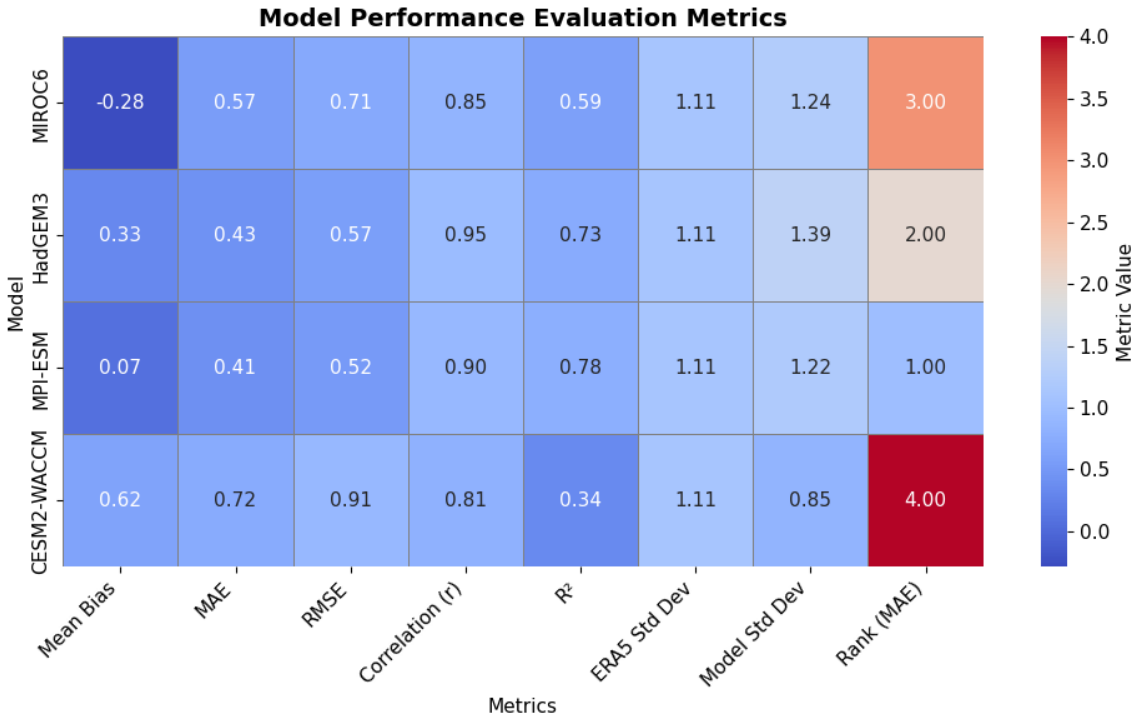

Figure 17: Heat map presenting quantitative performance metrics for the CMIP6 models.

3.7. Projection of future wind speed over west africa using MPI-ESM-LR model under ssp2-4.5 and ssp5-8.5 scenarios.

3.7.1.Projected near surface wind (10 m) speed distribution and spatial trends in west Africa: SSP Scenario Comparison MPI-ESM1-2LR (2025-2075)

The figure shows maps and trend analyses of projected near-surface wind speeds over West Africa under both moderate SSP2-4.5 and worst SSP5-8.5 climate scenarios using the MPI-ESM1-2LR CMIP6 model. Specifically, the top panels present the spatial distributions of mean wind speed for the two scenarios and their difference, while the lower panels quantify the decadal trends in wind speed and their difference between the scenarios.

We note that projected annual mean wind speed is consistently higher under the moderate SSP2-4.5 scenario compared to the high emission SSP5-8.5, especially in southern and central West Africa, where differences reach up to -0.9m/s.

Decadal trends show that SSP58.5 brings larger and more significant areas of decreasing wind speed, as indicated by the stippling. The trend difference map futther demonstrates that emission pathway selection has a huge impact on the projected wind resource,with negatives locations indicating stronger declines in wind speed under high emissions.

This also demonstrates the critical impact of climate change on regional wind resources (Solaun & Cerdá, 2019).

Overall, under both scenarios the model tends to reproduce the gradient of the climatology early presented with the observations from reanalysis ERA5. More specifically, under both scenarios, the model projects a plausible decrease in mean wind speed across the entire region except the coastal zone. Considering our regional subdivision, the Sahelian, southern coastal and most importantly the sub-Saharan regions appear to be the most affected with a huge decrease in mean wind speed (4 to1 m/s) observed particularly in West-Eastern and more in South-Eastern parts of the region according to both scenarios but more amplified under SSP5-8.5. In contrast, the model projects strongest near-surface winds along the coastal region margin and offshore corridor (5-8 m/s), moderate winds also show up over the Saharan zone (3-5 m/s). These results are consistent with studies conducted by Akinsanola et al. (2021) who used the CMIP6 multi-model ensemble mean to project changes in wind speed and wind energy potential over West Africa. It was found that there is a robust increase in wind speed and power density (WPD) over the Guinea coast and parts of the coastal regions, especially towards the end of the century (2070–2099), with increases exceeding 70% in some seasons. In contrast, the Sahel region was expected to experience decreases in wind speed and WPD in the same region.

Furthermore, Sawadogo et al. (2019a) came to the same conclusions using eleven multi-model multi-ensemble simulations from CORDEX RCMs projection under the global warming of 1.5 °C and above. However, all studies are not converging towards the same results. For instance, K.O et al. (2022) found different results using CORDEX ensemble simulation over West Africa. His findings revealed a projected decline in wind power production of up to 12% in the near future (2021–2050), especially in the Guinea and Savannah zones, followed by a substantial increase of about 24–30% towards the end of the century (2071–2100) in most areas, particularly in the Sahel zone similar. Moreover Ndiaye et al. (2022) used the REMO model to project a decrease of about 10% in much of the region in the near future (2021–2050) and by the end of the century (2071–2100). Spatially, increases in WPD are mainly expected in the Sahel, with gains between 10 and 20%.

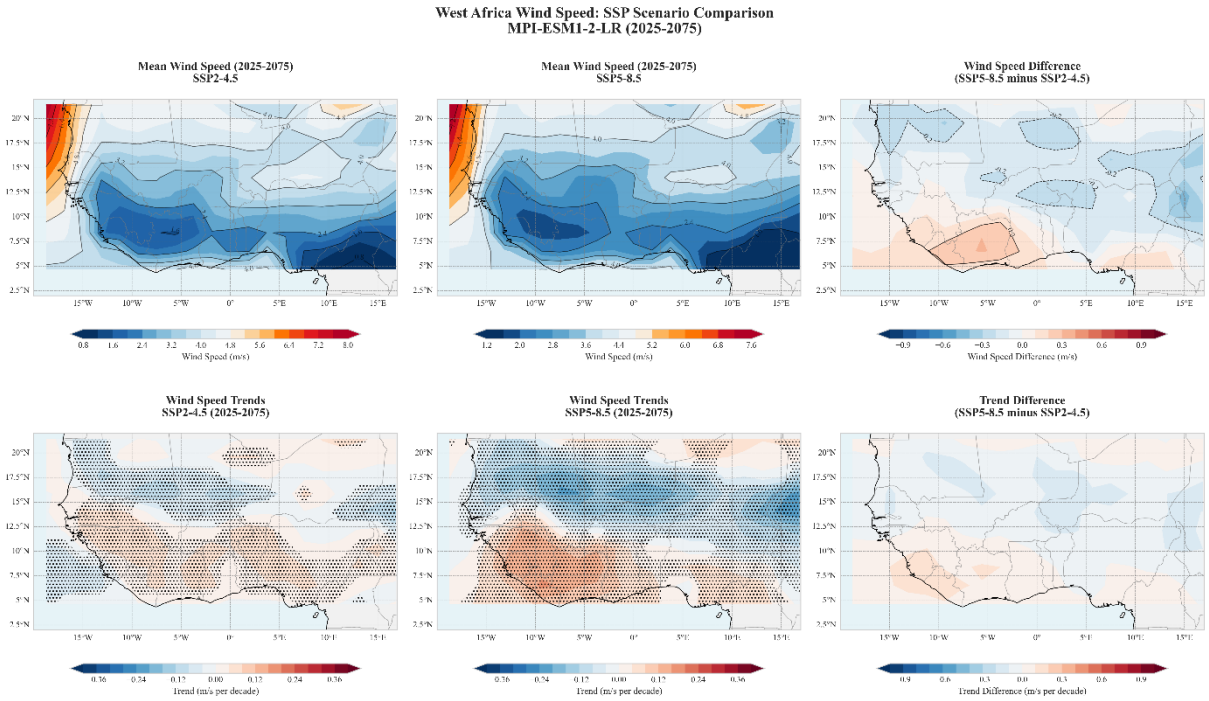

Figure 18:Annual mean and trend maps of near-surface wind speed (10 m) over West Africa as simulated by the MPI-ESM1-2LR CMIP6 model for the period 2025–2075 under the SSP2-4.5 and SSP5-8.5 scenarios. Top panels show contour maps of mean wind speed (m/s) for each scenario and their absolute difference (SSP5-8.5 minus SSP2-4.5). Bottom panels present decadal wind speed trends (m/s per decade) and trend differences; stippling indicates statistically significant trend areas ($p < 0.05$)

3.7.2.Projected seasonal (DJF, JJA) near surface wind (10 m) speed in west Africa: MPI-ESM1-2LR (2025-2075)

The figure above systematically compares seasonal wind speed distributions dry season (DJF, top row) and wet season (JJA, bottom row) under both SSP2-4.5 and SSP5-8.5 scenarios for the mid-21st century. In the context of west Africa wind resource assessment understanding the seasonal analysis is important as they often indicate wind resource availability in the region.

In our special case, distinct patterns emerge: Wind speeds are consistently lower in the both scenarios but most intense in high-emission scenario (SSP5-8.5) for both seasons, with the greatest absolute and relative reductions seen in southern and coastal West Africa during the wet season (JJA). Under the SSP2-4.5 scenario the model shows stronger wind in DJF than in JJA, especially in the Saharan zone and north-eastern part of the Sahelian region.

Local losses above 18% are shown by the percentage difference. This reduction has a significant impact on the feasibility of wind energy. During DJF, decreases are less pronounced

over the region but still significant. This highlights the importance of seasonality in wind resource sensitivity to climate change.

These results strongly align with the conclusions of K.O et al. (2022) , who reported marked seasonal variability and scenario sensitivity in West African wind resources. Seasonal analysis showed greater reductions during winter months (DJF) and improvements during the monsoon season (JJA). In support to this Akinsanola et al. (2021) projected significant seasonal and regional variations in future wind characteristics over West Africa. Notably, the Guinea coast is identified as the most promising subregion, showing robust increases in wind speed and wind power density (WPD), particularly during the (JJA) season, with increases exceeding 70% towards the end of the century. In contrast, the Sahel region is expected to experience decreases in wind speed and WPD, especially during the (DJF) and (MAM) seasons, indicating reduced potential for wind energy there in the future.

Ultimately, the regional and seasonal wind speed projection using the single model MPI-ESM-LR under climate change scenarios (SSP2-4.5 and SSP5-8.5) has shown how wind resources could be influenced by climate change, causing a strong decline in wind patterns under both scenarios focusing only on DJF and JJA seasons. This is reliable as findings they are consistent with some of the previous studies using Global or Regioanl multi-model ensemble means as a way to reduce bias and uncertainties. Therefore, the MPI-ESM-LR model can be trusted and used as single reliable model for further studies in West Africa in particular and Africa in general.

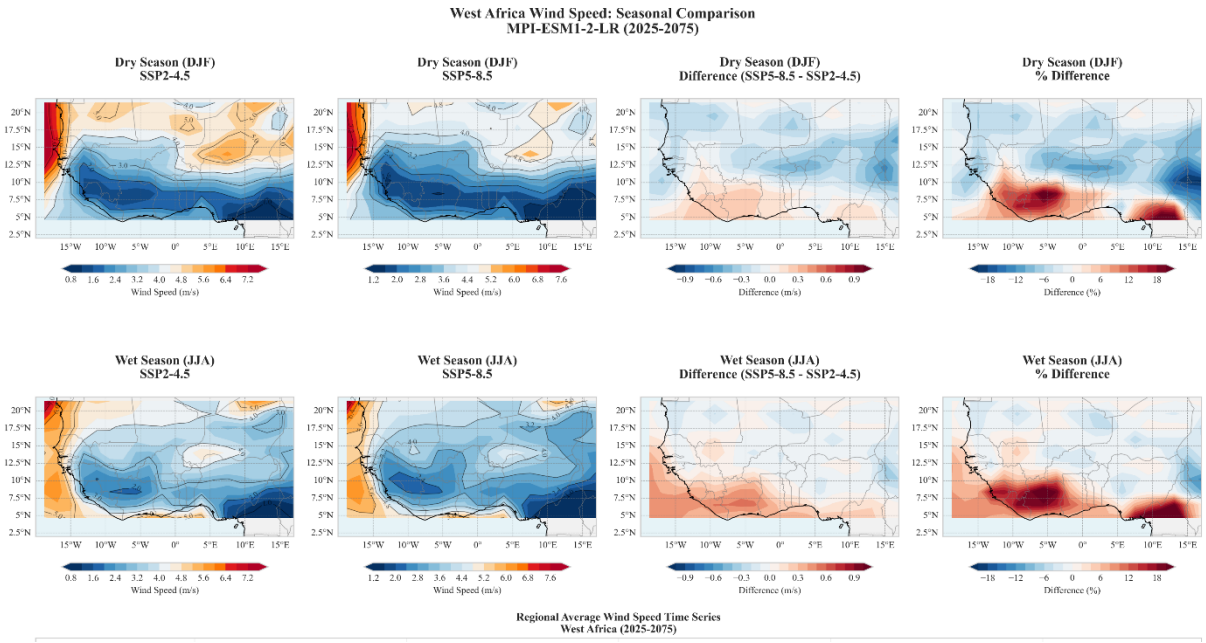

Figure 19: Seasonal distribution and scenario comparison of 10 m near-surface wind speed over West Africa for the MPI-ESM1-2LR model projections (2025–2075).

Overall, the findings reveal significant spatiotemporal variations in wind fields across West Africa, influenced by both regional climatic factors and large-scale variability. While ERA5 reanalysis data provides a valuable baseline reference, model comparisons reveal persistent biases that must be carefully evaluated during planning applications. The investigation of extreme events and anomalies underscores the critical importance of wind event persistence and duration factors often overlooked in macro-climate assessments. Projected changes under CMIP6 scenarios indicate that different regions will face differentiated impacts, holding significant implications for the siting and reliability of future wind energy facilities. The overarching conclusions of this work, grounded in these perspectives, bridge the cognitive gap between atmospheric variability and applied energy planning.

GENERAL CONCLUSION AND PERSPECTIVES

GENERAL CONCLUSION AND PERSPECTIVES

In this study, we assessed West Africa's wind resource with a dual objective: first of all, we characterised the historical distribution, anomalies, and variability of near-surface and hub-height winds across five planning-relevant sub-regions (Atlantic Coastal, Southern Coastal, Sub-Saharan, Sahelian, and Saharan); second, we evaluated the skill of four CMIP6 models (MIROC6, HadGEM3-GC3.1-MM, CESM2-WACCM, and MPI-ESM1-2LR) against a reanalysis baseline and generate forward projections using the best performer under SSP2-4.5 and SSP5-8.5. The analysis linked regional circulation regimes to operationally salient metrics (seasonality, intra-annual variability, and anomalies), ranked models for historical fidelity, and translated projected changes in wind speed into concrete implications for energy planning and policy.The results of this study can be gathered as follows:

1. The Atlantic coastal zone and the Saharan fringe have the highest average winds. But the sub-Saharan zone has the lowest. At the hub, the gradient is intensified.This improves the prospects for coastal implementation. The interior still stay marginal.
2. The southern Coastal and the sub-Saharan zones have higher coefficients of variation and shorter constant durations. This indicates a greater operational risk and a need for storage and hybridization. In contrast, the Atlantic coastal zone offers more stable and favourable conditions for the network.
3. Seasonal speed vary by region, with peaks on the Atlantic coast in the DJF-MAM and peaks on the southern coast in the JJA. Saharan seasonality is bimodal (DJF or SON). While that of the Sahel and sub-Saharan Africa is attenuated or mixed. These patterns correspond to the monsoon-harmattan dipole and help define complementary operation with solar photovoltaic.
4. The global climate driver AMO modulates multidecadal wind patterns over West Africa. The lagged correlation analysis shows stronger associations when the AMO precedes wind anomalies by several years. Correlations increase from around 0.2 for short negative lags to around 0.4–0.45 for positive lags of around +5 to +10 years.
5. The model evaluation demonstrated that all the four CMIP6 models reproduce broad spatial features in historical projections, with MPI-ESM1-2HR achieving the best overall skill. This model was therefore used for projections.

6. The projections under both SSPs keep the historical gradient but show widespread inland weakening, smaller and patchier under SSP2-4.5. They show more extensive under SSP5-8.5. Coastal resources remain comparatively robust. The Southern Coastal and interior Sub-Saharan experience the strongest JJA-season reductions. The Saharan zone maintains moderate winds with seasonally mixed signals.
7. The sub-regional planning priorities include grid-connected coastal and offshore projects and transmission network reinforcement in the Atlantic coast. Combining wind, photovoltaic and storage to manage JJA variability in the southern coastal. Adopting hybrid tactics and targeted micro-siting in the sub-Saharan and Sahelian regions. Assessing utility-scale prospects in the Saharan zone, considering dust or maintenance risks and long-distance transmission.

The findings of this study may be improved in many ways. Main limitations include reliance on a single reanalysis as the historical baseline, power-law extrapolation to hub height, a single best-model pathway for projections, and coarse model resolution that smooths coastal jets and complex terrain, sparse in-situ observations further constrain independent validation and bias correction.10 meter wind speed data was mostly considered in the evaluations. These constraints do not invalidate the conclusions but do bound their confidence and suggest a conservative stance for capacity planning and bankability assessments.

Looking ahead, decision-relevant evidence can be strengthhened by (i) using multi-model ensemble means with explicit model-agreement diagnostics for projections; (ii) applying bias-correction against reanalysis and available station data; (iii) designing cost-effective generation portfolios for each sub-region under moderate and worst-case scenarios, including adequacy and flexibility analyses; (iv) benchmarking machine-learning downscaling and projection methods against CMIP6 to improve spatial detail; and (v) conducting techno-economic studies that integrate siting, grid reinforcement, storage, and seasonal operations; (vi) conducting a study to critically evaluate global and regional climate drivers' influence on multidecadal wind speed on local variability over West Africa. Taken together, these steps will translate the climatological signals identified here into robust, policy-informed roadmaps for wind deployment and resilient power-sector planning across West Africa and hopefully in other parts of Africa.

BIBLIOGRAPHIC REFERENCES

BIBLIOGRAPHIC REFERENCES

Abatan, A. A., Collins, M., Babel, M. S., Khadka, D., & De Silva, Y. K. (2021). Assessment of the Ability of CMIP6 GCMS to Simulate the Boreal Summer Intraseasonal Oscillation Over Southeast Asia. *Frontiers in Climate*, *3*. https://doi.org/10.3389/fclim.2021.716129

Abbas, G., Ali, A., Mushtaq, Z., Rehman, A. U., Hussen, S., & Hamam, H. (2025). Advancing wind energy potential estimation through multidistribution wind speed analysis in coastal Pakistan. *Scientific Reports*, *15*(1). https://doi.org/10.1038/s41598-025-03322-y

Abiodun, B. J., Adeyewa, Z. D., Oguntunde, P. G., Salami, A. T., & Ajayi, V. O. (2012). Modeling the impacts of reforestation on future climate in West Africa. *Theoretical and Applied Climatology*, *110*(1–2), 77–96. https://doi.org/10.1007/s00704-012-0614-1

Abolude, A. T., Zhou, W., & Akinsanola, A. A. (2020). Evaluation and projections of wind power resources over China for the energy industry using CMIP5 models. *Energies*, *13*(10). https://doi.org/10.3390/en13102417

Adekunle, E. P., Adedoyin, B. A., Theophilus, E., A. A. Osinowo, Ogundare, M. O., Raheemat, A. O., Abe, J. Sunday., A. S. Ifanegan, & Okunlola, B. A. (2025). Exploration of Wind-Wave Energy Potentials for Renewable Energy Development in Parts of Ondo Coastal and Offshore Locations, Southwestern Nigeria. *Indian Journal of Energy and Energy Resources*, *4*(2), 1–10. https://doi.org/10.54105/ijeer.B1039.04020225

Ajah, S. N. (2019). Solar Energy: A Source of Renewable Energy and a Disruptive Innovation Creating Business Opportunities in Nigeria. In *Human Behavior, Development and Society* (Vol. 20, Issue 3).

Akhator, P. E., Obanor, A. I., & Sadjere, E. G. (2019). Electricity situation and potential development in Nigeria using off-grid green energy solutions. *Journal of Applied Sciences and Environmental Management*, *23*(3), 527. https://doi.org/10.4314/jasem.v23i3.24

Akinsanola, A. A., Ogunjobi, K. O., Abolude, A. T., & Salack, S. (2021). Projected changes in wind speed and wind energy potential over West Africa in CMIP6 models. *Environmental Research Letters*, *16*(4). https://doi.org/10.1088/1748-9326/abed7a

Akinsanola, A. A., & Zhou, W. (2019). Projections of West African summer monsoon rainfall extremes from two CORDEX models. *Climate Dynamics*, *52*(3–4), 2017–2028. https://doi.org/10.1007/s00382-018-4238-8

Aksay, E., Çoban, E., & Güçlü, Y. S. (2025). Normalized innovative trend analysis model and Mann-Kendall test for solar data. *Modeling Earth Systems and Environment*, *11*(5). https://doi.org/10.1007/s40808-025-02550-5

Alamirew, N. K., Todd, M. C., Ryder, C. L., Marsham, J. H., & Wang, Y. (2018). The early summertime Saharan heat low: Sensitivity of the radiation budget and atmospheric heating to water vapour and dust aerosol. *Atmospheric Chemistry and Physics*, *18*(2), 1241–1262. https://doi.org/10.5194/acp-18-1241-2018

Alemzero, D., Acheampong, T., & Huaping, S. (2021). Prospects of wind energy deployment in Africa: Technical and economic analysis. *Renewable Energy*, *179*, 652–666. https://doi.org/10.1016/j.renene.2021.07.021

Aliyu, A. K., Modu, B., & Tan, C. W. (2018). A review of renewable energy development in Africa: A focus in South Africa, Egypt and Nigeria. In *Renewable and Sustainable Energy Reviews* (Vol. 81, pp. 2502–2518). Elsevier Ltd. https://doi.org/10.1016/j.rser.2017.06.055

Almazroui, M., Saeed, F., Saeed, S., Nazrul Islam, M., Ismail, M., Klutse, N. A. B., & Siddiqui, M. H. (2020). Projected Change in Temperature and Precipitation Over Africa from CMIP6. *Earth Systems and Environment*, *4*(3), 455–475. https://doi.org/10.1007/s41748-020-00161-x

Ando, T., Higuchi, T., Hotta, H., Iwakiri, T., Jinno, T., Kino, K., Takano, Y., Toda, M., Yamazaki, K., Chikira, M., Kodama, T., Michibata, T., Miura, H.-R., Nitta, T., Ogura, T., Saito, F., Sekiguchi, M., Suzuki, T., Suzuki, K., … Yoshimura, K. (2021). *Description of MIROC6 AGCM MIROC6 AGCM document writing team *.* https://doi.org/10.15083/0002000180

Aririguzo, J. C., & Ekwe, E. B. (2019). Weibull distribution analysis of wind energy prospect for Umudike, Nigeria for power generation. *Robotics and Computer-Integrated Manufacturing*, *55*, 160–163. https://doi.org/10.1016/j.rcim.2018.01.001

Atsu, B., Foli, K., Addo, K. A., Ansong, J. K., & Wiafe, G. (1976). *Evaluation of ECMWF and NCEP Reanalysis Wind Fields for Long-Term Historical Analysis and Ocean Wave Modelling in West Africa*. https://doi.org/10.1007/s41976-021-00052-3/Published

Attabo, A. A., Ajayi, O. O., Oyedepo, S. O., & Afolalu, S. A. (2023). Assessment of the wind energy potential and economic viability of selected sites along Nigeria's coastal and offshore locations. *Frontiers in Energy Research*, *11*. https://doi.org/10.3389/fenrg.2023.1186095

Attanayake, K., Wickramage, I., Samarasinghe, U., Ranmini, Y., Ehalapitiya, S., Jayathilaka, R., & Yapa, S. (2024). Renewable energy as a solution to climate change: Insights from a comprehensive study across nations. *PLoS ONE*, *19*(6 June). https://doi.org/10.1371/journal.pone.0299807

Ayodele, T. R., Mosetlhe, T. C., Yusuff, A. A., & Ogunjuyigbe, A. S. O. (2021). Off-grid hybrid renewable energy system with hydrogen storage for South African rural community health clinic. *International Journal of Hydrogen Energy*, *46*(38), 19871–19885. https://doi.org/10.1016/j.ijhydene.2021.03.140

Ayugi, B., Tan, G., Gnitou, G. T., Ojara, M., & Ongoma, V. (2020). Historical evaluations and simulations of precipitation over East Africa from Rossby centre regional climate model. *Atmospheric Research*, *232*. https://doi.org/10.1016/j.atmosres.2019.104705

AYUGI, B., Zhidong, J., Zhu, H., Ngoma, H., Babaousmail, H., Rizwan, K., & Dike, V. (2021). *Comparison of CMIP6 and CMIP5 Models in Simulating Mean and Extreme Precipitation over East Africa*. https://doi.org/10.20944/preprints202102.0111.v1

Azorin-Molina, C., Vicente-Serrano, S. M., McVicar, T. R., Revuelto, J., Jerez, S., & López-Moreno, J. I. (2017). Assessing the impact of measurement time interval when calculating wind speed means and trends under the stilling phenomenon. *International Journal of Climatology*, *37*(1), 480–492. https://doi.org/10.1002/joc.4720

Babaousmail, H., Hou, R., Ayugi, B., Ojara, M., Ngoma, H., Karim, R., Rajasekar, A., & Ongoma, V. (2021). Evaluation of the performance of cmip6 models in reproducing rainfall patterns over north africa. *Atmosphere*, *12*(4). https://doi.org/10.3390/atmos12040475

Batibeniz, F., Hauser, M., & Seneviratne, S. I. (2023). Countries most exposed to individual and concurrent extremes and near-permanent extreme conditions at different global warming levels. *Earth System Dynamics*, *14*(2), 485–505. https://doi.org/10.5194/esd-14-485-2023

Biasutti, M. (2019). Rainfall trends in the African Sahel: Characteristics, processes, and causes. In *Wiley Interdisciplinary Reviews: Climate Change* (Vol. 10, Issue 4). Wiley-Blackwell. https://doi.org/10.1002/wcc.591

Bloomfield, H. C., Wainwright, C. M., & Mitchell, N. (2022). Characterizing the variability and meteorological drivers of wind power and solar power generation over Africa. *Meteorological Applications*, *29*(5). https://doi.org/10.1002/met.2093

Boadu, S., & Otoo, E. (2024). A comprehensive review on wind energy in Africa: Challenges, benefits and recommendations. In *Renewable and Sustainable Energy Reviews* (Vol. 191). Elsevier Ltd. https://doi.org/10.1016/j.rser.2023.114035

Burton, Tony. (2011). *Wind energy handbook*. Wiley.

Climate Change Impacts on Biodiversity and Protected Areas in West Africa. (2016). www.unep-wcmc.org

Climate Impacts in the Sahel and West Africa (West African Papers, Vol. 2). (2016). https://doi.org/10.1787/5jlsmktwjcd0-en

Compo, G. P., Whitaker, J. S., Sardeshmukh, P. D., Matsui, N., Allan, R. J., Yin, X., Gleason, B. E., Vose, R. S., Rutledge, G., Bessemoulin, P., BroNnimann, S., Brunet, M., Crouthamel, R. I., Grant, A. N., Groisman, P. Y., Jones, P. D., Kruk, M. C., Kruger, A. C., Marshall, G. J., … Worley, S. J. (2011). The Twentieth Century Reanalysis Project. In *Quarterly Journal of the Royal Meteorological Society* (Vol. 137, Issue 654, pp. 1–28). John Wiley and Sons Ltd. https://doi.org/10.1002/qj.776

Danso, D. K., Anquetin, S., Diedhiou, A., Lavaysse, C., Kobea, A., & Touré, N. E. (2019). Spatio-temporal variability of cloud cover types in West Africa with satellite-based and reanalysis data. *Quarterly Journal of the Royal Meteorological Society*, *145*(725), 3715–3731. https://doi.org/10.1002/qj.3651

Davis, N. N., Badger, J., Hahmann, A. N., Hansen, B. O., Mortensen, N. G., Kelly, M., Larsén, X. G., Olsen, B. T., Floors, R., Lizcano, G., Casso, P., Lacave, O., Bosch, A., Bauwens, I., Knight, O. J., Potter van Loon, A., Fox, R., Parvanyan, T., Krohn Hansen, S. B., … Drummond, R. (2023). The Global Wind Atlas: A High-Resolution Dataset of Climatologies and Associated Web-Based Application. *Bulletin of the American Meteorological Society*, *104*(8), E1507–E1525. https://doi.org/10.1175/BAMS-D-21-0075.1

Dee, D. P., Uppala, S. M., Simmons, A. J., Berrisford, P., Poli, P., Kobayashi, S., Andrae, U., Balmaseda, M. A., Balsamo, G., Bauer, P., Bechtold, P., Beljaars, A. C. M., van de Berg, L., Bidlot, J., Bormann, N., Delsol, C., Dragani, R., Fuentes, M., Geer, A. J., … Vitart, F. (2011). The ERA-Interim reanalysis: Configuration and performance of the data assimilation system. *Quarterly Journal of the Royal Meteorological Society*, *137*(656), 553–597. https://doi.org/10.1002/qj.828

Deng, K., Azorin-Molina, C., Minola, L., Zhang, G., & Chen, D. (2020). *Global Near-Surface Wind Speed Changes over the Last Decades Revealed by Reanalyses and CMIP6 Model Simulations*. https://doi.org/10.1175/JCLI-D-20

Diallo, I., Sylla, M. B., Giorgi, F., Gaye, A. T., & Camara, M. (2012). Multimodel GCM-RCM ensemble-based projections of temperature and precipitation over West Africa for the Early 21st Century. *International Journal of Geophysics*, *2012*. https://doi.org/10.1155/2012/972896

Dosio, A., Turner, A. G., Tamoffo, A. T., Sylla, M. B., Lennard, C., Jones, R. G., Terray, L., Nikulin, G., & Hewitson, B. (2020). A tale of two futures: Contrasting scenarios of future precipitation for West Africa from an ensemble of regional climate models. *Environmental Research Letters*, *15*(6). https://doi.org/10.1088/1748-9326/ab7fde

Dunn, J. H. R., Willett, M. K., Parker, E. D., & Mitchell, L. (2016). Expanding HadISD: Quality-controlled, sub-daily station data from 1931. *Geoscientific Instrumentation, Methods and Data Systems*, *5*(2), 473–491. https://doi.org/10.5194/gi-5-473-2016

Enfield, D. B., Mestas-Nuñez, A. M., & Trimble, P. J. (2001). The Atlantic multidecadal oscillation and its relation to rainfall and river flows in the continental U.S. *Geophysical Research Letters*, *28*(10), 2077–2080. https://doi.org/10.1029/2000GL012745

Esnaola, G., Ulazia, A., Sáenz, J., & Ibarra-Berastegi, G. (2024). Future changes of global Annual and Seasonal Wind-Energy Production in CMIP6 projections considering air density variation. *Energy*, *307*. https://doi.org/10.1016/j.energy.2024.132706

Eyring, V., Bony, S., Meehl, G. A., Senior, C. A., Stevens, B., Stouffer, R. J., & Taylor, K. E. (2016). Overview of the Coupled Model Intercomparison Project Phase 6 (CMIP6) experimental design and organization. *Geoscientific Model Development*, *9*(5), 1937–1958. https://doi.org/10.5194/gmd-9-1937-2016

Fall, M., Dieng, A. L., Eymard, L., Coëtlogon, G. De, Sall, S. M., & Sane, Y. (2025). Atmospheric Dynamics of Extreme Precipitation over the West African Sahel. *American Journal of Climate Change*, *14*(01), 119–145. https://doi.org/10.4236/ajcc.2025.141007

Feng, H. (2022). The Impact of Renewable Energy on Carbon Neutrality for the Sustainable Environment: Role of Green Finance and Technology Innovations. *Frontiers in Environmental Science*, *10*. https://doi.org/10.3389/fenvs.2022.924857

Fujiwara, M., Wright, J. S., Manney, G. L., Gray, L. J., Anstey, J., Birner, T., Davis, S., Gerber, E. P., Lynn Harvey, V., Hegglin, M. I., Homeyer, C. R., Knox, J. A., Krüger,

K., Lambert, A., Long, C. S., Martineau, P., Molod, A., Monge-Sanz, B. M., Santee, M. L., … Zou, C. Z. (2017). Introduction to the SPARC Reanalysis Intercomparison Project (S-RIP) and overview of the reanalysis systems. *Atmospheric Chemistry and Physics*, *17*(2), 1417–1452. https://doi.org/10.5194/acp-17-1417-2017

Gaetani, M., Flamant, C., Bastin, S., Janicot, S., Lavaysse, C., Hourdin, F., Braconnot, P., & Bony, S. (2017). West African monsoon dynamics and precipitation: the competition between global SST warming and CO2 increase in CMIP5 idealized simulations. *Climate Dynamics*, *48*(3–4), 1353–1373. https://doi.org/10.1007/s00382-016-3146-z

Ganea, D., & Rusu, L. (2024). Assessment of the offshore wind energy along the European cost line. *2024 IEEE Conference on Advanced Topics on Measurement and Simulation, ATOMS 2024*, 331–334. https://doi.org/10.1109/ATOMS60779.2024.10921547

Gbode, I. E., Babalola, T. E., Diro, G. T., & Intsiful, J. D. (2023). Assessment of ERA5 and ERA-Interim in Reproducing Mean and Extreme Climates over West Africa. *Advances in Atmospheric Sciences*, *40*(4), 570–586. https://doi.org/10.1007/s00376-022-2161-8

Gebrechorkos, S., Leyland, J., Slater, L., Wortmann, M., Ashworth, P. J., Bennett, G. L., Boothroyd, R., Cloke, H., Delorme, P., Griffith, H., Hardy, R., Hawker, L., McLelland, S., Neal, J., Nicholas, A., Tatem, A. J., Vahidi, E., Parsons, D. R., & Darby, S. E. (2023). A high-resolution daily global dataset of statistically downscaled CMIP6 models for climate impact analyses. *Scientific Data*, *10*(1). https://doi.org/10.1038/s41597-023-02528-x

Gernaat, D. E. H. J., de Boer, H. S., Daioglou, V., Yalew, S. G., Müller, C., & van Vuuren, D. P. (2021). Climate change impacts on renewable energy supply. *Nature Climate Change*, *11*(2), 119–125. https://doi.org/10.1038/s41558-020-00949-9

Gleixner, S., Demissie, T., & Diro, G. T. (2020). Did ERA5 improve temperature and precipitation reanalysis over East Africa? *Atmosphere*, *11*(9). https://doi.org/10.3390/atmos11090996

Gruber, K., Klöckl, C., Regner, P., Baumgartner, J., & Schmidt, J. (2019). Assessing the Global Wind Atlas and local measurements for bias correction of wind power generation simulated from MERRA-2 in Brazil. *Energy*, *189*. https://doi.org/10.1016/j.energy.2019.116212

Gruber, K., Regner, P., Wehrle, S., Zeyringer, M., & Schmidt, J. (2022). Towards global validation of wind power simulations: A multi-country assessment of wind power simulation from MERRA-2 and ERA-5 reanalyses bias-corrected with the global wind atlas. *Energy*, *238*. https://doi.org/10.1016/j.energy.2021.121520

Gugliani, G. K., Sarkar, A., Ley, C., & Mandal, S. (2018). New methods to assess wind resources in terms of wind speed, load, power and direction. *Renewable Energy*, *129*, 168–182. https://doi.org/10.1016/j.renene.2018.05.088

Gunnell, Y., Mietton, M., Touré, A. A., & Fujiki, K. (2023). Potential for wind farming in West Africa from an analysis of daily peak wind speeds and a review of low-level jet dynamics. In *Renewable and Sustainable Energy Reviews* (Vol. 188). Elsevier Ltd. https://doi.org/10.1016/j.rser.2023.113836

Gunnell, Y., Mietton, M., Touré, A. A., Fujiki, K., Gunnell, Y., Mietton, M., Touré, A. A., & Fujiki, K. (2023). *Potential for wind farming in West Africa from an analysis of daily peak wind speeds and a review of low-level jet dynamics*.

Guo, H., Bao, A., Chen, T., Zheng, G., Wang, Y., Jiang, L., & De Maeyer, P. (2021). Assessment of CMIP6 in simulating precipitation over arid Central Asia. *Atmospheric Research*, *252*. https://doi.org/10.1016/j.atmosres.2021.105451

Hahmann, A. N., S¯ Ile, T., Witha, B., Davis, N. N., Dörenkämper, M., Ezber, Y., García-Bustamante, E., Fidel González-Rouco, J., Navarro, J., Olsen, B. T., & Söderberg, S. (2020). *The Making of the New European Wind Atlas-Part 1: Model Sensitivity*. https://map.neweuropeanwindatlas.eu/

Haidi, T., & Cheddadi, B. (2022). Wind energy integration in Africa: development, impacts and barriers. *International Journal of Electrical and Computer Engineering*, *12*(5), 4614–4622. https://doi.org/10.11591/ijece.v12i5.pp4614-4622

Han, Q., & Chu, F. (2021). Directional wind energy assessment of China based on nonparametric copula models. *Renewable Energy*, *164*, 1334–1349. https://doi.org/10.1016/j.renene.2020.10.149

Heinzeller, D., Dieng, D., Smiatek, G., Olusegun, C., Klein, C., Hamann, I., Salack, S., Bliefernicht, J., & Kunstmann, H. (2018). The WASCAL high-resolution regional climate simulation ensemble for West Africa: Concept, dissemination and assessment. *Earth System Science Data*, *10*(2), 815–835. https://doi.org/10.5194/essd-10-815-2018

Hersbach, H., Bell, B., Berrisford, P., Hirahara, S., Horányi, A., Muñoz-Sabater, J., Nicolas, J., Peubey, C., Radu, R., Schepers, D., Simmons, A., Soci, C., Abdalla, S.,

Abellan, X., Balsamo, G., Bechtold, P., Biavati, G., Bidlot, J., Bonavita, M., … Thépaut, J. N. (2020a). The ERA5 global reanalysis. *Quarterly Journal of the Royal Meteorological Society*, *146*(730), 1999–2049. https://doi.org/10.1002/qj.3803

Hersbach, H., Bell, B., Berrisford, P., Hirahara, S., Horányi, A., Muñoz-Sabater, J., Nicolas, J., Peubey, C., Radu, R., Schepers, D., Simmons, A., Soci, C., Abdalla, S., Abellan, X., Balsamo, G., Bechtold, P., Biavati, G., Bidlot, J., Bonavita, M., … Thépaut, J. N. (2020b). The ERA5 global reanalysis. *Quarterly Journal of the Royal Meteorological Society*, *146*(730), 1999–2049. https://doi.org/10.1002/qj.3803

Hueging, H., Haas, R., Born, K., Jacob, D., & Pinto, J. G. (2013). Regional changes in wind energy potential over Europe using regional climate model ensemble projections. *Journal of Applied Meteorology and Climatology*, *52*(4), 903–917. https://doi.org/10.1175/JAMC-D-12-086.1

IFC. (2020, November 2). *New Analysis Shows Onshore Wind Potential Across Africa Enough to Power the Entire Continent Many Times Over*. World Bank . https://www.ifc.org/en/pressroom/2020/new-analysis-shows-onshore-wind-potential-across-africa-enough-to-power-the-entire-continent-many-times-over

IPCC. (2021). *Climate Change 2021: The Physical Science Basis. Working Group I Contribution to the IPCC Sixth Assessment Report*. https://doi.org/https://dx.doi.org/10.1017/9781009157896

IRENA. (2025). *RENEWABLE CAPACITY STATISTICS 2025 STATISTIQUES DE CAPACITÉ RENOUVELABLE 2025 ESTADÍSTICAS DE CAPACIDAD RENOVABLE 2025 About IRENA*. www.irena.org

Jabbar, R. I. (2021). Statistical Analysis of Wind Speed Data and Assessment of Wind Power Density Using Weibull Distribution Function (Case Study: Four Regions in Iraq). *Journal of Physics: Conference Series*, *1804*(1). https://doi.org/10.1088/1742-6596/1804/1/012010

Joly, M., & Voldoire, A. (2009). Influence of ENSO on the West African monsoon: Temporal aspects and atmospheric processes. *Journal of Climate*, *22*(12), 3193–3210. https://doi.org/10.1175/2008JCLI2450.1

Jung, C., & Schindler, D. (2021). The role of the power law exponent in wind energy assessment: A global analysis. *International Journal of Energy Research*, *45*(6), 8484–8496. https://doi.org/10.1002/er.6382

Jurasz, J., Mikulik, J., Dabek, P. B., Guezgouz, M., & Kaźmierczak, B. (2021). Complementarity and 'resource droughts' of solar and wind energy in poland: An era5-based analysis. *Energies*, *14*(4). https://doi.org/10.3390/en14041118

Kaufman, Y. J., Boucher, O., Tanré, D., Chin, M., Remer, L. A., & Takemura, T. (2005). Aerosol anthropogenic component estimated from satellite data. *Geophysical Research Letters*, *32*(17), 1–4. https://doi.org/10.1029/2005GL023125

Kikumoto, H., Ooka, R., Sugawara, H., & Lim, J. (2017). Observational study of power-law approximation of wind profiles within an urban boundary layer for various wind conditions. *Journal of Wind Engineering and Industrial Aerodynamics*, *164*, 13–21. https://doi.org/10.1016/j.jweia.2017.02.003

Klutse, N. A. B., Ajayi, V. O., Gbobaniyi, E. O., Egbebiyi, T. S., Kouadio, K., Nkrumah, F., Quagraine, K. A., Olusegun, C., Diasso, U., Abiodun, B. J., Lawal, K., Nikulin, G., Lennard, C., & Dosio, A. (2018). Potential impact of 1.5 °c and 2 °c global warming on consecutive dry and wet days over West Africa. *Environmental Research Letters*, *13*(5). https://doi.org/10.1088/1748-9326/aab37b

Knight, J. R., Folland, C. K., & Scaife, A. A. (2006a). Climate impacts of the Atlantic multidecadal oscillation. *Geophysical Research Letters*, *33*(17). https://doi.org/10.1029/2006GL026242

Knight, J. R., Folland, C. K., & Scaife, A. A. (2006b). Climate impacts of the Atlantic multidecadal oscillation. *Geophysical Research Letters*, *33*(17). https://doi.org/10.1029/2006GL026242

K.O, O., V.O, A., A.H, F., & O.W, I. (2022). Projected changes in wind energy potential using CORDEX ensemble simulation over West Africa. *Meteorology and Atmospheric Physics*, *134*(3). https://doi.org/10.1007/s00703-022-00880-y

Kouogang Tchuenkam, F. C., Mama, A. C., Gah-Muti, S. Y., & Araujo, M. (2022). Variability of Sea Breezes Over the Cameroonian Coast and Their Interaction With the West African Monsoon. *Frontiers in Earth Science*, *10*. https://doi.org/10.3389/feart.2022.848684

Kruger, W., & Eberhard, A. (2018). Renewable energy auctions in sub-Saharan Africa: Comparing the South African, Ugandan, and Zambian Programs. In *Wiley Interdisciplinary Reviews: Energy and Environment* (Vol. 7, Issue 4). John Wiley and Sons Ltd. https://doi.org/10.1002/wene.295

Kunchala, R. K., Attada, R., Karumuri, R. K., Seelanki, V., Singh, B. B., Ashok, K., & Hoteit, I. (2024). Climatology, trends, and future projections of aerosol optical depth

over the Middle East and North Africa region in CMIP6 models. *Frontiers in Climate*, *6*. https://doi.org/10.3389/fclim.2024.1384202

Lakku, N. K. G., & Behera, M. R. (2022). Skill and Inter-Model Comparison of Regional and Global Climate Models in Simulating Wind Speed over South Asian Domain. *Climate*, *10*(6). https://doi.org/10.3390/cli10060085

Laura El-Katiri. (2021). *Sunny-side-up_Maximising-the-European-Green-Deals-potential-for-North-Africa-and-Europe*.

Li, Z. B., Xu, Y., Yuan, H. S., Chang, Y., & Shen, C. (2024a). AMO footprint of the recent near-surface wind speed change over China. *Environmental Research Letters* , *19*(11). https://doi.org/10.1088/1748-9326/ad7ee4

Li, Z. B., Xu, Y., Yuan, H. S., Chang, Y., & Shen, C. (2024b). AMO footprint of the recent near-surface wind speed change over China. *Environmental Research Letters* , *19*(11). https://doi.org/10.1088/1748-9326/ad7ee4

Lübbecke, J. F., Rodríguez-Fonseca, B., Richter, I., Martín-Rey, M., & Losada, T. (2011). *Article Title: Equatorial Atlantic variability-modes, mechanisms, and global teleconnections Article Type: Advanced review x*. https://core.ac.uk/download/pdf/158572105.pdf

Maidment, R. I., Allan, R. P., & Black, E. (2015). Recent observed and simulated changes in precipitation over Africa. *Geophysical Research Letters*, *42*(19), 8155–8164. https://doi.org/10.1002/2015GL065765

Martin, E. R., & Thorncroft, C. D. (2014). The impact of the AMO on the West African monsoon annual cycle. *Quarterly Journal of the Royal Meteorological Society*, *140*(678), 31–46. https://doi.org/10.1002/qj.2107

McSweeney, C. F., Jones, R. G., Lee, R. W., & Rowell, D. P. (2015). Selecting CMIP5 GCMs for downscaling over multiple regions. *Climate Dynamics*, *44*(11–12), 3237–3260. https://doi.org/10.1007/s00382-014-2418-8

Mcvicar, T. R., Roderick, M. L., Donohue, R. J., & Van Niel, T. G. (2012). Less bluster ahead? ecohydrological implications of global trends of terrestrial near-surface wind speeds. *Ecohydrology*, *5*(4), 381–388. https://doi.org/10.1002/eco.1298

Mentis, D., Hermann, S., Howells, M., Welsch, M., & Siyal, S. H. (2015). Assessing the technical wind energy potential in africa a GIS-based approach. *Renewable Energy*, *83*, 110–125. https://doi.org/10.1016/j.renene.2015.03.072

Merven, B., Burton, J., & Lehmann-Grube, P. (2021). *Assessment of new coal generation capacity targets in South Africa's 2019 Integrated Resource Plan for Electricity*.

Meulenbroeks, R., De Jongh, J., & Smulders, P. (1989). *A LITERATURE SURVEY ON THE WIND ENERGY POTENTIAL IN THE SAHEL*.

Miao, H., Xu, H., Huang, G., & Yang, K. (2023). Evaluation and future projections of wind energy resources over the Northern Hemisphere in CMIP5 and CMIP6 models. *Renewable Energy*, *211*, 809–821. https://doi.org/10.1016/j.renene.2023.05.007

Molina, M. O., Gutiérrez, C., & Sánchez, E. (2021). Comparison of ERA5 surface wind speed climatologies over Europe with observations from the HadISD dataset. *International Journal of Climatology*, *41*(10), 4864–4878. https://doi.org/10.1002/joc.7103

Monerie, P. A., Wainwright, C. M., Sidibe, M., & Akinsanola, A. A. (2020). Model uncertainties in climate change impacts on Sahel precipitation in ensembles of CMIP5 and CMIP6 simulations. *Climate Dynamics*, *55*(5–6), 1385–1401. https://doi.org/10.1007/s00382-020-05332-0

Natarajan, N., Rehman, S., Nandhini, S. S., & Vasudevan, M. (2020). Evaluation of Wind Energy Potential of the State of Tamil Nadu, India Based on Trend Analysis. *FME Transactions*, *49*(1), 244–251. https://doi.org/10.5937/FME2101244N

Ndiaye, A., Moussa, M. S., Dione, C., Sawadogo, W., Bliefernicht, J., Dungall, L., & Kunstmann, H. (2022). Projected Changes in Solar PV and Wind Energy Potential over West Africa: An Analysis of CORDEX-CORE Simulations. *Energies*, *15*(24). https://doi.org/10.3390/en15249602

Nefabas, K. L., Söder, L., Mamo, M., & Olauson, J. (2021). Modeling of ethiopian wind power production using era5 reanalysis data. *Energies*, *14*(9). https://doi.org/10.3390/en14092573

Niang, S. A. A., Gueye, A., Drame, M. S., Ba, A., Sarr, A., Nebon, B., Ndiaye, S. O., Niang, D. N., Dioum, A., & Talla, K. (2024a). Analysis of wind resources in Senegal using 100-meter wind data from ERA5 reanalysis. *Scientific African*, *26*. https://doi.org/10.1016/j.sciaf.2024.e02480

Niang, S. A. A., Gueye, A., Drame, M. S., Ba, A., Sarr, A., Nebon, B., Ndiaye, S. O., Niang, D. N., Dioum, A., & Talla, K. (2024b). Analysis of wind resources in Senegal using 100-meter wind data from ERA5 reanalysis. *Scientific African*, *26*. https://doi.org/10.1016/j.sciaf.2024.e02480

Nicholson, S. E. (2013). The West African Sahel: A Review of Recent Studies on the Rainfall Regime and Its Interannual Variability. *ISRN Meteorology*, *2013*, 1–32. https://doi.org/10.1155/2013/453521

Nkrumah, F., Quagraine, K. A., Leger Davy Quenum, G. M., Visioni, D., Koffi, H. A., & Browne Klutse, N. A. (2025). Assessing Regional Climate Trends in West Africa Under Geoengineering: A Multimodel Comparison of UKESM1 and CESM2. *Journal of Geophysical Research: Atmospheres*, *130*(13). https://doi.org/10.1029/2024JD043117

Nooni, I. K., Ogou, F. K., Chaibou, A. A. S., Nakoty, F. M., Gnitou, G. T., & Lu, J. (2023a). Evaluating CMIP6 Historical Mean Precipitation over Africa and the Arabian Peninsula against Satellite-Based Observation. *Atmosphere*, *14*(3). https://doi.org/10.3390/atmos14030607

Nooni, I. K., Ogou, F. K., Chaibou, A. A. S., Nakoty, F. M., Gnitou, G. T., & Lu, J. (2023b). Evaluating CMIP6 Historical Mean Precipitation over Africa and the Arabian Peninsula against Satellite-Based Observation. *Atmosphere*, *14*(3). https://doi.org/10.3390/atmos14030607

Ogunjobi, K. O., Adamu, Y., Akinsanola, A. A., & Orimoloye, I. R. (2018). Spatio-temporal analysis of land use dynamics and its potential indications on land surface temperature in Sokoto Metropolis, Nigeria. *Royal Society Open Science*, *5*(12). https://doi.org/10.1098/rsos.180661

Olujobi, O. J., Okorie, U. E., Olarinde, E. S., & Aina-Pelemo, A. D. (2023). Legal responses to energy security and sustainability in Nigeria's power sector amidst fossil fuel disruptions and low carbon energy transition. *Heliyon*, *9*(7). https://doi.org/10.1016/j.heliyon.2023.e17912

O'Neill, B. C., Tebaldi, C., Van Vuuren, D. P., Eyring, V., Friedlingstein, P., Hurtt, G., Knutti, R., Kriegler, E., Lamarque, J. F., Lowe, J., Meehl, G. A., Moss, R., Riahi, K., & Sanderson, B. M. (2016). The Scenario Model Intercomparison Project (ScenarioMIP) for CMIP6. *Geoscientific Model Development*, *9*(9), 3461–3482. https://doi.org/10.5194/gmd-9-3461-2016

Otunla, T. A., & Umoren, A. K. (2022). Wind Characteristics and Potentials of Two-Parameter Weibull Distribution and Maximum Entropy-Based Distribution Functions at an Equatorial Location. *Journal of Science and Technology*, *14*(2). https://doi.org/10.30880/jst.2022.14.02.005

Ouammi, A., Dagdougui, H., Sacile, R., & Mimet, A. (2010). Monthly and seasonal assessment of wind energy characteristics at four monitored locations in Liguria region (Italy). *Renewable and Sustainable Energy Reviews*, *14*(7), 1959–1968. https://doi.org/10.1016/j.rser.2010.04.015

Parker, D. J., Burton, R. R., Diongue-Niang, A., Ellis, R. J., Felton, M., Taylor, C. M., Thorncroft, C. D., Bessemoulin, P., & Tompkins, A. M. (2005). The diurnal cycle of the West African monsoon circulation. *Quarterly Journal of the Royal Meteorological Society*, *131*(611), 2839–2860. https://doi.org/10.1256/qj.04.52

Pillot, B., Muselli, M., Poggi, P., & Dias, J. B. (2019). Historical trends in global energy policy and renewable power system issues in Sub-Saharan Africa: The case of solar PV. *Energy Policy*, *127*, 113–124. https://doi.org/10.1016/j.enpol.2018.11.049

Piotrowski, P., Rutyna, I., Baczyński, D., & Kopyt, M. (2022). Evaluation Metrics for Wind Power Forecasts: A Comprehensive Review and Statistical Analysis of Errors. In *Energies* (Vol. 15, Issue 24). MDPI. https://doi.org/10.3390/en15249657

Poli, P., Hersbach, H., Dee, D. P., Berrisford, P., Simmons, A. J., Vitart, F., Laloyaux, P., Tan, D. G. H., Peubey, C., Thépaut, J. N., Trémolet, Y., Hólm, E. V., Bonavita, M., Isaksen, L., & Fisher, M. (2016). ERA-20C: An atmospheric reanalysis of the twentieth century. *Journal of Climate*, *29*(11), 4083–4097. https://doi.org/10.1175/JCLI-D-15-0556.1

Prospero, J. M., & Mayol-Bracero, O. L. (2013). Understanding the transport and impact of African dust on the Caribbean Basin. *Bulletin of the American Meteorological Society*, *94*(9), 1329–1337. https://doi.org/10.1175/BAMS-D-12-00142.1

Pryor, S. C., & Barthelmie, R. J. (2010). Climate change impacts on wind energy: A review. In *Renewable and Sustainable Energy Reviews* (Vol. 14, Issue 1, pp. 430–437). https://doi.org/10.1016/j.rser.2009.07.028

Ramon, J., Lledó, L., Torralba, V., Soret, A., & Doblas-Reyes, F. J. (2019). What global reanalysis best represents near-surface winds? *Quarterly Journal of the Royal Meteorological Society*, *145*(724), 3236–3251. https://doi.org/10.1002/qj.3616

Rehman, A., Alam, M. M., Ozturk, I., Alvarado, R., Murshed, M., Işık, C., & Ma, H. (2023). Globalization and renewable energy use: how are they contributing to upsurge the CO2 emissions? A global perspective. *Environmental Science and Pollution Research*, *30*(4), 9699–9712. https://doi.org/10.1007/s11356-022-22775-6

Rohrig, K., Berkhout, V., Callies, D., Durstewitz, M., Faulstich, S., Hahn, B., Jung, M., Pauscher, L., Seibel, A., Shan, M., Siefert, M., Steffen, J., Collmann, M., Czichon, S., Dörenkämper, M., Gottschall, J., Lange, B., Ruhle, A., Sayer, F., … Wenske, J. (2019). Powering the 21st century by wind energy - Options, facts, figures. *Applied Physics Reviews*, *6*(3). https://doi.org/10.1063/1.5089877

Sawadogo, W., Abiodun, B. J., & Okogbue, E. C. (2019a). Projected changes in wind energy potential over West Africa under the global warming of 1.5 °C and above. *Theoretical and Applied Climatology*, *138*(1–2), 321–333. https://doi.org/10.1007/s00704-019-02826-8

Sawadogo, W., Abiodun, B. J., & Okogbue, E. C. (2019b). Projected changes in wind energy potential over West Africa under the global warming of 1.5 °C and above. *Theoretical and Applied Climatology*, *138*(1–2), 321–333. https://doi.org/10.1007/s00704-019-02826-8

Schepanski, K., Heinold, B., & Tegen, I. (2017). Harmattan, Saharan heat low, and West African monsoon circulation: Modulations on the Saharan dust outflow towards the North Atlantic. *Atmospheric Chemistry and Physics*, *17*(17), 10223–10243. https://doi.org/10.5194/acp-17-10223-2017

Sedzro, K. S. A., Salami, A. A., Agbessi, P. A., & Kodjo, M. K. (2022). Comparative Study of Wind Energy Potential Estimation Methods for Wind Sites in Togo and Benin (West Sub-Saharan Africa). *Energies*, *15*(22). https://doi.org/10.3390/en15228654

Siyi, W. (2024). *Social and Economic Impacts of Renewable Energy Development in Morocco in the Context of International Relations: Opportunities and Challenges* (pp. 39–45). https://doi.org/10.2991/978-94-6463-459-4_5

Solaun, K., & Cerdá, E. (2019). Climate change impacts on renewable energy generation. A review of quantitative projections. In *Renewable and Sustainable Energy Reviews* (Vol. 116). Elsevier Ltd. https://doi.org/10.1016/j.rser.2019.109415

Spinoni, J., Barbosa, P., Bucchignani, E., Cassano, J., Cavazos, T., Christensen, J. H., Christensen, O. B., Coppola, E., Evans, J., Geyer, B., Giorgi, F., Hadjinicolaou, P., Jacob, D., Katzfey, J., Koenigk, T., Laprise, R., Lennard, C. J., Kurnaz, M. L., Delei, L. I., … Dosio, A. (2020). Future global meteorological drought hot spots: A study based on CORDEX data. *Journal of Climate*, *33*(9), 3635–3661. https://doi.org/10.1175/JCLI-D-19-0084.1

Sterl, S., Liersch, S., Koch, H., Lipzig, N. P. M. V., & Thiery, W. (2018). A new approach for assessing synergies of solar and wind power: Implications for West Africa. *Environmental Research Letters*, *13*(9). https://doi.org/10.1088/1748-9326/aad8f6

Storm, B., Dudhia, J., Basu, S., Swift, A., & Giammanco, I. (2009). Evaluation of the weather research and forecasting model on forecasting low-level jets: Implications for wind energy. *Wind Energy*, *12*(1), 81–90. https://doi.org/10.1002/we.288

Sultan, B., & Janicot, S. (2003). *The West African Monsoon Dynamics. Part II: The "'Preonset'" and " 'Onset'" of the Summer Monsoon*.

Sultan, B., Janicot, S., & Diedhiou, A. (2003). The West African monsoon dynamics, Part I : Intra-seasonal variability The West African Monsoon Dynamics. Part I: Documentation of Intraseasonal Variability. *Journal of Climate*, *16*, 3389–3406. https://doi.org/10.1175/1520

Taguela, T. N., Akinsanola, A. A., Adeliyi, T. E., Rhoades, A., & Nazarian, R. H. (2025). Understanding drivers and uncertainty in projected African precipitation. *Npj Climate and Atmospheric Science*, *8*(1). https://doi.org/10.1038/s41612-025-01123-8

Taylor, K. E., Stouffer, R. J., & Meehl, G. A. (2012). An overview of CMIP5 and the experiment design. In *Bulletin of the American Meteorological Society* (Vol. 93, Issue 4, pp. 485–498). https://doi.org/10.1175/BAMS-D-11-00094.1

Thomas, S. R., Nicolau, S., Martínez-Alvarado, O., Drew, D. J., & Bloomfield, H. C. (2021). *How Well Do Atmospheric Reanalyses Reproduce Observed Winds in Coastal Regions of Mexico?*

Todzo, S., Bichet, A., & Diedhiou, A. (2020). Intensification of the hydrological cycle expected in West Africa over the 21st century. *Earth System Dynamics*, *11*(1), 319–328. https://doi.org/10.5194/esd-11-319-2020

Toolan, C. A., Amooli, J. A., Wilcox, L. J., Samset, B. H., Turner, A. G., & Westervelt, D. M. (2024). *Strong inter-model differences and biases in CMIP6 simulations of PM 2.5 , aerosol optical depth, and precipitation over Africa*. https://doi.org/10.5194/egusphere-2024-3057

Toste, R., Assad, L. P. de F., & Landau, L. (2018). Downscaling of the global HadGEM2-ES results to model the future and present-day ocean conditions of the southeastern Brazilian continental shelf. *Climate Dynamics*, *51*(1–2), 143–159. https://doi.org/10.1007/s00382-017-3911-7

Troccoli, A., Zambon, F., Hodges, K. I., & Marani, M. (2012). Storm surge frequency reduction in Venice under climate change. *Climatic Change*, *113*(3–4), 1065–1079. https://doi.org/10.1007/s10584-011-0093-x

Tushar K. Ghosh and Mark A. Prelas. (2011). *Energy Resources and Systems*.

van der Zwaan, B., Kober, T., Longa, F. D., van der Laan, A., & Jan Kramer, G. (2018). An integrated assessment of pathways for low-carbon development in Africa. *Energy Policy*, *117*, 387–395. https://doi.org/10.1016/j.enpol.2018.03.017

Wang, Z., & Liu, W. (2021). Wind energy potential assessment based on wind speed, its direction and power data. *Scientific Reports*, *11*(1). https://doi.org/10.1038/s41598-021-96376-7

Yaro, J. A., & Hesselberg, J. (2016). *Adaptation to Climate Change and Variability in Rural West Africa*. https://doi.org/10.1007/978-3-319-31499-0

Yeo, K., Yoroba, F., & Oluleye, A. (2025). Spatio-Temporal Trends of Dust Storms Drivers and Their Role in the Decline of Dust Activity over North Africa. *Journal of Geoscience and Environment Protection*, *13*(07), 191–208. https://doi.org/10.4236/gep.2025.137012

Youm, I., Sarr, J., Sall, M., Ndiaye, A., & Kane, M. M. (2005). Analysis of wind data and wind energy potential along the northern coast of Senegal. *Journal of Renewable Energies*, *8*(2), 95–108. https://doi.org/10.54966/jreen.v8i2.855

Zeng, Z., Ziegler, A. D., Searchinger, T., Yang, L., Chen, A., Ju, K., Piao, S., Li, L. Z. X., Ciais, P., Chen, D., Liu, J., Azorin-Molina, C., Chappell, A., Medvigy, D., & Wood, E. F. (2019). A reversal in global terrestrial stilling and its implications for wind energy production. *Nature Climate Change*, *9*(12), 979–985. https://doi.org/10.1038/s41558-019-0622-6

Zha, J., Chuan, T., Wu, J., Zhao, D., Luo, M., Feng, J., Fan, W., Shen, C., & Jiang, H. (2024). Attribution of Terrestrial Near-Surface Wind Speed Changes Across China at a Centennial Scale. *Geophysical Research Letters*, *51*(7). https://doi.org/10.1029/2024GL108241

Zha, J., Shen, C., Li, Z., Wu, J., Zhao, D., Fan, W., Sun, M., Azorin-Molina, C., & Deng, K. (2021). Projected changes in global terrestrial near-surface wind speed in 1.5 °c-4.0 °c global warming levels. *Environmental Research Letters*, *16*(11). https://doi.org/10.1088/1748-9326/ac2fdd

Zhang, R., & Delworth, T. L. (2006). Impact of Atlantic multidecadal oscillations on India/Sahel rainfall and Atlantic hurricanes. *Geophysical Research Letters*, *33*(17). https://doi.org/10.1029/2006GL026267

Zhang, Z. (2025). Exploring the nexus: Climate change concerns, renewable energy, and carbon emissions. *Journal of Environmental Management*, *376*. https://doi.org/10.1016/j.jenvman.2025.124413

Zhang, Z., & Li, G. (2022). Uncertainty in the projected changes of Sahel summer rainfall under global warming in CMIP5 and CMIP6 multi-model ensembles. *Climate Dynamics*, *59*(11–12), 3579–3597. https://doi.org/10.1007/s00382-022-06284-3

Zhao, C., Geng, X., & Qi, L. (2022). Atlantic Multidecadal Oscillation Modulates the Relation of ENSO With the Precipitation in the Central-Western Indian Ocean. *Frontiers in Earth Science*, *10*. https://doi.org/10.3389/feart.2022.866241

Zhao, L., Jin, S., Liu, X., Wang, B., Song, Z., Hu, J., & Guo, Y. (2021). Assessment of CMIP6 Model Performance for Wind Speed in China. *Frontiers in Climate*, *3*. https://doi.org/10.3389/fclim.2021.735988

APPENDICES

Table A1: Variability analysis, seasonal mean wind speed with standard deviations

Region seasonal averages					
Seasons	Atlantic coastal	Saharan	Southern Coastal	Sub-Sahara	Sahel
	Mean±SD (m/s)	Mean±SD (m/s)	Mean±SD (m/s)	Mean±SD(m/s)	Mean ±SD(m/s)
DJF	4.186 ±0.516	3.74 ±0.721	2.262 ± 0.394	1.715 ± 0.291	2.846 ±0.578
MAM	4.026 ±0.597	2.421 ± 0.622	2.430 ± 0.570	1.811 ± 0.278	2.012 ± 0.628
JJA	3.490 ± 0.711	2.325 ± 0.822	3.779 ± 0.459	1.952 ± 0.379	2.110 ± 0715
SON	3.024 ±0.582	3.394 ±0.743	2.200 ± 0.424	1.370 ± 0.215	2.308 ± 0.75

Table A2: Variability analysis, summary statistics

Statistics	Atlantic coastal	Saharan	Southern Coastal	Sub-Sahara	Sahel
counts	21600	21600	21600	21600	21600
mean	3.68	2.97	2.67	1.71	2.32
SD	0.76	0.95	0.80	0.37	0.74
min	1.51	0.81	0.90	0.77	0.61
25%	3.11	2.24	2.08	1.43	1.75
50%	3.74	2.99	2.45	1.68	2.29
75%	4.26	3.64	3.25	1.96	2.85
max	6.08	6.96	4.95	3.28	5.48

Table A3: Wind Extreme Statistics summary sub-Sahara

	Basic statistics	Extreme events
Sub-sahara	• Data coverage: 21,600 time points • Mean wind speed: 1.71 ± 0.37 m/s • Wind speed range: 0.77 - 3.28 m/s • 90th percentile threshold: 2.19 m/s • 95th percentile threshold: 2.34 m/s • 99th percentile threshold: 2.67 m/s	• Moderate events (≥90th percentile): 2160 • Total extreme events (≥95th percentile): 1,080 • Total severe events (≥99th percentile): 216 • Extreme event frequency: 5.00% of total time
Seasonal distribution	Event duration statistics (hours)	Top 3 longest events
• DJF Dry: 22 events (2.0%) • MAM Trans: 168 events (15.6%) • JJA Wet: 890 events (82.4%) • SON Trans: 0 events (0.0%)	• Average duration: 4.2 • Median duration: 3.0 • Maximum duration: 22 • Minimum duration: 1 • Standard deviation: 4.2	• 1958-07-01 00:00 to 1958-07-01 21:00 Duration: 22 hours | Max speed: 3.23 m/s | Season: JJA Wet • 2024-08-01 00:00 to 2024-08-01 21:00 Duration: 22 hours | Max speed: 3.19 m/s | Season: JJA Wet • 1954-07-01 01:00 to 1954-07-01 21:00 Duration: 21 hours | Max speed: 3.28 m/s | Season: JJA Wet

Table A4: Wind Extreme Statistics summary Atlantic coastal

	Basic statistics	Extreme events
Atlantic coastal	• Data coverage: 21,600 time points • Mean wind speed: 3.68 ± 0.76 m/s • Wind speed range: 1.51 - 6.08 m/s • 90th percentile threshold: 4.64 m/s • 95th percentile threshold: 4.85 m/s • 99th percentile threshold: 5.16 m/s	• Moderate events (≥90th percentile): 2160 • Total extreme events (≥95th percentile): 1,080 • Total severe events (≥99th percentile): 216 • Extreme event frequency: 5.00% of total time
Seasonal distribution	Event duration statistics (hours)	Top 3 longest events

• DJF Dry: 320 events (29.6%) • MAM Trans: 679 events (62.9%) • JJA Wet: 81 events (7.5%) • SON Trans: 0 events (0.0%)	• Average duration: 5.8 • Median duration: 5.0 • Maximum duration: 24 • Minimum duration: 1 • Standard deviation: 4.1	• 1974-03-01 00:00 to 1974-03-01 23:00 Duration: 24 hours | Max speed: 5.75 m/s | Season: MAM Trans • 2009-02-01 00:00 to 2009-02-01 23:00 Duration: 24 hours | Max speed: 5.47 m/s | Season: DJF Dry • 2009-01-01 00:00 to 2009-01-01 16:00 Duration: 17 hours | Max speed: 6.08 m/s | Season: DJF Dry

Table A5: Wind Extreme Statistics summary Sahara

	Basic statistics	Extreme events
Sahara	• Data coverage: 21,600 time points • Mean wind speed: 2.97 ± 0.95 m/s • Wind speed range: 0.81 - 6.96 m/s • 90th percentile: 4.196 m/s • 95th percentile threshold: 4.54 m/s • 99th percentile threshold: 5.25 m/s	• Moderate events (≥90th percentile): 2160 • Total extreme events (≥95th percentile): 1,080 • Total severe events (≥99th percentile): 216 • Extreme event frequency: 5.00% of total time

Seasonal distribution	Event duration statistics (hours)	Top 3 longest events
• DJF Dry: 901 events (83.4%) • MAM Trans: 77 events (7.1%) • JJA Wet: 19 events (1.8%) • SON Trans: 83 events (7.7%)	• Average duration: 5.3 • Median duration: 4.0 • Maximum duration: 24 • Minimum duration: 1 • Standard deviation: 4.6	• 1983-01-01 00:00 to 1983-01-01 23:00 Duration: 24 hours | Max speed: 6.96 m/s | Season: DJF Dry • 1961-02-01 00:00 to 1961-02-01 17:00 Duration: 18 hours | Max speed: 6.23 m/s | Season: DJF Dry • 1967-01-01 00:00 to 1967-01-01 17:00 Duration: 18 hours | Max speed: 6.15 m/s | Season: DJF Dry

Table A6: Wind Extreme Statistics summary Sahel

	Basic statistics	Extreme events
SaheL	• Data coverage: 21,600 time points • Mean wind speed: 2.32 ± 0.74 m/s • Wind speed range: 0.61 - 5.48 m/s • 90th percentile: 3.29 m/s • 95th percentile threshold: 3.60 m/s • 99th percentile threshold: 4.12 m/s	• Moderate events (≥90th percentile): 2160 • Total extreme events (≥95th percentile): 1,080 • Total severe events (≥99th percentile): 216 • Extreme event frequency: 5.00% of total time
Seasonal distribution	Event duration statistics (hours)	Top 3 longest events
• DJF Dry:750 events (69.4%) • MAM Trans: 22 events (2.0%) • JJA Wet: 276 events (25.6%) • SON Trans: 32 events (3.0%)	• Average duration: 4.0 • Median duration: 3.0 • Maximum duration: 18 • Minimum duration: 1 • Standard deviation: 2.6	• 1983-01-01 00:00 to 1983-01-01 17:00 Duration: 18 hours | Max speed: 5.48 m/s | Season: DJF Dry • 1997-02-01 00:00 to 1997-02-01 16:00 Duration: 17 hours | Max speed: 5.07 m/s | Season: DJF Dry • 1989-01-01 06:00 to 1989-01-01 16:00 Duration: 11 hours | Max speed: 4.82 m/s | Season: DJF Dry

Table A7: Wind Extreme Statistics summary Southern coastal

	BASIC STATISTICS	EXTREME EVENTS
Southern coastal	• Data coverage: 21,600 time points • Mean wind speed: 2.67 ± 0.80 m/s • Wind speed range: 0.90 - 4.95 m/s • 90th percentile threshold: 3.95 m/s • 95th percentile threshold: 4.18 m/s • 99th percentile threshold: 4.52 m/s	• Moderate events (≥90th percentile): 2160 • Total extreme events (≥95th percentile): 1,080 • Total severe events (≥99th percentile): 216 • Extreme event frequency: 5.00% of total time
Seasonal distribution	Event duration statistics (hours)	Top 3 longest events
• DJF Dry: 0 events (0.0%) • MAM Trans: 0 events (0.0%) • JJA Wet: 1029 events (95.3%) • SON Trans: 51 events (4.7%)	• Average duration: 8.4 • Median duration: 8.0 • Maximum duration: 24 • Minimum duration: 1 • Standard deviation: 5.7	• 2024-07-01 00:00 to 2024-07-01 23:00 Duration: 24 hours | Max speed: 4.60 m/s | Season: JJA Wet • 2024-08-01 00:00 to 2024-08-01 23:00 Duration: 24 hours | Max speed: 4.69 m/s | Season: JJA Wet • 1954-07-01 01:00 to 1954-07-01 22:00 Duration: 22 hours | Max speed: 4.82 m/s | Season: JJA Wet

Table A8: Subregional Wind Speed Bias Summary (Model − ERA5)

Model	Region	Mean Bias (m/s)	Min Bias (m/s)	Max Bias (m/s)	Std Dev (m/s)
CESM2-WACCM	Atlantic Coastal Zone	0.332	-1.171	2.325	0.731
CESM2-WACCM	Saharan Zone	0.063	-0.762	1.676	0.306
CESM2-WACCM	Sahelian Zone	1.105	-0.161	1.954	0.448
CESM2-WACCM	Southern Coastal Zone	0.039	-1.580	1.399	0.469
CESM2-WACCM	Sub-Saharan Zone	0.858	-1.131	2.071	0.536
HadGEM3	Atlantic Coastal Zone	0.655	-0.288	1.826	0.378
HadGEM3	Saharan Zone	0.729	-1.338	1.787	0.508
HadGEM3	Sahelian Zone	0.108	-0.846	1.549	0.301
HadGEM3	Southern Coastal Zone	0.302	-1.166	1.394	0.378

Model	Region	Mean Bias (m/s)	Min Bias (m/s)	Max Bias (m/s)	Std Dev (m/s)
HadGEM3	Sub-Saharan Zone	0.143	-0.995	1.502	0.372
MIROC6	Atlantic Coastal Zone	0.284	-1.327	1.605	0.543
MIROC6	Saharan Zone	-0.625	-2.251	0.810	0.353
MIROC6	Sahelian Zone	0.170	-1.457	1.382	0.430
MIROC6	Southern Coastal Zone	-0.762	-3.066	0.584	0.687
MIROC6	Sub-Saharan Zone	-0.685	-2.899	0.592	0.583
MPI-ESM	Atlantic Coastal Zone	0.108	-1.135	1.548	0.417
MPI-ESM	Saharan Zone	0.095	-1.100	1.926	0.378
MPI-ESM	Sahelian Zone	0.429	-0.755	1.383	0.379

Model	Region	Mean Bias (m/s)	Min Bias (m/s)	Max Bias (m/s)	Std Dev (m/s)
MPI-ESM	Southern Coastal Zone	-0.537	-2.360	0.558	0.482
MPI-ESM	Sub-Saharan Zone	-0.217	-2.164	1.067	0.411

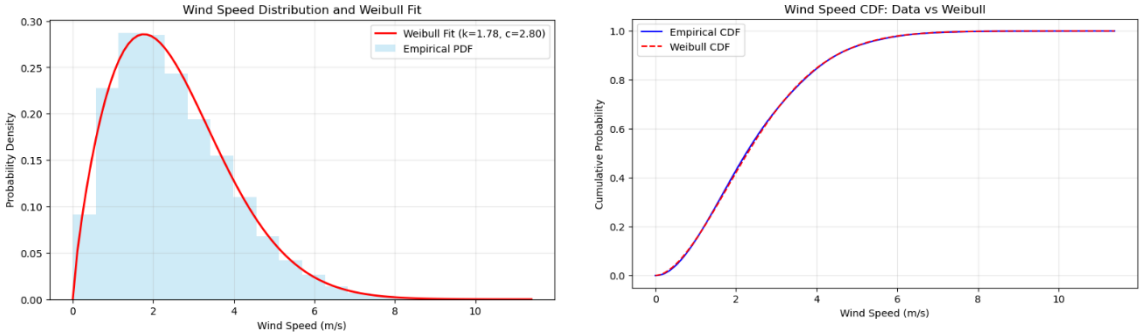

Figure A1:ERA5 10-m wind speeds at the study site, 1950–2024. (left panel) Histogram of wind speed. (right panel) Empirical cumulative distribution function (blue solid) versus the Weibull CDF (red dashed).

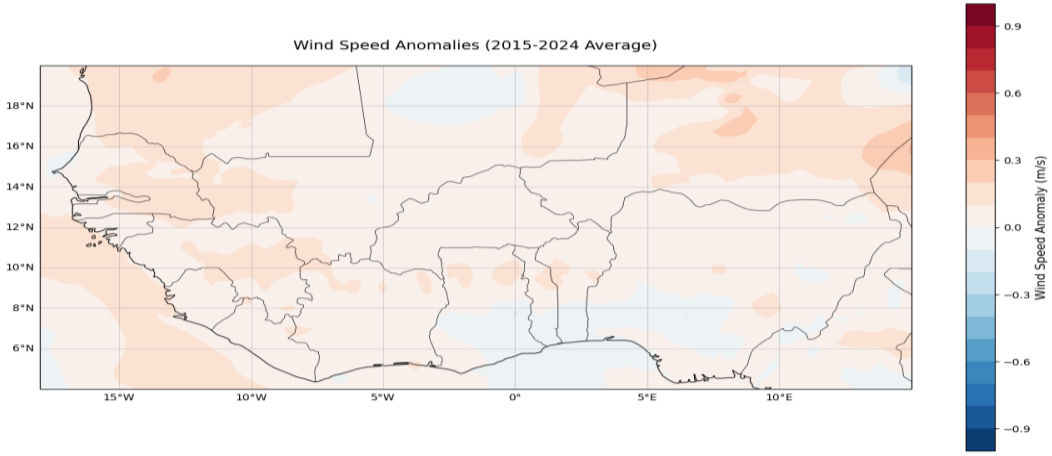

Figure A2: ERA5 reanalysis 10-m wind-speed anomalies over West Africa (4–20° N, 18° W–15° E), 1950–2024. Map of the 2015–2024 average anomaly (m/s), computed relative to the 1950–2024 climatology at each grid cell; red (blue) shading indicates above- (below-) average winds.

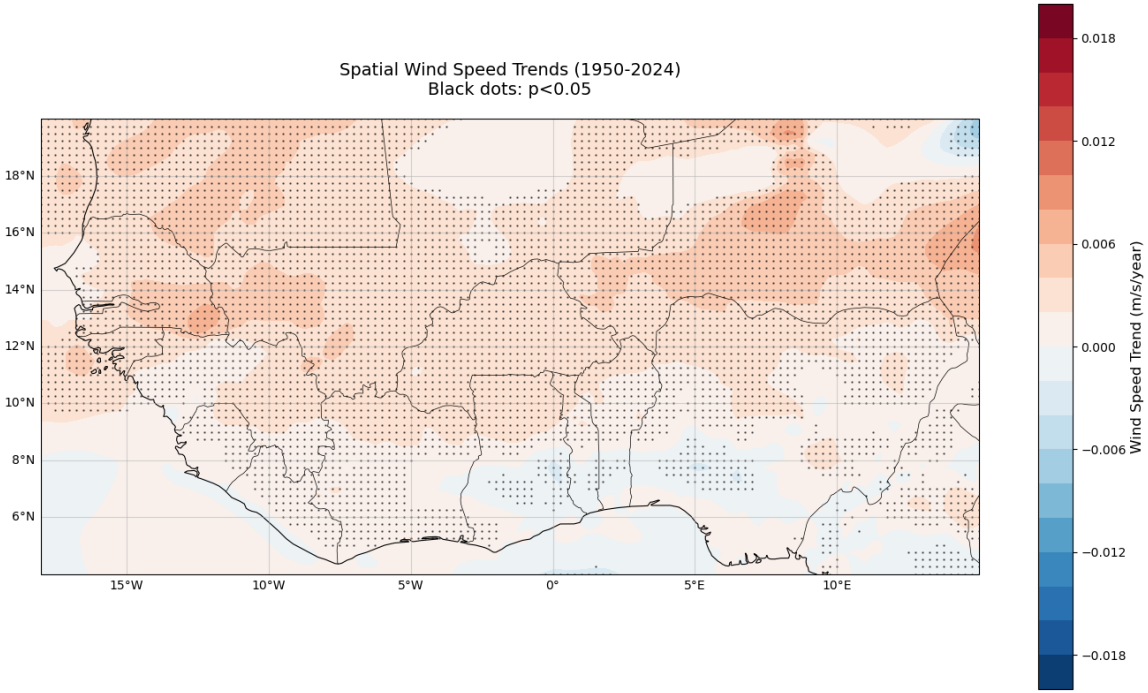

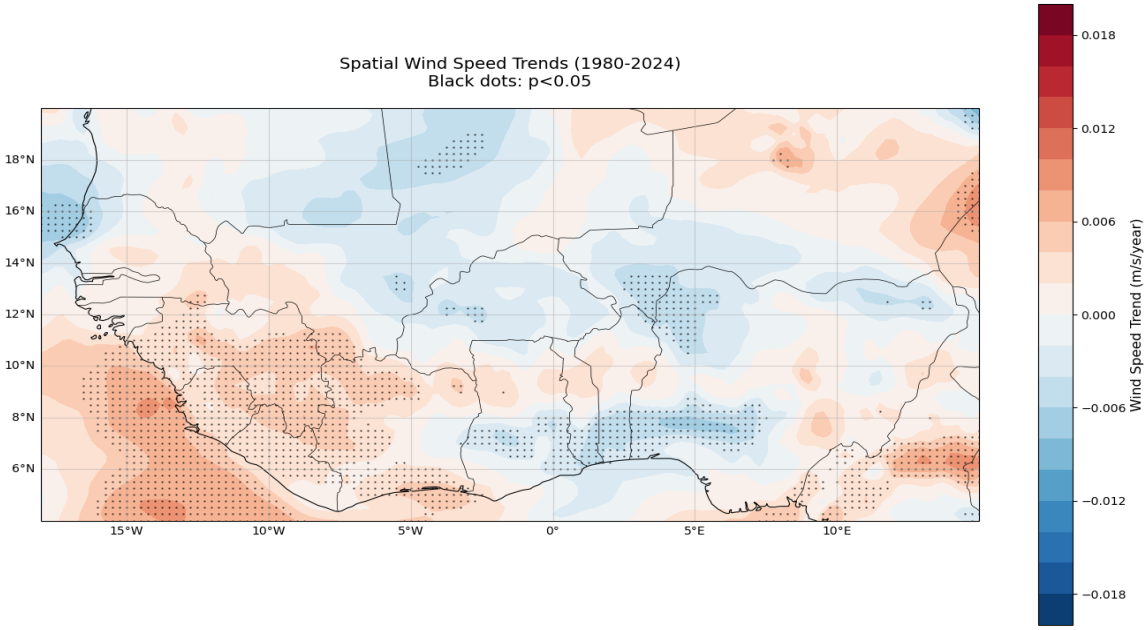

Figure A3:Spatial distribution of wind speed trends across West Africa from 1950-2024 at 10m (panel a) and from 1980-2024 (panel b) at 100m, showing linear trend coefficients in m/s per year. . Black dots indicate grid points where trends are statistically significant ($p < 0.05$).

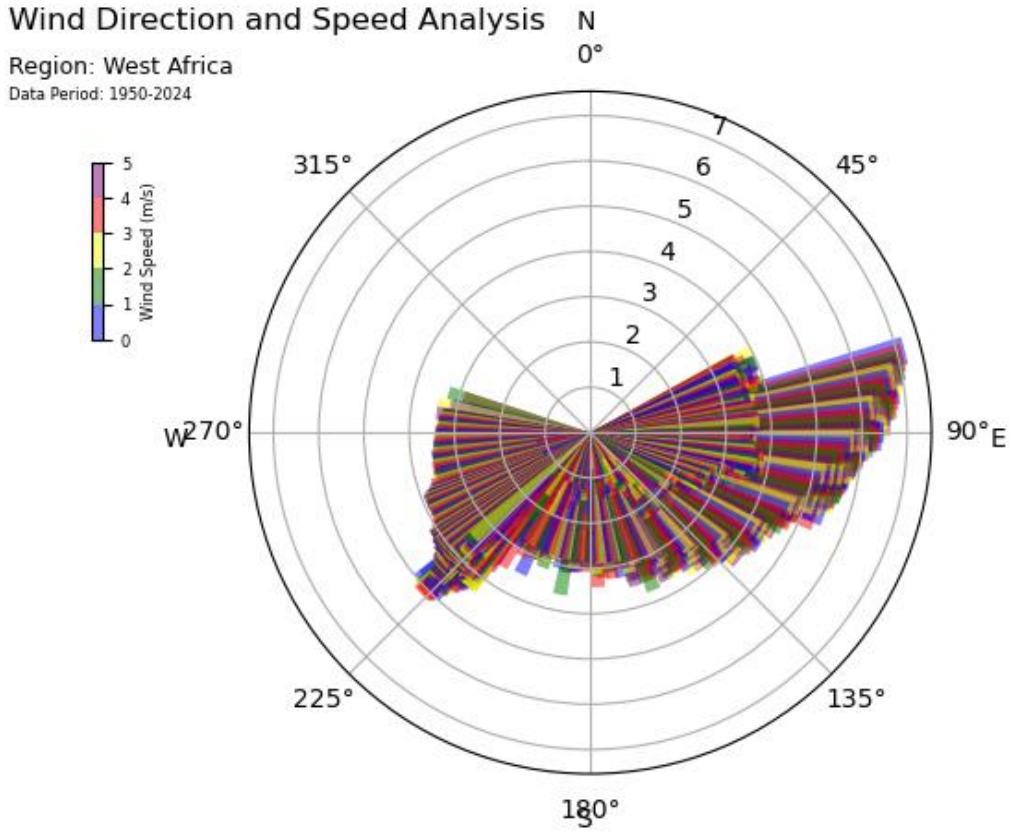

FigureA4:Wind direction and speed, West Africa (1950–2024). Polar wind-rose summarizing near-surface winds over West Africa. Angular position is meteorological direction (degrees clockwise from north); radial length indicates relative frequency (%).

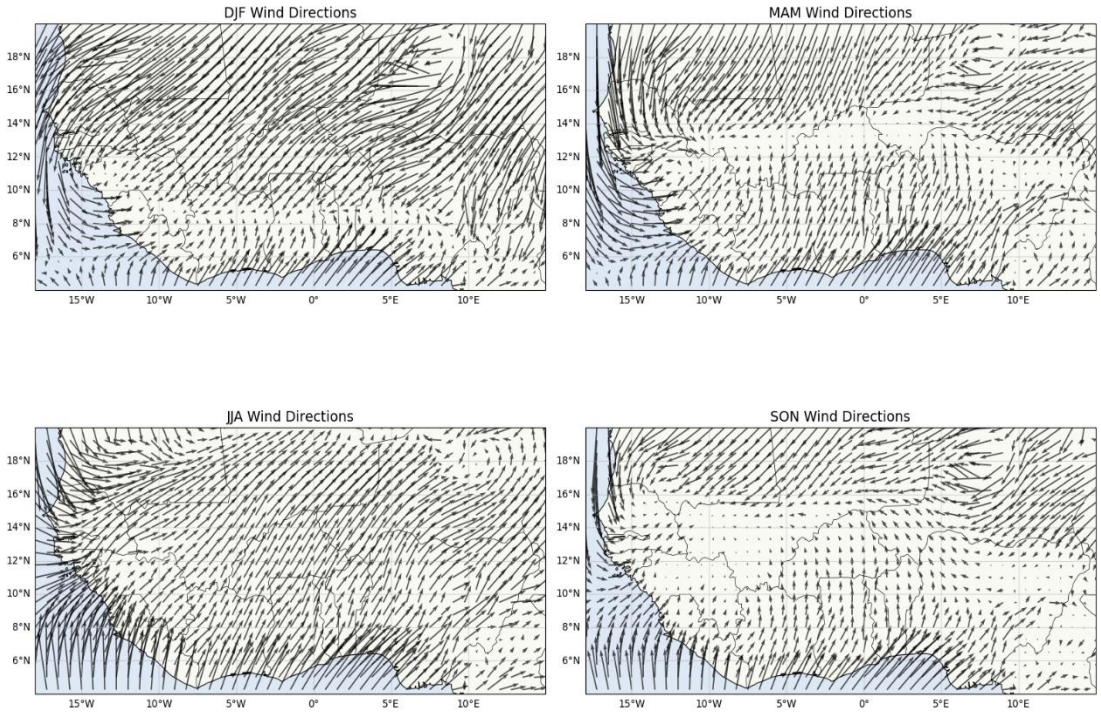

Figure A5: Seasonal surface wind vectors over West Africa (study period: 1950–2024; 10 m altitude). The scatter plots show the climate-averaged wind direction and relative wind speed for (top letf) DJF, (top right) MAM, (bottom left) JJA, and (bottom right) SON in the region ~18° W–15° E and 4–20° N. The direction of the arrows indicates the average wind direction, and the length of the arrows is proportional to the average wind speed at each grid point.

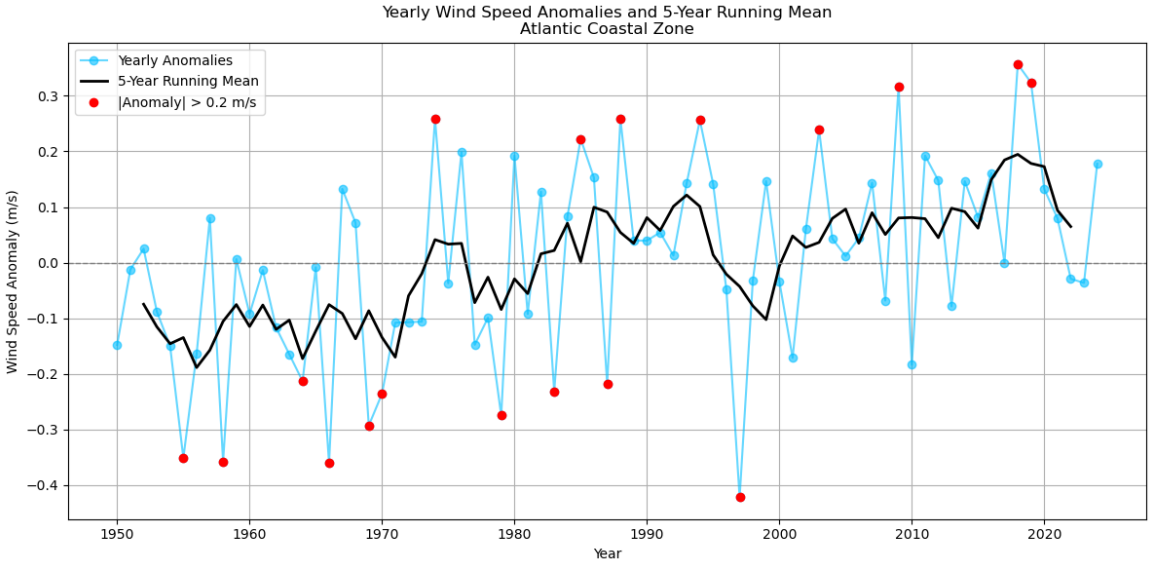

Figure A*6*:Annual anomalies of 10 m wind speed in the Atlantic Coastal zone (1950–2024).

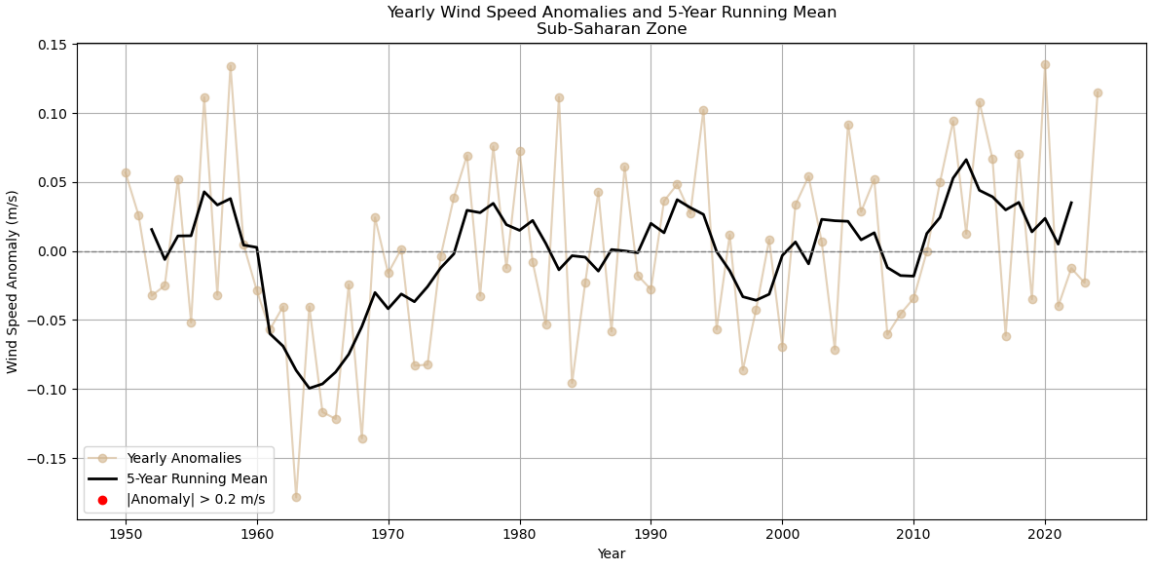

Figure A7:Annual anomalies of 10 m wind speed in the sub-Sahara zone (1950–2024).

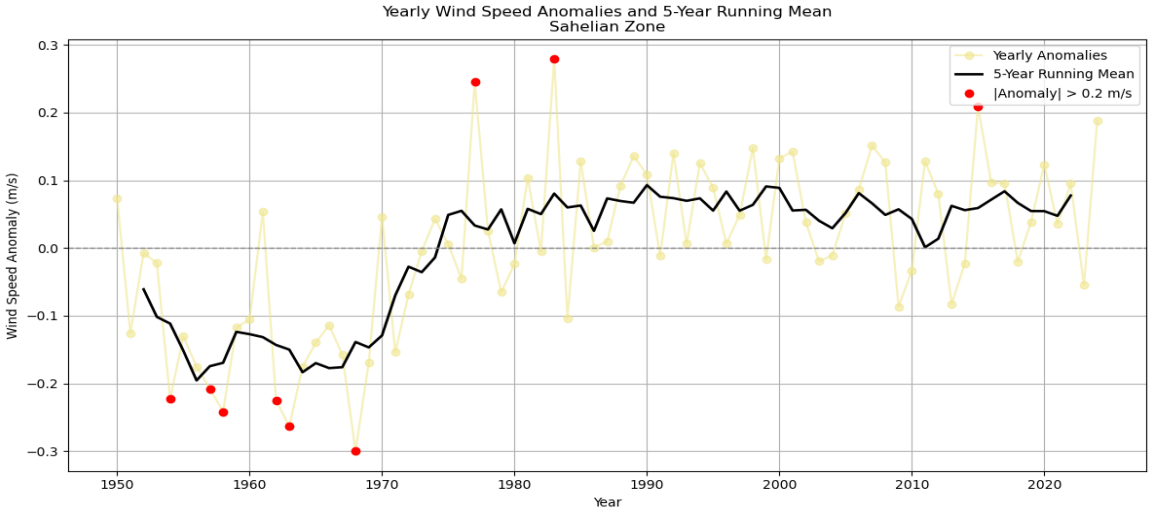

Figure A*8*:Annual anomalies of 10 m wind speed in the Sahelian zone (1950–2024).

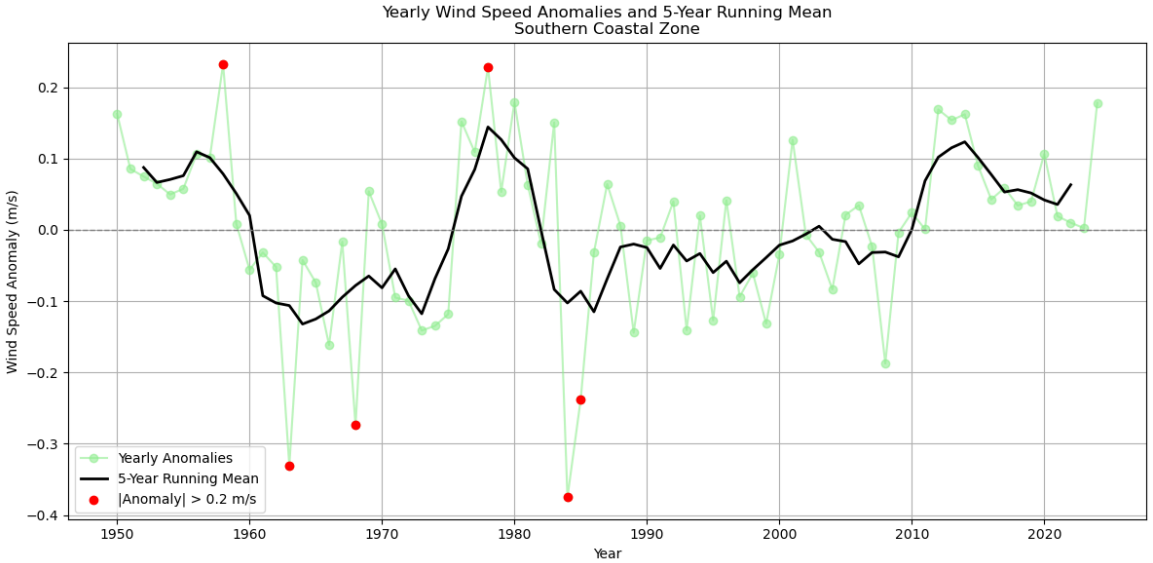

Figure A*9*:Annual anomalies of 10 m wind speed in the Southern Coastal zone (1950–2024).

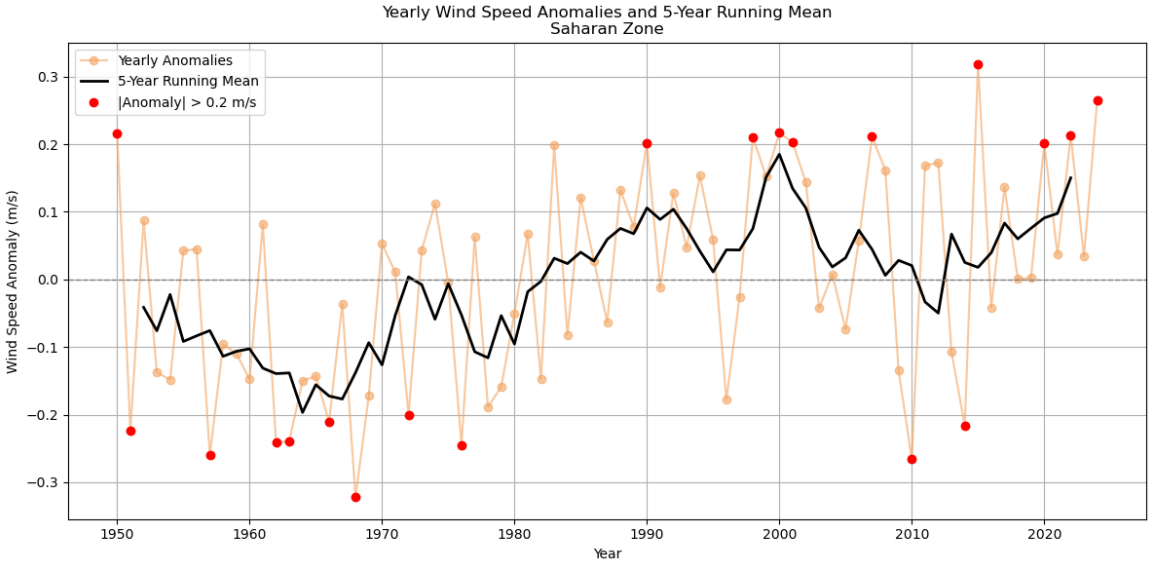

Figure A*10*:Annual anomalies of 10 m wind speed in the Sahara zone (1950–2024).

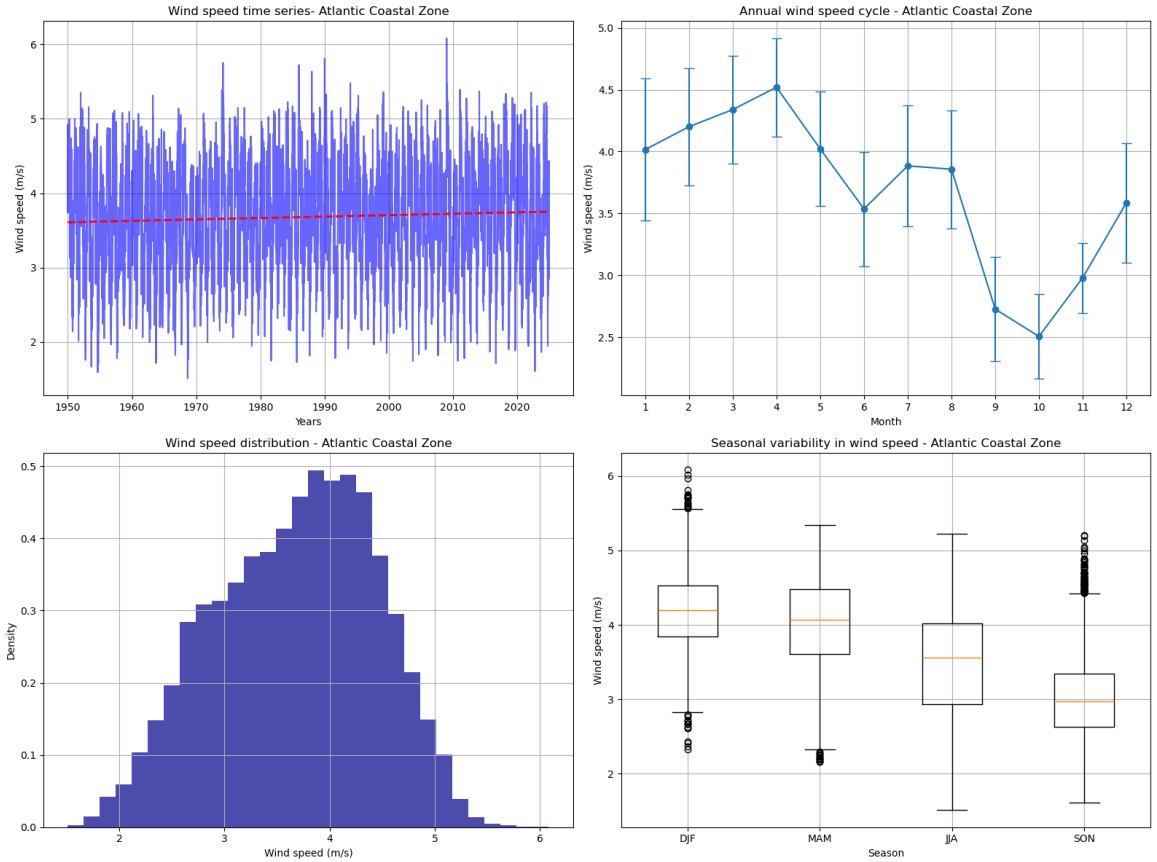

Figure A11: Wind speed Variability analysis Atlantic coastal

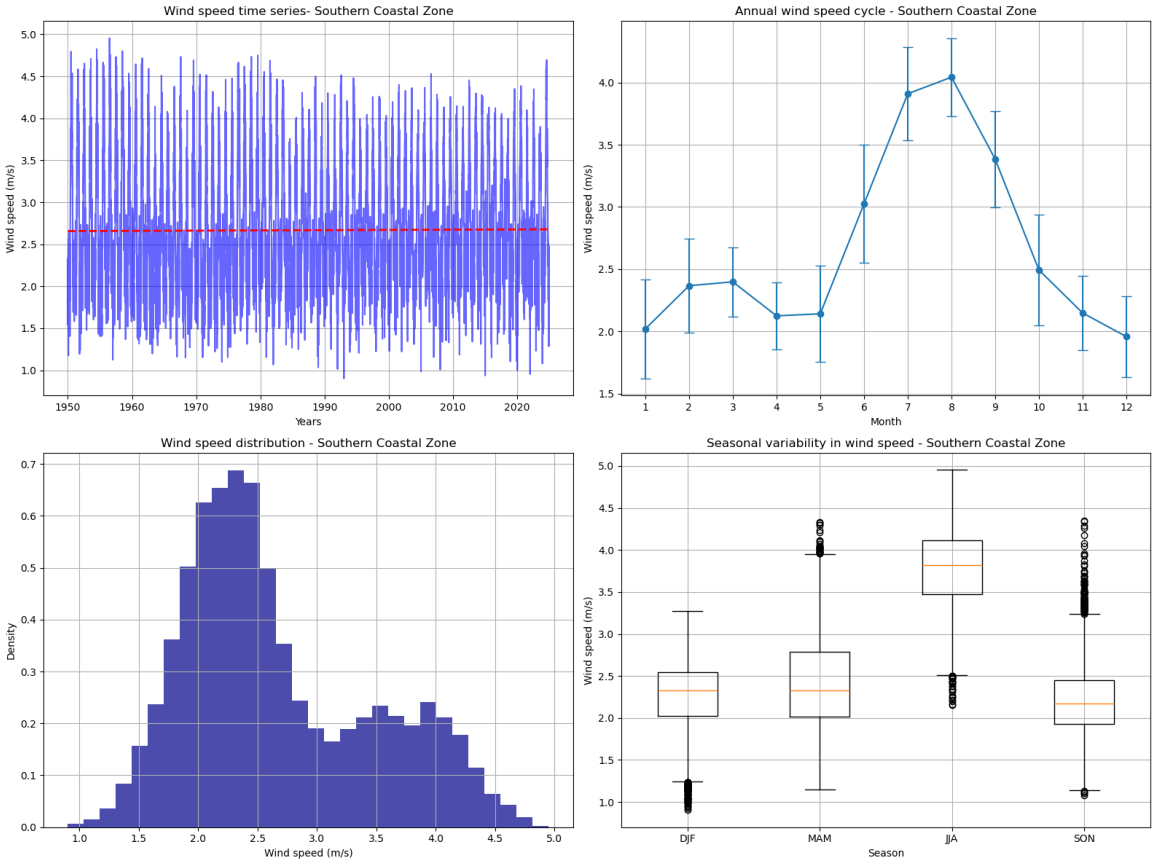

Figure A12: Wind speed Variability analysis Southern coastal

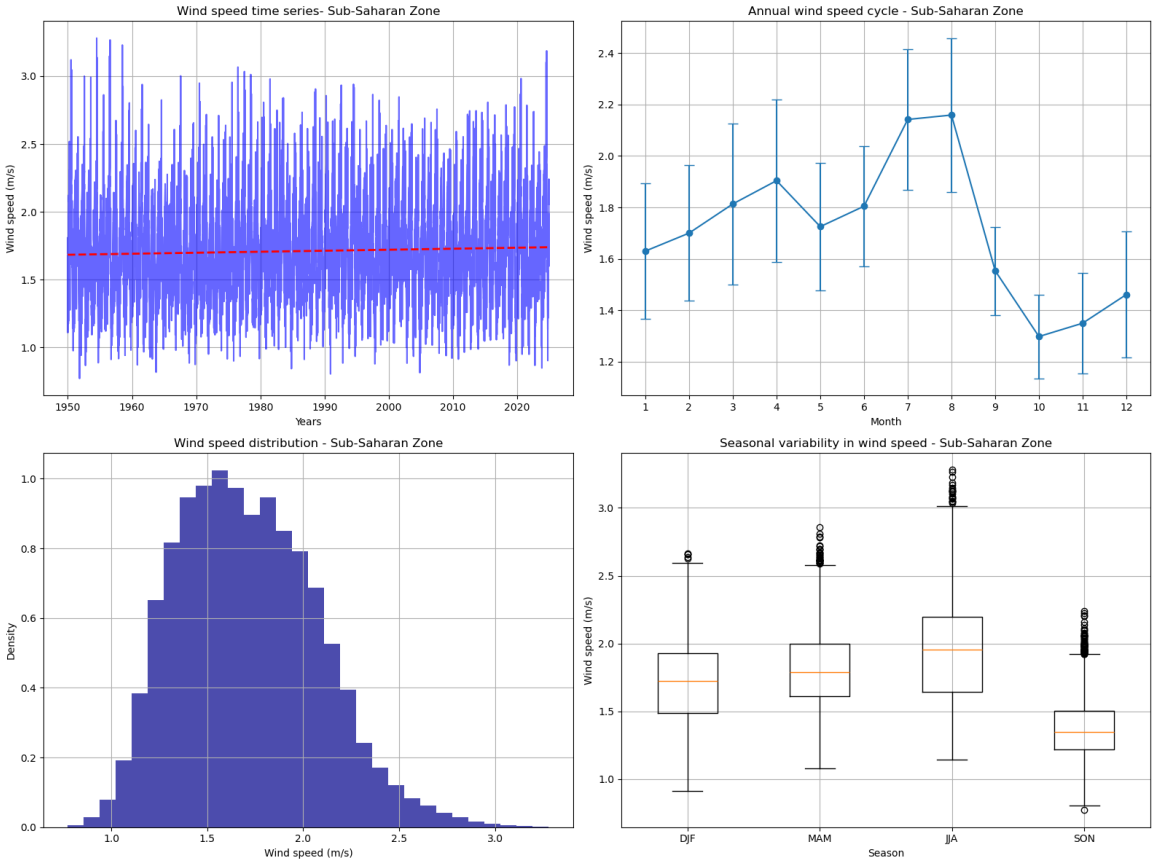

Figure A13: Wind speed Variability analysis sub-Sahara zone

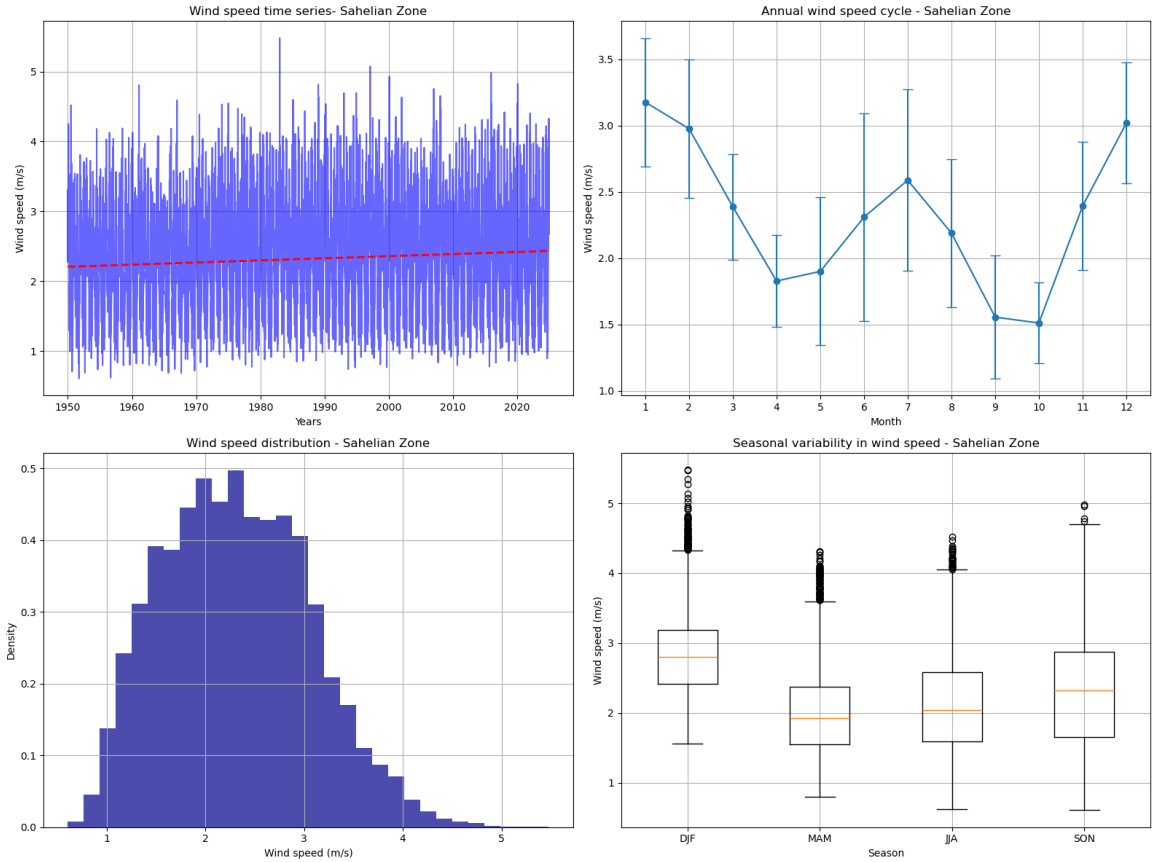

Figure A14: Wind speed Variability analysis Sahelian zone

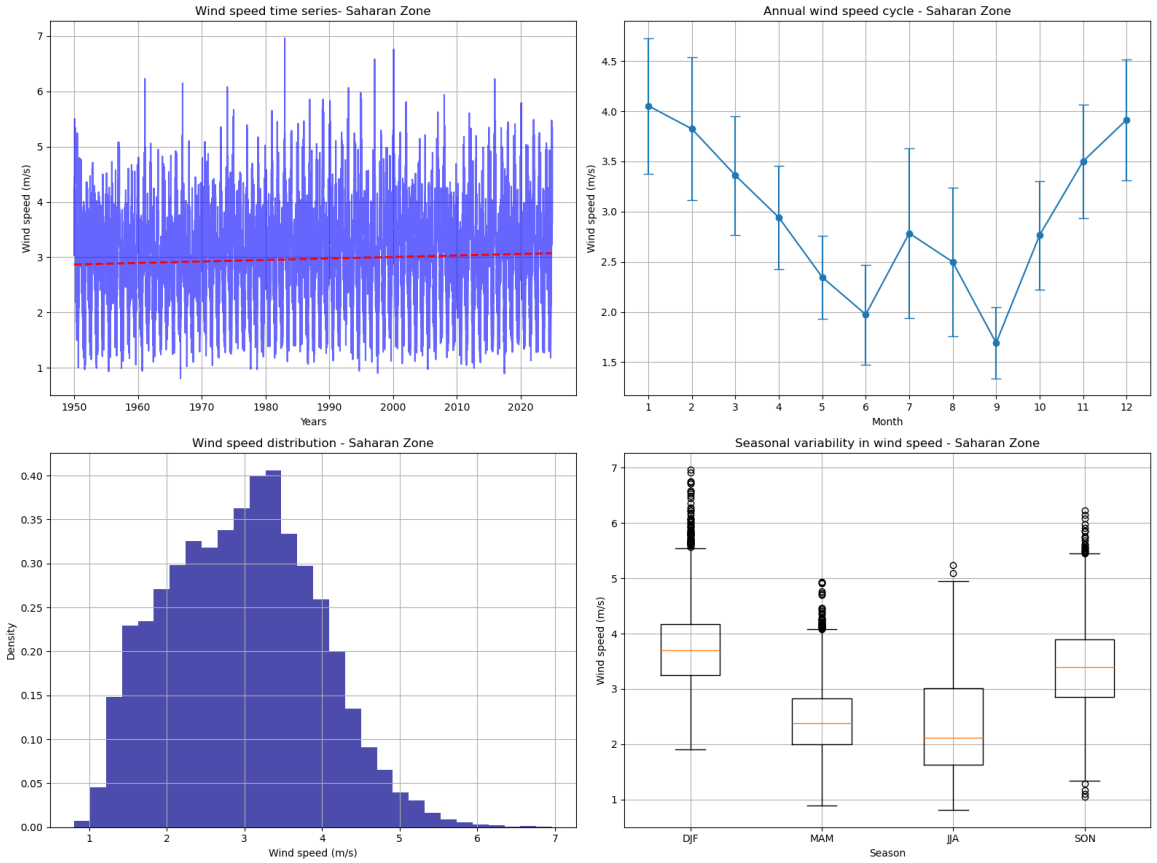

Figure A15: Wind speed Variability analysis Saharan zone

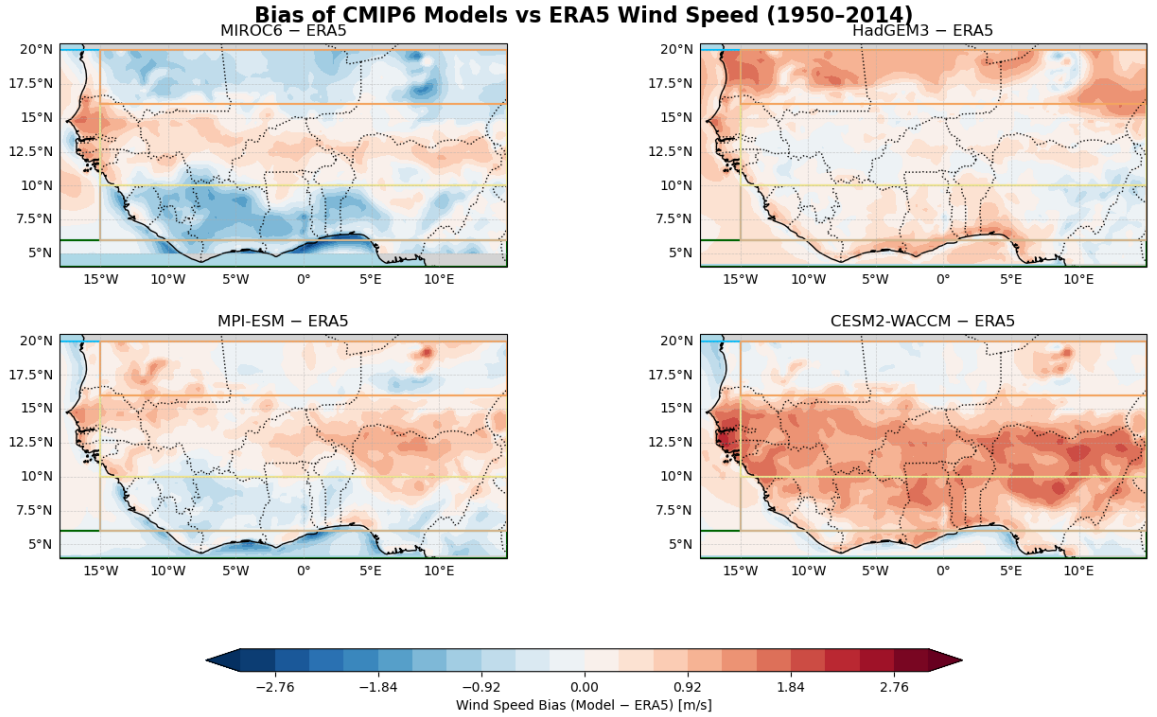

Figure A16 :Model bias in mean near-surface wind speed over West Africa for 1950–2014, computed as Model − ERA5 to assess departures from the ERA5 observational benchmark. Panels show (top-left) MIROC6, (top-right) HadGEM3, (bottom-letf) MPI-ESM, (bottom-right) CESM2-WACCM.

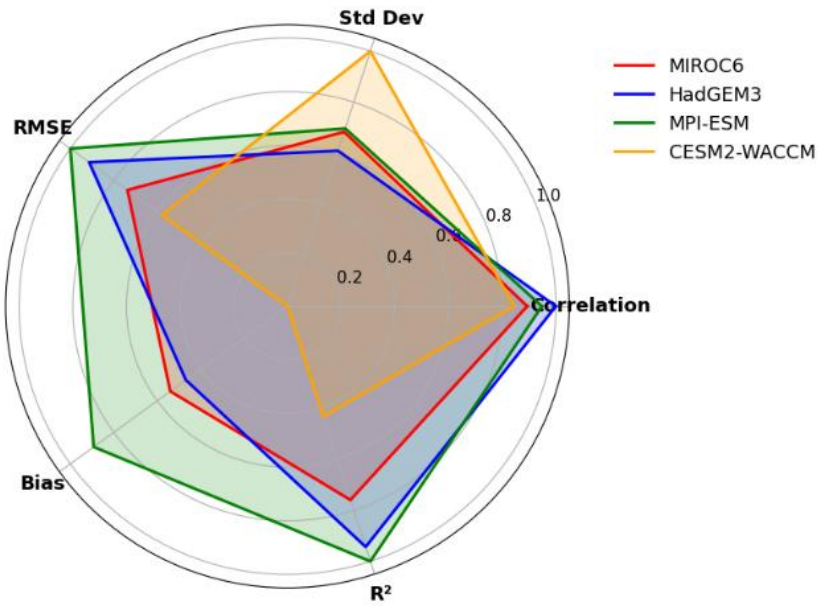

Figure A17:Radar chart summarizing normalized skill metrics of four CMIP6 models against the ERA5 benchmark over West Africa (1950–2014).